Universidade de Aveiro
2014

Seção Autónoma das Ciências da Saúde

Marta Sofia da Silva Correia

Identificação de potenciais biomarcadores de doença de Alzheimer no plasma usando FTIR

Identification of potential Alzheimer's disease biomarkers in plasma using FTIR

Marta Sofia da Silva Correia

Identificação de potenciais biomarcadores de doença de Alzheimer no plasma usando FTIR

Identification of potential Alzheimer's disease biomarkers in plasma using FTIR

Dissertação apresentada à Universidade de Aveiro para cumprimento dos requisitos necessários à obtenção do grau de Mestre em Biomedicina Molecular, realizada sob a orientação científica da Professora Doutora Carla Alexandra Pina da Cruz Nunes, Professora Auxiliar Convidada da Seção Autónoma das Ciências da Saúde da Universidade de Aveiro.

Este trabalho é dedicado aos meus pais e ao meu irmão, por serem as pessoas mais importantes da minha vida! Sem eles, nada seria possível.

o júri

presidente

Professora Doutora Odete Abreu Beirão da Cruz e Silva
Professora Auxiliar com Agregação da Seção Autónoma de Ciências da Saúde da Universidade de Aveiro

Professora Doutora Ivonne Delgadillo Giraldo
Professora Associada com Agregação do Departamento de Química da Universidade de Aveiro

Professora Doutora Carla Alexandra Pina da Cruz Nunes
Professora Auxiliar Convidada da Seção Autónoma de Ciências da Saúde da Universidade de Aveiro

agradecimentos

Um agradecimento muito especial à Professora Doutora Alexandra Nunes pela orientação e apoio ao longo de todo o projeto. Obrigada pelo encorajamento e dedicação durante todo este período.

À Professora Doutora Odete da Cruz e Silva e à Doutora Ilka Rosa pela disponibilização das amostras e dados clínicos importantes para este trabalho.

À Professora Doutora Ana Gabriela Henriques pela disponibilidade, sugestões e informação relativa às amostras utilizadas neste projeto.

Ao departamento de Química e ao Grupo dos Produtos Naturais e Alimentares da Universidade de Aveiro por facultarem o sistema de FTIR, e ao Centro de Biologia Celular da Universidade de Aveiro pelo material disponibilizado.

A todos os pacientes, obrigada por se terem voluntariado para este estudo.

À Susana, ao Daniel, à Sandra e à Margarida, obrigada pela vossa amizade, apoio e por me acompanharem ao longo de todo o meu percurso académico. Ao Christian, que apesar da distância, permanece por perto. A todos os meus colegas e amigos de mestrado, pelo apoio e momentos de boa disposição.

À minha família, que está desde sempre a meu lado, obrigada por toda a confiança que depositam em mim.

Aos meus pais pelo amor incondicional e por me apoiarem desde sempre em todas as circunstâncias da minha vida!

Ao meu irmão, pela importância que tem na minha vida e por acrescentar um colorido especial aos meus dias.

A Deus, por me acompanhar todos os dias, iluminando o meu caminho!

palavras-chave

Doença de Alzheimer, espectroscopia de infravermelho, biomarcadores no plasma, metabolómica, diagnóstico precoce.

resumo

Os atuais critérios clínicos de diagnóstico da doença de Alzheimer geralmente identificam a patologia apenas quando os pacientes já atingiram a fase de demência, ou seja, o estágio mais avançado da doença. Isto revela-se demasiado tarde para que qualquer tipo de terapêutica seja bem-sucedida e, consequentemente é necessário desenvolver uma metodologia de diagnóstico que permita um reconhecimento mais precoce da doença. Desta forma, é preciso adotar diferentes abordagens para a descoberta de novos biomarcadores para a doença de Alzheimer, tais como a utilização de técnicas de metabolómica (ex. FTIR). O potencial do FTIR no campo clínico recebeu recentemente particular atenção, sendo que esta técnica utiliza as frequências de vibração das moléculas presentes na amostra analisada para produzir uma "impressão digital" metabólica, a qual é específica para cada amostra.

Esta dissertação tem como objetivo a identificação de potenciais alterações bioquímicas que possam estar relacionadas com demência, tornando possível a distinção entre grupos controlo e de doentes no seio do conjunto de amostras de plasma analisadas. A utilização de amostras de plasma torna o processo minimamente invasivo, de entre outras vantagens clínicas. Para além da colheita das amostras de sangue utilizadas neste projeto, os voluntários foram submetidos a uma avaliação cognitiva através da realização do MMSE e do CDR, com outra informação clínica relevante a ser também recolhida. Todas as amostras analisadas foram emparelhadas de acordo com a idade e o sexo.

Para uma melhor distinção entre amostras controlo e de doentes foi aplicada a metodologia de PCA aos dados dos espectros obtidos em regiões específicas, nomeadamente em 3500-2700 cm^{-1}, 1700-1400 cm^{-1}, e 1200-900 cm^{-1}. Isto permitiu identificar as principais alterações patológicas que ocorrem a nível bioquímico durante o desenvolvimento da doença neurodegenerativa. Na primeira região espectral referida, as amostras dos doentes apresentaram um maior conteúdo de lípidos saturados comparativamente aos não saturados, o que se traduz num potencial risco cerebral maior. Para além disso, foi observada a presença de ácidos carboxílicos, usualmente relacionados com hiperoxidação de lípidos, produção de carbonilos reativos e alterações estruturais e funcionais de proteínas. Por sua vez, a região espectral 1700-1400 cm^{-1} permitiu identificar diferenças na conformação de proteínas entre amostras controlo e de doentes, tendo estas últimas sido ainda relacionadas com a ocorrência de agregados proteicos. Por outro lado, a região 1200-900 cm^{-1} pôde ser relacionada com presença de danos celulares provocados por *stress* oxidativo nas amostras de doentes.

Como importante nota a reter, a análise por FTIR pode ter o potencial para ser aplicada no futuro não apenas para diagnóstico de disfunção cognitiva, mas também para identificação do estádio da doença e realização de prognósticos, para além da avaliação do risco de desenvolvimento da doença em sujeitos controlo.

keywords

Alzheimer's disease, infrared spectroscopy, plasma biomarkers, metabolomics, early diagnosis.

abstract

Current clinical AD diagnosis criteria used to identify the disorder in patients who have already overt the advanced stage of dementia. This is too late for some kind of successful disease adjustment and consequently, early recognition of AD needs to be improved. Therefore, it is really needed different approaches for discovering new AD biomarkers, such as the application of metabolomics techniques (e.g. FTIR). The potential of FTIR in the clinical field has recently received particular attention, since it uses vibration frequencies of molecules present in the analysed sample to produce a metabolic fingerprint, which is then specific for each sample.

This dissertation aims to identify biochemical alterations that might be related to dementia, being possible to distinguish between control and disease groups of plasma samples, through application of FTIR methodology at the 4000-600 cm^{-1} spectral region. Using plasma samples makes the process being minimally invasive, with other relevant clinical advantages. Besides the collection of blood samples used in this project, the volunteers were also submitted to cognitive evaluation trough Mini Mental State Examination (MMSE) and Clinical Dementia Rating (CDR), with other relevant clinical information being also collected. All the analysed samples were matched by age and sex.

For a better discrimination between control and disease samples, Principal Component Analysis (PCA) was applied to spectra data at specific regions, namely 3500-2700 cm^{-1}, 1700-1400 cm^{-1}, and 1200-900 cm^{-1}. This allowed to identify the main pathological changes that occurred at the biochemical level during neurodegenerative disorder development. In the former spectral region, disease samples presented a higher content of saturated lipids in relation to the unsaturated ones, which translates in a high potential brain damage. Besides, it was also noted the presence of carboxylic acids that are usually related to lipid hyperoxidation, production of reactive carbonyls and proteins structural and functional alterations. In turn, the spectral region 1700-1400 cm^{-1} allowed to identify differences in protein conformation between control and disease samples, and these last ones were still related with occurrence of protein aggregates. In other hand, the 1200-900 cm^{-1} region could be associated to cellular damage provoked by oxidative stress in disease samples.

As an important note to take, FTIR analysis could have the potential to be applied in future not only for cognitive impairment diagnosis but also for identification of disease stage and prognostic evaluation, besides assessment of disease developing risk for control subjects.

INDEX

INDEX OF FIGURES

INDEX OF TABLES

Abbreviations

AD	Alzheimer's disease
ADAS-Cog	Alzheimer's Disease Assessment Scale-Cognitive
ADDL	Aβ-derived diffusible ligands
ADL	Activities of daily living
ADRDA	Alzheimer's Disease and Related Disorders Association
AICD	APP intracellular C-terminal domain
ANN	Artificial Neural Network
APOE	Apolipoprotein E
APP	Amyloid precursor protein
ATR	Attenuated Total Reflectance
Aβ	Amyloid-β
BACE1	β-site amyloid precursor protein-cleaving enzyme 1
BBB	Blood-brain barrier
BIOMARKAPD	Biomarkers for Alzheimer's disease and Parkinson's disease
CA	Cluster Analysis
CAA	Cerebral Amyloid Angiopathy
CALM	Clathrin assembly lymphoid-myeloid leukemia gene
CANTAB	Cambridge Neuropsychological Test Automated Battery
CDK5	Cyclin-dependent kinase 5
CDR	Clinical dementia rating scale
CLU	Clusterin
CNS	Central Nervous System
CSF	Cerebrospinal Fluid
CTFα	membrane-bound C-terminal fragment α
CTFβ	membrane-bound C-terminal fragment β
DA	Discriminant Analysis
DLB	Dementia with Lewy bodies
DM	Diabetes mellitus
DMS-IV	Diagnostic and Statistical Manual of Mental Disorders
DREL	Clock drawing test
EAA	Excitatory Amino Acid
EDTA	Ethylenediamine Tetraacetic Acid
ELISA	Enzyme-Linked Immunosorbent Assay
EOAD	Early-onset Alzheimer's disease
FAD	Familiar Alzheimer's Disease
FDA	Food and Drug Administration
FDG	Fluorodeoxyglucose
FTIR	Fourier Transform Infra-red spectroscopy
FTLD	Frontotemporal lobar degeneration
GABA	γ-Aminobutyric Acid
GDS	Geriatric Depression Scale

GSK3β	Glycogen synthase kinase 3β
HTN	Hypertension
ICD-10	International Statistical Classification of Diseases
IDE	Insulin-degrading enzyme
LOAD	Late-onset Alzheimer's disease
LRP1	LDL receptor-related protein 1
MAP	Microtubule Associated Protein
MCI	Mild Cognitive Impairment
MMSE	Mini-mental state examination
MoCA	Montreal Cognitive Assessment
MRI	Magnetic resonance imaging
MRS	Magnetic resonance spectroscopy
MS	Mass spectrometry
MSI	Metabolomics Standard Initiative
NAA	N-acetyl aspartate
NEP	Neprilysin
NFT	Neurofibrillary tangles
NINCDS	National Institute of Neurological and Communicative Disorders and Stroke
NMDA	N-Methyl-D-aspartate
NMR	Nuclear magnetic resonance
NSAID	Nonsteroidal anti-inflammatory drug
PCA	Principal Component Analysis
PDD	Parkinson's disease dementia
PET	Positron emission tomography
PHF	Paired Helical Filaments
PiB	Pittsburgh compound B
PICALM	Phosphatidylinositol-binding clathrin assembly protein
PP2A	Protein phosphatase-2A
PUFA	Polyunsaturated Fatty Acid
RCT	Randomised controlled trial
RNS	Reactive nitrogen species
ROS	Reactive oxygen species
SOD	Superoxide Dismutase
SORL1	Sortilin-related receptor 1
SP	Senile plaques
SPECT	Single-proton emission CT
TNF-α	Tumor Necrosis Factor α
VaD	Vascular dementia
WHO	World Health Organization
8-OHdG	8-hydroxydeoxyguanosine

CHAPTER 1

1. EPIDEMIOLOGY

Alzheimer's disease (AD) is the most common and most debilitating neurodegenerative disorder among older population, being usually developed after 65 years old with incidence of 67 per 1000 in these ages. The risk of developing AD doubles with each 5 years of age, with more incidence among women. The estimated number in 2005 of AD patients was 24 million people worldwide, and leaning to grow at 81 million in 2040, with the major percentage of cases occurring in developing countries [1,2]. At an aging population as we have nowadays, diseases associated with old age are prone to become increasingly prevalent. Most of the increase in AD prevalence is projected to occur with people of the over-85 age group [3].

Furthermore, AD substantially reduces life expectancy with the median survival time after diagnosis being around of 8,3 years for individuals diagnosed at 65 years old, which means an approximated 67% reduction in media life span [4].

AD is also the commonest dementia, accounting for over 65% of dementia in any age group [5]. Dementia is a major cause of disability in the older adult population. Although the actual prevalence of dementia is unknown, estimates range from 2,5% to 24,6% of those older than 65 years of age, with the number increasing with advanced age [6]. According to a WHO report, dementia could contributed 11,2% of years spent living with a disability in people over 60 years old – more than stroke, cardiovascular disease and cancer [7].

According to European studies until 2009, in Portugal there are 153 000 people suffering with dementia, from which 90 000 have AD. This means that about 1% of total Portuguese population suffer from this pathology [8].

2. PATHOLOGICAL CARACTERIZATION

AD has a gradual onset and a progressive course over several to 10 or more years, with death in a state of extreme cognitive decline [5]. This pathology is manifested by a progressive decline in several cognitive abilities, like memory, with functional and behavioural degeneration. It is thought that those clinical symptoms take place at 15 to 20 years after the beginning of pathological mechanisms behind of AD [2].

The progressive loss of intellectual functions turns sufficient severe by interfering significantly with normal activities of daily living (ADL) and social relationships. It is important to differentiate AD from some benign age-related episodes of forgetfulness by its inevitable, progressive and irreversible declines in memory, time and space orientation, performance of routine tasks,

language and communication skills, abstract thinking, learning ability and, in a more advanced stage, personality changes and impairment of judgment [3]. Disturbance of gait, motor and occasionally sensory abnormalities and seizures are prone to occur in a later stage. AD cardinal clinical features are summarized in Table 1 and clinical stages are presented in Table 2 [5,6].

Table 1| Main clinical features present in AD.

Main Clinical Features of AD
Progressive loss of ability to learn, retain and process new information (i.e. memory loss)
Decline in language, with difficulty in naming and in understanding what is being said
Apraxia – impaired ability to carry out skilled motor activities
Agnosia – failure to recognize objects (e.g. clothing), places or people
Progressive loss of executive function (organizing, planning and sequencing)
Behavioural change (manifestation of agitation, aggression, wandering and persecutory delusions)
Loss of insight, relative or complete
Depression – though severe depression is unusual, perhaps because of loss in insight

Table 2| Clinical staging of AD, characterized by progressive degenerative changes. Adapted from [6].

Stage 1	*Initial stage that may last 2 to 4 years* • Memory loss • Lack of spontaneity • Subtle personality changes • Disorientation to time and date
Stage 2	*Confusional stage that may last several years* • Impaired cognition and abstract thinking • Restlessness and agitation • Wandering, "sundown syndrome" • Inability to carry out ADL • Impaired judgment, lack of insight, inappropriate social behaviour • Repetitive behaviour • Voracious appetite
Stage 3	*Terminal stage that usually last for 1 to 2 years, with some exceptions* • Emaciation, indifference to food • Inability to communicate • Urinary and fecal incontinence • Seizures

2.1. Macroscopic characterization

At a more gross level, there is an atrophy of neocortex and often of hippocampus and amygdala as well – all key sites involved in thinking and memory function. Atrophy is then most pronounced in the association cortices and is accompanied of widened sulci and narrowed gyri. Besides this, the

ventricular system is often enlarged, contributing to the atrophy (Figure 1). Also, melanin-pigmented neurons are often much paler than normal [3,9].

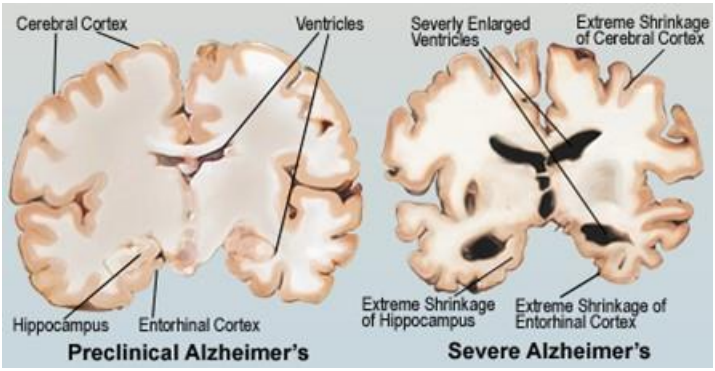

Figure 1|Schematic representation from a longitudinal section of preclinical AD brain (left) and brain in AD severe stage (right), with emphasis on the progressive character of ventricles enlargement and cortex shrinkage. Adapted from [10].

Despite of classical relevance of atrophy in AD morphological characterization, this is more prominent in younger patients where disparity with control cases is bigger. Therefore, while atrophy is of cursory diagnostic value in younger individuals, in majority of cases this is not used in the routine pathologic diagnosis of AD. Nonetheless, AD brains do tend to be about 8% - 15% smaller than age-matched controls [9].

2.2. Microscopic characterization

At a microscopic level, the most common and distinctive hallmark lesions present within the AD brain are amyloid or senile plaques (SP), which consists on intracellular aggregates of amyloid-β (Aβ) peptides, and neurofibrillary tangles (NFT), that results from the accumulation of hyperphosphorylated tau protein. These AD pathological hallmarks affect firstly the medial temporal and parietal lobe, and part of the frontal cortex of the brain, resulting in the symptomatic pattern already mentioned above [1,9]. Other closely related lesions include neuropil threads and dystrophic neurites (terminal neuritic swellings) that occur within neuritic plaques, in the case of neuropil threads specifically in corona of these plaques. Neuropil threads represent swollen dendrites with thread like accumulations of phosphorylated tau (p-tau) within grey and white matter neuropil, occurring in the same topography as NFT and mainly present at earlier stages of disease. Neuronal and dendritic loss, cerebral amyloid angiopathy, Hirano bodies and granulovacuolar degeneration are also typical of the AD brain [9,11].

2.2.1. Senile Plaques (SP)

Senile, or neural, plaques are spherical extracellular lesions with 10 to 200 µm of diameter (Figure 2), which can be found in both intellectually normal individuals and dementia patients. They are distributed predominantly within the cortical and various neocortical areas. Two major subtypes of these plaques are recognized: neuritic and diffuse [3,9].

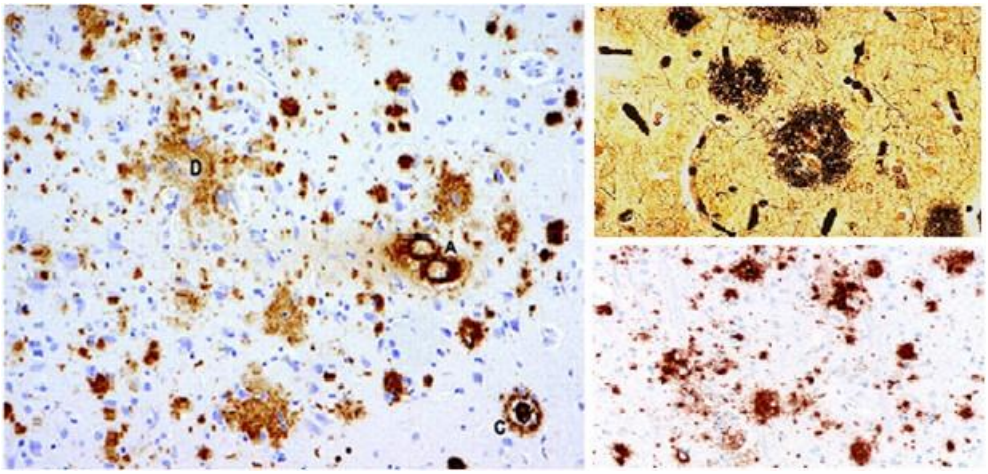

Figure 2|Several microscopic presentations of Aβ aggregation with emphasis for senile plaques. Left: presence of β-amyloidosis in the frontal lobe, showing a diffuse plaque (D), a neuritic plaque with its central core and corona well demarcated (C), and cerebral amyloid angiopathy (A); β-amyloid (10D5) immunohistochemistry. Upper right corner: senile plaques with neurites fragmentation within neuropil grey matter; Bielschowsky silver stain. Down right corner: diffuse plaques in a cerebral cortex sample, Aβ (4G8) immunohistochemistry. Adapted from [9,12,13].

The typical neuritic, classical, or compact plaques are strongly associated with AD and consists in spherical extracellular structures of 10 to 50 µm in diameter, with thickened neuronal processes (or neurites) surrounding an amyloid central fibrillar core that is made of 6 to 10 nm Aβ proteins filaments arranged as bundles radiating from the centre. Furthermore, these neuritic plaques contain dense bodies thought to be the remains of lysosomes, mitochondria and paired helical filaments (PHF, in plaques periphery). Aβ protein, amyloid precursor protein (APP), tau and neurofilament proteins, are all found in the peripheral region of neuritic plaques [3,9,14]. The invariable presence of activated microglia in these plaques comprises the basis for the hypothesis that AD is a disease of excessive inflammation within the brain [9].

In other hand, diffuse plaques lack abnormal neurites, appear more amorphous and contain little if any fibrillar amyloid, in other words, they do contain amyloid but in a diffuse form. They tend to be more heterogeneous in size with a frequency that decreases with increasing size such that most diffuse deposits are less than 20 µm in diameter. Diffuse plaques are the earliest cerebral lesions in

AD and it has been proposed that they may progress to neuritic plaques, depending on several factors (e.g. longevity). However, even in severe and longstanding AD cases, diffuse plaques account for the majority of Aβ protein-immunoreactive material. Furthermore, this does not necessarily imply an evolution from one type to another and might represent diverse mechanisms of SP formation that follows different morphogenic kinetics [3,9].

Giving the progressive degeneration process, SP are followed by neuron apoptosis with a marked reduction in choline acetyltransferase, acetylcholine, noradrenaline and serotonin, as it seen ahead (2.2.5 and 6.2) [5].

2.2.2. Neurofibrillary Tangles (NFT)

NFTs are intracellular clusters found within neuronal cell bodies or dendrites and composed mostly of PHFs, which consists in 10 nm protein filaments helically twisted about each other in pairs. These PHFs proteins are abnormally phosphorylated forms of tau protein, which is usually a microtubule associated protein (MAP), and are complexed with ubiquitin that is a protein normally used by cell to label proteins destined for degradation. Tangle-bearing neurons also contain structures known as neuropil threads, which are composed of either paired helical or nonhelical filaments in their axons or dendrites or both (Figure 3) [3,5,9,15].

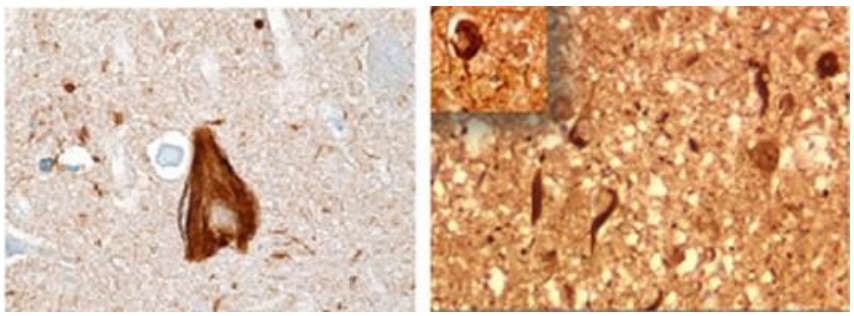

Figure 3| Neurofibrillary tangle microscopic presentation after immunohistochemical stain for tau protein (AT8). Special reference to the neuropil threads in the background (left), and flame-shaped NFTs and its globose form in the inset at 200x magnification (right). Adapted from [9,11]

Some clinicopathologic findings indicate that p-tau typically occupies viable cells and accumulates with age, often in significant amounts. In fact, NFTs are also found in non-demented adults, its deposition begins around to 30 years and increases with age. Recently, it has been suggested that tau lesions may be a manifestation of protection or cellular adaptation with age [9,16]. Nevertheless, NFT number in AD affected brain is approximately six times greater than NFT number present in most severely affected intellectually capable individuals [3].

NFTs are located primarily in large pyramidal neurons of Ammon's horn (hippocampus) and in the cerebral neocortex, although it is also encountered in deep structures, including midbrain, pontine tegmentum, basal nucleus of Meynert and hypothalamus [9]. In intellectually normal old individuals, NFTs may be found at the anterior temporal lobe, but rarely appear in other brain regions such as the neocortex [3].

Despite being hallmark lesions for AD, NFT can also be present in other neurological disorders, which could difficult making of differentiate diagnosis [3].

2.2.3. Cerebral Amyloid Angiopathy (CAA)

CAA consists in the Aβ deposition within the walls of leptomeningeal, cerebral cortical and cerebellar blood vessels, with tendency to formation of highly insoluble fibrils. It appears in 90% of AD patients, nevertheless there is no evidence suggesting that progression of cognitive decline differs between those subjects with and without CAA. Further, the severity of this deposition differs widely, and it is sometimes found in aged healthy brains [3,4,9]. Like SP and NFT, CAA are seen especially within hippocampus and frontal, temporal and parietal cortices [5].

This condition may lead to vascular rupture and multiple lobar haemorrhages, with APOE ε2 allele, considered a protective factor for AD development, being associated with an increased risk of CAA-related haemorrhage [4,9].

2.2.4. Other Lesions

Hirano bodies are intraneuronal rod-like inclusions of 15 to 30 μm in length, which are located primarily in hippocampus and whose frequency generally increases with normal aging and in AD, besides their usually presence in Pick disease and alcoholism. It is thought that a breakdown of the microfilament system is involved in their formation. Although their accumulation is an age-associated phenomenon, Hirano bodies role in AD pathogenesis is doubtful [9].

Granulovacuolar degeneration corresponds to granules, within a membrane-limited vacuole about 3 to 5 μm in diameter, which are frequently located in cytoplasm of pyramidal neurons of the hippocampal formation, and also found in smaller numbers at neocortex of AD brains. This is not specific for AD and it is also present in healthy aged individuals, albeit at lower frequency, as well as in other neurologic conditions [9].

2.2.5. Neuronal Loss

Pyramidal cells, the most abundant cortical neurons, appear to be the main substrate of neurodegeneration. This is because pyramidal neurons use EAAs (namely glutamate and aspartate) as neurotransmitters and receive prominent excitatory inputs, and it is thought that changes in EAA

neurotransmission are the major cause of AD cognitive impairments, particularly memory function. Besides, these neurons are responsible for connecting entorhinal cortex with hippocampus (perforant pathway), whose neurodegeneration is a very early change in AD. In the other hand, evidences suggest that loss of noradrenergic and serotonergic neurons in AD contributes to behavioural and psychological symptoms of dementia, including depression, psychosis, anxiety and aberrant motor activity [15].

Associating the progression of neuron loss with SP and NFT distribution allows the establishment of three pathological stages, as AD neurodegeneration spread (Table 3). Perforant pathway begins to be lost in the transentorhinal stage and progresses through the next stages, limbic and isocortical. Loss of the ascending cholinergic, serotonergic and noradrenergic neurons (from nbM, RN and LC, respectively) begins at the limbic stage and progresses further in the isocortical stage, when GABAergic interneurons start to degenerate [15].

Table 3|Stages of AD progression, according to SP and NFT anatomical distribution and advancement of neuronal loss. Arrow direction relates to different disease stages order, affecting diverse SNC regions. Adapted from [15].

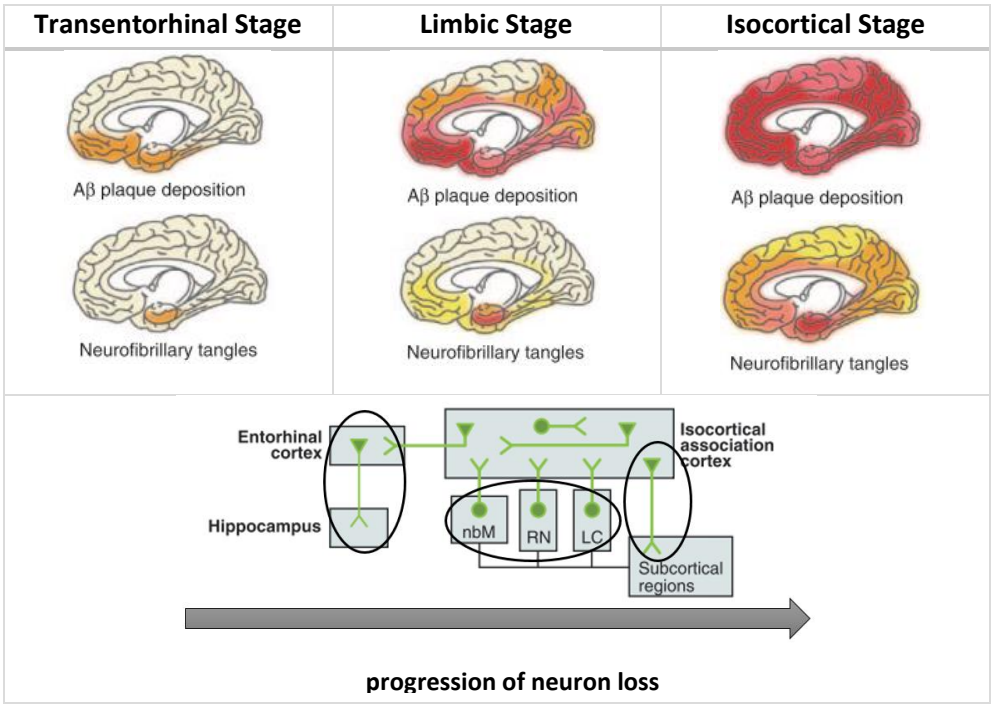

Besides neurotransmitters depletion, the normally high levels of neurotrophin receptors in cholinergic neurons of the basal forebrain are severely reduced in late-stage AD. This contribute for

synaptic failure in AD, since neurotrophins promote proliferation, differentiation and survival of neurons and glia, besides their role mediating learning, memory and behaviour [17].

3. TYPES OF ALZHEIMER'S DISEASE

According to age of onset, AD can be divided into early (<60-65 years) and late (>60-65 years) onset forms. In other hand, according to family history, AD may be classified as autosomal dominant, familial or sporadic, with the latter mainly presenting a later onset of disease [4].

3.1. Familial AD

Autosomal dominant familial AD, being termed early-onset AD (EOAD) or familial AD (FAD), accounts for less than 5% of all AD cases and its onset occurs predominantly before 65 years old. Genetic studies have shown linkage between familial (presenile) AD and loci on chromosome 1 (presenilin, PS1 gene), chromosome 14 (presenilin, PS2 gene) and chromosome 21 (amyloid β-protein precursor, APP gene). This last one can explain the increased incidence of AD among Down's syndrome patients, whose have an extra copy of APP gene since they have one more 21 chromosome than other people (gene dosage effect) [5,14,15]. In fact, all individuals afflicted with Down's syndrome develop symptoms indistinguishable from those of AD by the age 50, and they show diffuse plaques as early as the age 12 [3]. Nevertheless, the finding that age of onset of cognitive decline differs substantially between those with isolated APP duplication and those with chromosome 21 trisomy suggests that Down's syndrome is not a faithful model of EOAD, let alone LOAD [16].

Duplication of APP gene gives rise to Aβ deposition in brain neuropil and/or in cerebral blood vessels, with clinical pictures of AD or recurrent brain haemorrhages. These findings are reminiscent of Down's syndrome, although brain haemorrhages are rarely observed [14].

Between the aforesaid mutations, the one in PSEN1 is the most common cause of EOAD, and in the opposite frequency position is mutations in PSEN2, with both of genes encoding a component of the proteolytic enzyme γ-secretase. All mutations known to cause EOAD are associated with abnormal APP proteolytic processing that leads to increased production of $A\beta_{42}$, the most abundant APP-derived component of SP [9,15]. Indeed, presenilin gene mutations increase the ratio of $A\beta_{42}$ to $A\beta_{40}$, which appears to result from a change in function that manifests itself in reduced γ-secretase activity [14].

3.2. Sporadic AD

Late-onset AD (LOAD), or sporadic AD, represents the great majority of AD cases (>95%) and is probably a heterogeneous disorder. Evidence suggests a link between AD and atherosclerosis, inflammation and cholesterol. LOAD is not associated with deterministic gene mutations, it is instead genetically influenced. It has been found relation between AD and a gene locus on chromosome 19q, with special relevance for gene encoding apolipoprotein E (APOE), which has three alleles (ε2, ε3, ε4). APOE is a protein, in CNS secreted mainly by astrocytes and microglia, with physiological function that supports transporting lipids among CNS cells to keep lipid homeostasis, repairing injured neurons, maintaining synaptic connections and scavenging toxins. The APOE ε4 allele is the major genetic risk factor in AD, increasing the risk for developing LOAD – individuals with two of these alleles have more than seven times increased risk of suffering from AD compared with those who have APOE ε3 alleles. Besides, it is possible that Aβ accumulation is more extensive in those with this allele than those lacking it. In the other hand, it is thought that the under-represented ε2 allele is protective against AD, and ε3 allele, the most common APOE allele found in general population, plays a neutral role in disease. Therefore, although an APOE ε4 allele is not deterministic for AD, having this allele tends to move up age of onset in those perhaps destined to develop AD anyway [5–7,15,16,18].

An increased risk for AD is also associated with genes linked to cytokines, chemokines and nitric oxide synthases. Besides, APOE ε4 allele is associated with other aspects that may contribute to AD as low glucose usage, mitochondrial abnormalities and cytoskeletal dysfunction [7,14].

4. PATHOGENESIS

The complex molecular mechanisms of AD are supported by Aβ, tau and cholinergic theories, besides its genetic basis that accounts for the difference in symptomatology processes activation among human population [19]. Currently available evidence strongly supports the position that initiating event in AD is related to abnormal processing of Aβ peptide, that leads to excess production or reduced clearance of Aβ in the cortex and ultimately to Aβ plaques formation, leading to all AD associated clinical, histopathological, molecular and biochemical manifestations. This is known as amyloid cascade hypothesis and occurs while individuals are still cognitively normal [16,20].

4.1. Aβ cascade hypothesis

4.1.1. APP processing and Aβ formation, clearance and transport mechanisms

Aβ peptide is produced by proteolytic processing of the amyloid precursor protein (APP), an integral membrane glycoprotein, which is firstly cleaved by either α or β-secretase producing soluble sAPPα or sAPPβ fragments and membrane-bound C-terminal fragments (CTFα or CTFβ), respectively. When CTFα is cleaved by γ-secretase there is liberation of p3 peptide, while when γ-secretase cleaves CTFβ the product is Aβ (as it is cleaved at two different sites, it is generated two Aβ forms – $Aβ_{40}$ and $Aβ_{42}$) and APP intracellular C-terminal domain (AICD), as it shows Figure 4. Comparing the 40 or 42 amino acids long Aβ species, the more amyloidogenic $Aβ_{42}$ form is deposited first [1,14,18]. The availability of APP to α-secretase (nonamyloidogenic pathway) or β-secretase (amyloidogenic pathway) determines how much of the pathogenic Aβ peptide will be produced. Since these two secretases/pathways are likely to be spatially separated within the cell (Figure 4), it is possible that changes in APP trafficking, caused by lipid alterations, may be the primary cause of AD process [1]. Indeed, a possible defect in cholesterol metabolism ties together the APOE genetic risk, amyloid production and aggregation, and vasculopathy of AD. Cholesterol is an essential component of neuron membrane being concentrated in lipid rafts (Figure 4), which are platforms for the assembly of β and γ-secretases and processing of APP into Aβ. Furthermore, Aβ generation and aggregation are promoted and its clearance from the brains is reduced when an overabundance of esterified cholesterol decreases membrane lipid turnover [17].

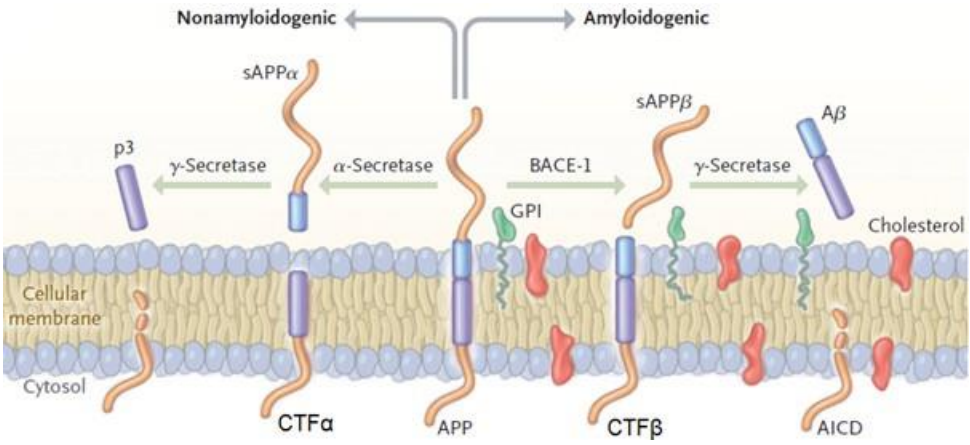

Figure 4| APP processing via nonamyloidogenic and amyloidogenic pathway. The β-site amyloid precursor protein-cleaving enzyme 1 (BACE-1) is the main β-secretase cleaving APP. It is shown a lipid raft that is a tightly packed membrane micro-environment enriched in sphingomyelin, cholesterol and glycophosphatidylinositol (GPI) – all of them are anchored proteins. Adapted from [17].

After being produced, Aβ is secreted outside the cell and binds to various isoforms of APOE, which will allow Aβ to undergo in different metabolism pathways (e.g. clearance via BBB, degradation by insulin-degrading enzyme (IDE) or neprilysin (NEP), deposition or trafficking into the cell). Affinity of APOE4 to Aβ is lower than that of APOE2 or APOE3. Thus, while this two later isoforms help Aβ to be cleared by transport or degradation, APOE4 mainly induce Aβ aggregation implicating it to be a high risk factor for AD (as aforesaid). Besides, contrarily to the other isoforms, APOE4 is more sensitive to stress or injury, which causes neuron-specific proteolysis with formation of a bioactive toxic C-terminal fragment that could induce tau phosphorylation. There is a feedback mechanism to keep Aβ homeostasis: when Aβ is produced, AICD is released and translocated into the nucleus initiating neprilysin transcription, which will degrade Aβ and hereby reduces Aβ to a proper level. If this Aβ levels balance is disrupted, Aβ will be oligomerized and lead to formation of fibrillar Aβ protein (fAβ), which can inhibit proteolytic activity of NEP and IDE, leading to the generation of a positive feedback that accelerates amyloid deposition. Both expression and activity of NEP are significantly decreased in AD brain, with NEP levels declining in an age-dependent manner and inversely correlating with insoluble Aβ levels in temporal and frontal cortex. IDE mRNA and protein levels are markedly decreased in hippocampus of AD patients carriers of APOE ε4 allele, besides IDE levels and activity presented significantly reduced in MCI subjects and appear to continuously decrease during MCI to AD progression [17,18].

It was further proposed that, via regulation of gene transcription, AICD facilitated creation of a feedback loop through which APP protein status could modulate transcriptional activation of APP gene itself [16]. APP shows having physiological functions especially in regulation of synaptic function and neuronal activity. Besides, APP processing regulates cholesterol metabolism and present a normal negative feedback function in modulating Aβ levels, to maintain proper neuronal activity [18].

Aβ transport across the blood-brain barrier (BBB) occurs through LDL receptor-related protein 1 (LRP1), and once in vascular system Aβ is cleared via transport into the blood or via the perivascular fluid drainage pathway. However, in AD brain the clearance via LRP1 is disturbed, resulting in the accumulation and aggregation of Aβ peptide [14,21]. Furthermore, during the onset of disease, the transfer of autophagic vesicles to the lysosomes is impeded, thus promoting Aβ accumulation, and secondly microglia cells cannot destroy efficiently abundant Aβ monomers through phagocytosis [19].

Aβ is a normal secreted product, which suggests that it has a physiological function, although it is still unknown. APP mutations increase Aβ production or lead to an increased proportion of $A\beta_{42}$.

Missense mutations in Aβ lead to vascular deposits, parenchymal plaques or both, since mutations in Aβ have little effect on APP processing but, in other hand, they increase the Aβ propensity to form fibrils [14].

4.1.2. Senile plaques and the triggering of AD neurodegeneration process

In the amyloid cascade hypothesis, Aβ deposits are toxic and cause synaptic dysfunction and neuronal cell death (Figure 5). Aβ oligomers are able to bind specifically to excitatory pyramidal neurons and affect their synaptic structure, composition and density, as well as membrane expression of NMDA receptors. Furthermore, Aβ plays an important role in activity-dependent presynaptic vesicle release [7,18]. Besides, it proposes that changes in tau and consequent NFT formation are triggered by toxic concentrations of Aβ, although the linking between Aβ and tau are not yet clearly understood, as well as NFT contribution for AD neurodegeneration [7,22].

Primary role of tau is to stabilize neuronal cytoskeleton, by interacting with microtubules. Decreased affinity and dissociation of tau from microtubules, probably by phosphorylation (the most common tau post-translational modification), results in microtubule destabilization with cytoskeleton damage. This leads to disruption of tau-dependent cellular functions including axonal growth, vesicle and organelle transport, as well as nervous signal propagation along microtubule nerve network. Newly soluble tau proteins are targeted by post-translational modification that directly or indirectly alter tau conformation, promoting tau dimerization. These tau dimers form tau oligomers, which continue aggregating and constitute subunits of filaments called protomers. Two protomers around each other formed PHFs, whose assembly make NFTs [17,22].

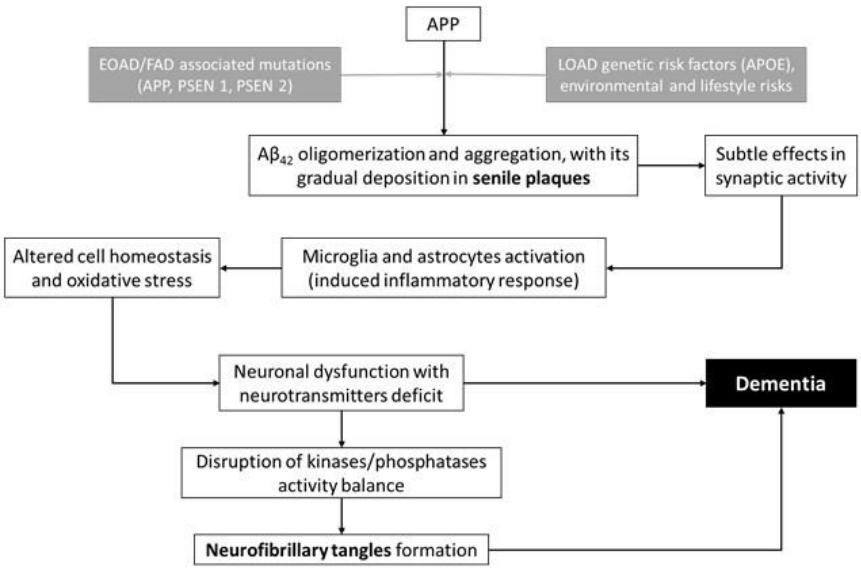

Figure 5| Neurodegeneration main steps according to the cascade amyloid hypothesis.

Tau phosphorylation level is mainly determined by a balance between kinases and phosphatases activity, which when disrupted contributes to tau abnormal phosphorylation observed in AD, especially overactivation of GSK3β and inhibition of PP2A (protein phosphatase-2A). In fact, PP2A activity has been shown to be decreased by 50% in AD brains, and alterations in expression and/or activity of some tau kinases (GSK3β, CDK5, DYRK1A, p38 and CK1) have been already reported in AD. Nonetheless, tau phosphorylation is not constantly accompanied by its aggregation, so it is thought that additional post-translational modification are required for development of NFTs, including cleavage, glycation and nitration. Regardless of this, tau by itself has been reported to mediate Aβ-induced neurotoxicity. In other hand, Aβ overproduction has been shown to induce caspase-3-dependent cleavage of tau, to activate GSK3β and to inhibit UPS activity, which promotes tau aggregation [22].

Aβ deposition is also associated with local inflammatory and immunologic alterations, with microglia around plaques maintaining their stability. Although Aβ may have direct neurotoxicity, at least some of its toxicity might be an indirect consequence of an Aβ protofibril-induced microglia activation and astrocyte recruitment. This inflammatory response may represent an attempt to clear Aβ deposition. However, it is also associated with release of cytokines, nitric oxide and other radical species, and complement factors that can injure neurons and promote ongoing inflammation. Indeed, levels of multiple cytokines and chemokines are elevated in AD brains, and certain pro-inflammatory gene polymorphisms have been related with AD [16,18].

Prudently named prionoids, Aβ aggregates have not yet been shown to be infectious (i.e. contagious) under natural conditions. However, demonstration of inter-individual transmissibility would warrant upgrading the status of such agents to bona fide prions [23]. In other hand, once filamentous tau has formed, it can be transmitted to other brain regions [7].

4.2. The role of aging in AD pathogenesis

The strong association of AD with aging suggests two possibilities: first, that there might be an intimate coupling of AD with an underlying process of aging, possibly involving the age-related increase of damage processes and decreased efficiency of repair mechanisms; second, that the disease might be dependent on some slow, time-dependent processes that take a long time to reach a critical threshold. In this second possibility, AD might not fit the strict definition of an age-related change. Furthermore, if AD actually be a similar sort of time-dependent process, then this would imply that individuals fated to develop AD should have brain characteristic abnormalities at an early, presymptomatic age [3].

Regardless of whether one is genetically predisposed or not, aging is an essential factor in AD, suggesting that an age-related process is involved in its development. It has been emphasized a discernible difference, clinical and pathologic, between AD and senile dementia (a manifestation of advanced age per se) [9].

4.3. Oxidative Stress

Since the brain is characterized by high energy consumption, mitochondria become crucial as an energy source, besides its role in controlling a wide range of cellular processes such as aging. Unfortunately, production of free radicals [hydrogen peroxide (H_20_2), hydroxyl (·OH) and superoxide ($O_2^{-}\cdot$)], in which the brain is especially vulnerable, is an undesirable consequence. The reactive oxygen species (ROS), generated as a by-product of ATP synthesis in mitochondria, have many targets such as lipids, proteins, RNA, DNA and mitochondrial DNA (mtDNA). Oxidative stress is increased during aging, similar to the increased susceptibility seen during AD. It has been strongly linked to neuronal dysfunction and death, and it has also been suggested as a central mediator of toxicity. Under degenerative conditions, cells capacity to maintain redox balance decreases resulting in mitochondrial and metabolic dysfunction, deregulation of metal homeostasis and changes in cell cycle [21,24].

Moreover, it is thought that increase in free radical formation and failure of antioxidant defences may contribute to neurodegeneration. In fact, superoxide dismutase (SOD), the free radical defence enzyme, is reduced by some 25% in AD frontal cortex and hippocampus [5]. Besides, evidence supports the close dependence between mitochondria and brain activity, so it is not surprising that significant reduction of intact mitochondria and microtubules has been found in AD. Furthermore, changes in mitochondrial enzymes, structure, localization and mobility are all involved in AD [24].

It is already known that oxidative stress, protein deposition and synaptic failure are crucially involved in AD neurodegeneration process. However, the order in which they appear during pathological progression and the identity of the mechanism that links them remains under extensive study. Evidence supports that mitochondrial and metallic abnormalities are direct precursors of oxidative stress during the early stages of disease [24].

NFTs are associated with impaired axonal transport of mitochondria between cell nucleus and synaptic terminal, which leads to severe energy dysfunction and imbalance in ROS and reactive nitrogen species (RNS) production, resulting in the AD typical synaptic failure. In other hand, data suggests that oxidative stress in synaptic terminals are able to affect downstream targets (e.g. GSK3β) that have direct repercussion in tau phosphorylation levels, whose balance appear to

determine whether tau contributes to synaptic formation or synaptic failure through NFTs. Thus, altered tau can create a pathological feedback loop with mitochondria that leads to synaptic failure [24].

According to one of the several hypotheses addressing Aβ toxicity, amyloid oligomers access intracellular organelles such as mitochondria and compromise their function [16]. Upon entering the mitochondria, Aβ binds to molecules that might play a cytoprotective role (e.g. ABAD, β-amyloid binding alcohol dehydrogenase, that detoxifies aldehydes as 4-HNE), inhibiting theirs action and leading to mitochondrial dysfunction and ROS production. Aβ induced mitotoxicity is still not clear, but may include several mechanisms such as increasing membrane permeability (interaction with MPTP), reducing of respiratory function and inclusive oxidative phosphorylation, enhancing vulnerability to other toxics, distressing calcium homeostasis, disturbing mitochondrial dynamics and distribution, inducing mitochondrial DNA/RNA mutations and even apoptosis, besides increasing ROS production. Furthermore, Aβ seems to decrease cytochrome c oxidase activity, leading to impairment of electron transport, ATP production (and Aβ-induced ATP synthase affection induces even more ATP depletion), oxygen consumption, and once again of mitochondrial membrane potential. Aβ tends also to increase mitochondrial fission, leading to its fragmentation and contributing to cell death. Oxidative stress resulting from excessive ROS production may be implicated in mitochondrial DNA and RNA point mutations in AD, nevertheless further studies are still required on this [17,21].

Lastly, Aβ and tau may act in synergy on oxidative stress and mitotoxicity, since both shown to affect respiratory capacity by acting on the cytochrome complexes [21]. In other hand, oxidative stress and mitochondrial damage, as cellular changes associated with aging per se, are able to contribute for amyloidosis development [16].

4.4. Other risk factors for AD development

Besides age and genetic factors, other issues associated with dementia include sex, comorbidity, environmental factors and lifestyle. Sex is an important risk factor for AD among elderly population, with several studies showing a higher prevalence of disease among women [25]. It could be associated with decrease in estrogen hormone in postmenopausal women that may have a more effective neuroprotective role than testosterone against AD development [19].

Several studies have observed that physical activity has a positive effect on cognitive function among older population, with significant reductions in cognitive decline. This protective effect of

physical training might results of reduced vascular risk and obesity, lower levels of inflammatory markers, enhanced fitness, neuronal health and positive behaviour [25].

Overweight and obesity are risk factors of AD, since weight loss can reflect underlying diseases and obesity can be related to subsequent vascular diseases. On average, around half of individuals with vascular cognitive impairment might develop dementia within 5 years after a stroke. As a whole, infections, vascular factors and related diseases, head injury and psychological conditions can share a common inflammatory pathway that contributes to the etiology of dementia. Furthermore, hyperinsulinemia and DM II (type 2 diabetes) is strongly associated with insulin resistance (inclusive central resistance), which is related to Aβ formation and presence of inflammatory agents in brain, with subsequent increased AD risk. Besides, resistance to insulin signalling renders neurons energy-deficient and vulnerable to oxidizing or other metabolic insults, and impairs synaptic plasticity. Hyperinsulinemia also damage directly the hippocampal structures, up-regulate GSK3β and reduce IDE levels in AD brain [17,25].

Some macronutrients, such as glucose, protein (tryptophan and tyrosine) and unsaturated fatty acids, have been linked to age-related changes in cognitive function among AD and VaD (vascular dementia) patients. Dementia can be exacerbated via oxidative stress as a result of higher energy and lower antioxidant intake. It is known that excessive intake of *n*-6 polyunsaturated fatty acids (PUFAs) or deficiency of *n*-3 PUFAs may lead to chronic inflammation, platelet aggregation or microvascular endothelial dysfunction [25].

An important early predictor of AD may be lower levels of mental activity at young ages. Furthermore, it has been already stated that high levels of education, verbal ability and/or continuing mental activity allows at least some individuals to function at normal behavioural and cognitive levels, despite the ravages of AD. This may be explained with the multiple additional neural pathways, by which information can get in and out, and that results from mental activity stimulation of complex neural circuits [3].

4.4.1.Genetic risk factors

A recent genome-wide association study of AD identified two loci that were not previously disease-associated: CLU (encoding clusterin) and PICALM (phosphatidylinositol-binding clathrin assembly protein), also known as CALM (clathrin assembly lymphoid-myeloid leukemia gene). Clusterin (apolipoprotein J), in a similar manner to APOE, may regulate both toxicity and solubility of Aβ. Furthermore, APOE and clusterin have been shown to cooperate in suppressing Aβ deposition, and they might modify Aβ clearance at the BBB, which could suggest a role for clusterin in the amyloidogenic pathway. Clusterin levels are increased in proportion to APOE ε4 allele dose levels,

suggesting an induction of clusterin in individuals with low APOE levels. In other hand, genetically directed changes in PICALM function may lead to synaptic dysfunction, possibly through synaptic vesicle cycling, thereby increasing risk for AD. Alternatively, PICALM could influence AD risk through APP processing via endocytic pathways, altering Aβ levels [9,20].

As aforesaid, inflammation is an important process in AD pathogenesis, with recent studies showing that polymorphisms of one of the inflammatory genes alone or in combination have comparable effects on AD risk to those for the APOE ε4 allele. Homozygous carriers of high-risk alleles, such as IL-1-α-889 and IL-1β+3953, or the combination of APOE ε4 allele and high-risk allele of TNF-α, could predict people at high AD risk [25].

Considered as a genetic risk factor, sortilin-related receptor 1 (SORL1), a γ-secretase substrate, is known to regulate APP trafficking and processing with enhancement of Aβ accumulation in both EOAD and LOAD, since SORL1 reduces interaction between APP and β-secretase. Furthermore, interaction between APOE4 and SORL1 single nucleotide polymorphisms on $A\beta_{42}$ CSF indicate the role that SORL1 genetic variants can have in regulating amyloidogenic pathway. An overexpression of SORL1 results in reduced Aβ production, which occurs with binding of SORL1 to APP. Thus, SORL1 concentrations are reduced in AD patients [7,19].

5. DIAGNOSIS

Nowadays, AD is fully diagnosed only by post-mortem analysis of the brain, and although the current clinical diagnosis criteria (DMS-IV, ICD-10 and NINCDS-ADRDA) presents an accuracy of about 80%, it used to identify AD in patients who have already overt dementia correspond to neuropathological advanced disease. This is too late for some kind of successful disease adjustment and consequently, early recognition of AD needs to be improved, especially since it was estimated that interventions capable of delayed clinical onset of dementia by one year would decrease disease prevalence in 2050 by 9 million cases [26,27].

Until recently, AD clinical diagnosis criteria established in 1984 by NINCDS-ADRDA have been used in common clinical practice and research, without modification. These criteria relies mainly on clinical history, physical examination, laboratory tests, neuroimaging and neuropsychological evaluation [20,26]. However, there is now a broad consensus that these criteria should be revised to incorporate new scientific knowledge that has been emerged in the last 30 years. The new proposed criteria differs manly from the 1984 criteria by incorporation of biomarkers of the underlying disease state and formalization of AD different stages [20,28].

It is made a distinction between syndromic labels that denote different qualitative and quantitative clinical expressions of disease (preclinical phase, pre-dementia or MCI phase, dementia phase), and pathophysiological process that underlies the syndrome acting as a neurodegenerative continuum. The core clinical criteria regarding AD dementia and MCI due to dementia are intended to guide diagnosis in the clinical setting, while the new recommendations for preclinical AD phase are intended only for research purposes, do not having any clinical utility at this time. It is important to note that in the preclinical phase, biomarkers are used to establish the presence of AD pathophysiology process in research subjects with no or very subtle overt symptoms. While, in both MCI and AD dementia criteria, clinical diagnoses are paramount and biomarkers are complimentary. Furthermore, development of biomarker standardization is needed before widespread adoption of these renewed guidelines at any AD stage [20].

MCI due to AD, symptomatic pre-dementia phase of the disease, corresponds to a degree of cognitive impairment that is not normal for age and that progress gradually to a state of dementia, when there is significant interference in the ability to function at work or in ADL [28,29]. The core clinical criteria for MCI comprises the following issues: concern regarding a change in cognition; impairment in one or more cognitive domains including memory (impairment in episodic memory is common in MCI patients that progress to AD dementia), executive function, language and visuospatial skills; independence preservation in functional abilities including ADL; without evidence of significant social or occupational impairment. Besides, cognitive tests scores of MCI patients usually present 1-1,5 standard deviations below the mean for their age and education matched peers [29].

The diagnosis of dementia state in AD is intended to encompass a severity spectrum, ranging from the mildest to the most severe stages of dementia. Thus, proposed AD dementia classification are the following: probable AD dementia; possible AD dementia (atypical clinical presentation); probable or possible AD dementia with evidence of AD pathophysiological process (currently intended terminology only for research purposes) [28].

Other two recent publications by an international working group also emphasize the importance of AD diagnostic criteria revision, being also proposed a panel of reviewed criteria and AD lexicon, with insight in potential diagnostic role of biomarkers and differentiation between AD stages, including separating various prodromal/preclinical AD phases [30,31]. Nonetheless, these proposed criteria have not been validated and there is discussion on which neurocognitive tests should be used for characterization and quantification of cognitive deficits, as well as on which are the best

auxiliary biomarkers, definition of their pathological threshold and their clinical value in each patient [11].

5.1. Genetic Tests

The amount of AD risk that is attributable to genetics is estimated to be around 70% [7]. The advance of high-throughput genotyping techniques (e.g. microarrays) and statistical tools have allowed extensive access to association between genetic factors and risk of dementia [25].

According to the American College of Medical Genetics (ACMG) and the National Society of Genetic Counsellors (NSGC), tests for EOAD associated genes (currently APP, PSEN1 and PSEN2) are useful for:

- Symptomatic patients with EOAD;
- Individuals with a family history of dementia with one or more cases of EOAD;
- Individuals with a relative affected by a known mutation of abovementioned genes [4].

Thus, for these rare autosomal dominant mutations, genetic tests are available in selected circumstances. In the other hand, although APOE genotyping is commercially available, this is not recommended at present due to limited clinical utility and poor predictive value. Otherwise, it cannot be used as a surrogate or substitute for clinical diagnosis [4,16].

5.2. Neuroimaging in AD diagnosis

To complement clinical observations and improve clinical trials research, it could be used several molecular imaging techniques such as structural resonance imaging (MRI), functional MRI (fMRI), proton-magnetic resonance spectroscopy (^{1}H-MRS) and positron emission tomography (PET) [27].

In MRI structural studies, it is correlated MRI-based volume with neuron numbers in specific brain regions [27]. In AD, main structural changes are global cerebral volumetric reduction, increased ventricular volumes and regional atrophy of medial temporal lobe. Novel quantitative techniques for structural imaging analysis, such as volumetric imaging, three-dimensional mapping of the hippocampus and cortical thickness measurement, are being investigated as promising markers for AD. These techniques and potential functional imaging with PET might address the metabolic changes that presumably antedate structural damage [7,32].

The blood oxygen-dependent level (BOLD) fMRI signal is a measure of the input and processing of neuronal information within a brain region, which might be associated to a hypoperfusion global pattern in AD. Further, studies of memory in AD patients using fMRI discovered a pattern of altered activation consistent with structural MRI results [27,32].

^{1}H-MRS provides quantitative analysis of the biochemical composition of brain tissue, being its best established marker the amino acid N-acetyl aspartate (NAA), which reflects the functional status of neuronal mitochondria. Indeed, a reduction in NAA levels independent of brain atrophy is a consistent finding in AD. Other metabolites are detectable with ^{1}H-MRS, but their potential as biomarkers candidates requires refined investigations [27].

PET with fluorodeoxyglucose (FDG), that represents neuronal glucose consumption as the main determinant of neuronal metabolism, enables a sensitive and specific detection of AD in its early stages. A reduce of glucose metabolism in bilateral temporal parietal regions and in the posterior cingulate cortex is the most commonly described diagnostic criterion for AD. PET with Aβ ligands, such as ^{11}C-labelled Pittsburgh compound B (PiB) and an ^{18}F-labelled Aβ ligand, can be used to directly visualise Aβ in vivo. The ^{11}C-PiB binding sites in brain are associated with Aβ sheets in neuritic and diffuse plaques, as well as CAA, it does not bind to soluble and oligomeric amyloid [7,27].

The SPECT comprises a radioisotopic scan accomplished with single-proton emission CT (SPECT), and is a useful neuroimaging technique for distinguishing AD from FTLD. Ligands have also been developed that visualise specific neurotransmitter systems with SPECT [7].

Ultrasound and optical imaging are the next promising techniques that can replace high energy radioisotopes and cost effective instruments largely employed in clinical settings. It could be possible to combine development of deep tissue multiphoton imaging systems with optical imaging to generate fusion image with better resolution. Besides, development of new molecular imaging technologies should use neurochemical biomarkers to detect the earliest AD pathogenic events, improve classification, track progression and assess in prediction [19].

5.3. Neuropsychological evaluation

Neuropsychological characterization remains essential to understanding individual deficits, contributing for nonpharmacologic interventions properly applied [33]. Several measures have been developed for helping to determine dementia severity, such as mini-mental state examination (MMSE) and clinical dementia rating scale (CDR) [34]. Other tests could be used: ADAS-Cog (Alzheimer's Disease Assessment Scale-Cognitive), considered more thorough than MMSE and focusing on language, orientation, executive functioning and memory skills; MoCA (Montreal Cognitive Assessment), that includes a clock-drawing test and a test of executive function, it is relatively simple and very useful; Clock Drawing Test, often used combined to other tests, it assess visual-spatial impairment, memory and executive functions; CANTAB (Cambridge

Neuropsychological Test Automated Battery), it consists in 13 interrelated computerized tests of memory and executive functioning and it appear to be quite sensitive to AD warning signs and relatively unbiased regarding culture issues [34,35].

MMSE is the most commonly used test for complaints of memory problems, helping clinicians in dementia diagnosis as well as assessing its progression and severity. It consists of a series of questions and tests with a possible total score of 30 points (Table 4). Different mental abilities are evaluated, including memory, attention and language. On average, AD patients who are not receiving treatment lose two to four MMSE points each year. It is important to note that some factors might influence MMSE total score, such as educational and cultural issues, mental impairment by another reason does not dementia, difficult hearing [36,37].

Table 4|Interpretation of MMSE scores, with correspondence to degree of impairment and need to proceed to a formal psychometric assessment.

Score	Degree of Impairment	Formal Psychometric Assessment
25-30	Questionably significant	Only if clinical signs of cognitive impairment are present
20-25	Mild	To better determine pattern and extent of deficits
10-20	Moderate	If there are specific clinical indications
0-10	Severe	Patient not likely to be testable

CDR is comprised of six cognitive and functional domains (memory, orientation, judgement and problem solving, community affairs, home and hobbies, personal care), which clinicians fulfil based on interview data from patient and a collateral source (e.g. caregiver) [34].

5.4. Differential Diagnosis

NINCDS-ADRDA criteria have been validated against neuropathological gold standards with diagnostic accuracy from 65-96%. However, specificity of these criteria against other dementias is only 23-88%. Currently criteria (1997 NIA/Reagan criteria) for neuropathological diagnosis of AD need to be updated trough improvement in definition and characterisation of non-AD dementias, since their methods are not robustly quantitative and/or not systematically qualitative [30,38].

In clinical practice it is often difficult to recognize each type of dementia, and to define landmarks that differentiate dementia from the mild decline in memory and cognitive function seen during aging. Following AD, the most common neurodegenerative dementias (Table 5) are frontotemporal lobar degeneration (FTLD), vascular dementia (VaD), dementia with Lewy bodies (DLB) and Parkinson's disease dementia (PDD) [5,11].

Table 5| Main neuropathological characteristics of the most common neurodegenerative dementias besides AD.

Disease	Main clinical, imaging and histopathological findings	Refs
AD	Hallmark lesions: Aβ extracellular deposition (amyloid plaques) and intracellular neurofibrillary tangles (accumulated p-tau) Clinical: prominent episodic memory impairment, with secondary deficits in word-finding skills, visual-spatial cognition and executive functions; common neuropsychiatric symptoms and personality alterations Imaging: PiB-PET positive amyloid tracer in prefrontal, medial parietal, lateral temporal and posterior cingulate cortices, and striatum; FDG-PET shows hypometabolism in posterior cingulate and temporo-parietal cortices; disproportionate atrophy on MRI in medial, basal and lateral temporal lobe, and medial parietal cortex	[4,39]
FTLD	Hallmark lesions: cellular inclusions constituted by MAPT (FTLD-tau), TDP-43 (FTLD-TDP) and FUS (FTLD-FUS) Clinical: progressive non-fluent aphasia (FTLD-tau), semantic dementia and motor neuron disease (FTLD-TDP), behavioural perturbations (FTLD-FUS); inefficient retrieval strategies; onset usually before 65 years old Imaging: structural MRI changes and salient hypometabolism in left perisylvian language regions (FTLD-tau and FTLD-TDP); atrophy and hypometabolism at bilateral frontal and anterior temporal areas (FTLD-FUS)	[4,11,32,39]
VaD	Hallmark lesions: multiple or strategically placed infarctions, ischemic brain injury and haemorrhagic lesions Clinical: relative abrupt onset, fluctuating cognition (often mild symptoms) related to stroke(s); executive dysfunction and focal neurological signs; depression, psychomotor retardation and affective disorders Imaging: widespread vessel disease on MRI	[5,32,39]
DLB	Hallmark lesions: α-synuclein deposits (Lewy bodies and Lewy neurites) Clinical: dementia with ADL impairment; fluctuating cognition (especially attention and awareness); recurrent visual and auditory hallucinations, delusions and transient loss of consciousness; symptoms of Parkinson's disease; REM sleep behaviour disorder and depression Imaging: SPECT or PET scan shows reduced dopaminergic activity in basal ganglia, hypometabolism and hypoperfusion in primary and association visual cortices	[4,32,39,40]
PDD	Hallmark lesions: α-synuclein deposits (Lewy bodies and Lewy neurites) Clinical: Queen Square Brain Bank criteria* for Parkinson's disease; impairment of more than one cognitive domain affecting ADL (mainly executive and visual-spatial functions, memory and speech); apathy, personality and mood alterations; hallucinations and delusions; increased daytime fatigue Imaging: MRI volumetry shows atrophy of basal ganglia, hippocampus, parahippocampal regions and anterior cingulate gyrus; SPECT or PET scan shows reduced dopaminergic activity in basal ganglia	[4,40,41]

MAPT: microtubule associated protein; TDP-43: transactive response DNA binding protein of 43 kD; FUS: fused in sarcoma protein

*Clinical criteria according to which, for a diagnosis of Parkinson's disease, it has to be present bradykinesia and at least one of the following symptoms: muscle rigidity, resting tremor, and/or postural instability; besides presence of supporting criteria (e.g. unilateral onset) and absence of exclusion criteria (e.g. no improvement after levodopa treatment).

Depression is a significant health problem among elderly population which can be accompanied by a pseudodementia state that is often included in differential diagnosis of dementia, since many of the features of an early dementia are apparent, especially memory impairment, slowed thinking and lack of spontaneity. However, patients with pseudodementia often have a previous history of depression or a family history of mood disorder, whose successful treatment restores intellectual function, unlike what happens with dementia [5,6]. Besides, contrarily to dementia, pseudodementia has rapid onset and relatively short symptomatology duration, patient might display marked variability in performing tasks of similar difficulty or may lack of interest in answering questions, further neurologic symptoms are not present [6].

6. ALZHEIMER'S TREATMENT AND THERAPEUTIC PERSPECTIVES

6.1. Pharmacological treatment

Several drugs have become available over the past two decades to help further cognitive decline in AD [6]. However, AD is reaching epidemic proportions, with a large human, social and economic burden, for which effective treatments are greatly needed. Current drugs for AD target cholinergic and glutamatergic neurotransmission, thus improving symptoms, although their neuroprotective activity is still debated. Much effort is directed towards identifying disease-modifying therapies, with several compounds in different phases of development and being subject of clinical trials [43].

6.2. Targeting cholinergic and glutamatergic neurotransmission

Cholinergic neurons are selectively (>70%) degenerated in AD, with the loss of cholinergic function being closely related to cognitive dysfunction. Therefore, therapeutics emphasis has been on increasing cholinergic synaptic transmission in areas of the brain that are concerned with memory and cognition. Acetylcholinesterase inhibitors (AChEIs), that inhibit the breakdown of acetylcholine released by still-intact neurons, are considered the best developed therapy stabilizing cognitive decline for up to 3-6 months, which corresponds to 1,5 - 2 points on the MMSE over 6-12 months. Moderate improvements in mood and social interaction have also been reported. However, no modification of disease duration or general disease progression has been accomplished, since they are not actually considered modifying-disease drugs, only symptomatic relievers. Currently, three AChEIs – donepezil, rivastigmine and galantamine – are available as cognitive-enhancing agents (Table 6) [6,7,9].

Table 6|Currently approved drugs for treatment in AD. Adapted from [9,10,42].

Drug	Disease stage	Symptomatic activity	Potential neuroprotective activity
AChEI			
Donepezil (Aricept®)	All stages	AChEI	Possibly decreases levels of APP, production of Aβ and other amyloidogenic compounds, and Aβ-induced toxicity; modulates expression of AChEI isoforms; increases expression of nicotinic receptors
Rivastigmine (Exelon®)	Mild to moderate	AChEI and BChEI	
Galantamine (Razadyne®)	Mild to moderate	AChEI (nicotinic receptor modulation)	
NMDA receptor antagonist			
Memantine (Namenda®)	Moderate to severe	Uncompetitive, voltage-dependent NMDA receptor antagonist	Decreases Aβ toxicity; prevents hyperphosphorylation of tau; decreases microglia-associated inflammation; increases release of neurotrophic factors from astroglia

BChEI: butyrylcholinesterase inhibitor; *AChEI*: *acetylcholinesterase inhibitors; NMDA: N-methyl D-aspartate*

There is evidence that combine therapy of memantine with an AChEI, namely donepezil, may provide better outcomes with regards to cognition, ADL, global outcome and behaviour [7,9].

Direct activation of postsynaptic cholinergic receptors by muscarinic agonists may decrease secretion of Aβ and increase secretion of nerve growth factor (NGF). In this insight, other substances besides rivastigmine that are capable of blocking butyrylcholinesterases, nonsynaptic (nonspecific) cholinesterases, are being explored [9].

6.2.1. Researching possible disease-modifying therapies

Apart from the ACIs already approved there has been little development of cholinergic drugs. Besides this drug category, other ones are being focus in drug development and research (Table 7), such as non-cholinergic modifying neurotransmission drugs, anti-amyloid therapies, drugs to target tau protein, targeting mitochondrial dysfunction therapies, neurotrophins, and other potential therapeutic strategies (e.g. antioxidant supplementation) [43].

Table 7| Main anti-AD drug categories that are being focus in drug research. Adapted from [15,43,44].

Anti-amyloid therapies
AD drug development is driven mainly by the amyloid hypothesis, thus most of clinical trials are designed to target Aβ.
Targeting of Aβ production
β-secretase inhibitors
Their development is challenging, since this enzyme has many substrates and a wide substrate binding domain. Furthermore, candidate drugs must cross the blood-brain barrier. Oral drugs for Type II DM, rosiglitazone and pioglitazone, act as β-secretase inhibitors by stimulating PPARγ. However, it was reported in clinical trial environment that there was no efficacy on cognition or global function, besides FDA warning for possible cardiac risks associated with the use of rosiglitazone.
γ-secretase inhibitors and modulators
Besides similar challenges presented to those for β-secretase inhibitors, this drug category are associated to collateral effects caused mainly by inhibition of Notch signalling pathway, which is involved in cell differentiation.
α-secretase activators
Several drugs have been tested in clinical trials, but no evidence supports their use in AD yet.
Targeting of Aβ aggregation
Peptidic and non-peptidic anti-aggregants have been tested, with promising results particularly from PBT2, that it was subject of a 12-week phase 2 RCT with mild AD patients.
Targeting of Aβ clearance
Apart from advantages and disadvantages of immunization strategies, evidence suggests that clearance of amyloid plaques alone cannot repair already damaged neurons and prevent disease progression.
Drugs to target tau protein
The only one tau-directed compound (valproate) that has reached phase 3 RCT presented disappointing results since there were no effects on cognition and functional status. More compounds that target tau-phosphorylating kinases, to prevent tau aggregation or to promote aggregate disassembly, are in development.
Targeting mitochondrial dysfunction therapies
A new approach to AD therapy, different from the protein-focused strategies that currently dominate research, since it is thought that mitochondrial dysfunction have a causal role in neurodegeneration. Although some promising results from phase II RCTs with latrepirdine, a non-selective antihistamine, phase III CONCERT trial presented in 2012 had disappointing results, leading to discontinuation of latrepirdine development for all indications.
Neurotrophins
Basal forebrain cholinergic neurons depend on NGF for survival and fibre outgrowth. Furthermore, recent findings have suggested a causal link between NGF imbalance, activation of amyloidogenic pathway and AD neurodegeneration. Several clinical trials with NGF delivery have been made and some are ongoing, particularly using gene therapy, but further research is needed.
Other potential therapeutic strategies
Other approaches such as omega-3 polyunsaturated fatty acids (e.g. docosahexaenoic acid), antioxidants (e.g. vitamin E), NSAIDs, statins or drugs that target phosphodiesterase have been tested in RCTs, some of them are ongoing. However, without much promising results yet.

Antioxidant supplementation is still a matter of discussion since high doses of vitamin E have been associated with increased mortality risk and no beneficial effects for AD patients, whereas it is thought that a combination of micronutrients could be more effective in neuroprotection [6,42]. Further, a more recent RCT in MCI patients did not report any benefit with vitamin E [7].

6.3. Non-pharmacological therapy

Over the 8 to 10 years of progressing dementia, patients became increasingly disabled in ADLs. Physical therapy can improve mobility despite the dementia. The approach to ADLs and social activities must take advantage of the ability of many AD patients to learn skills through procedural memory. This motor learning depends upon corticocerebellar and striatal structures, rather than upon the mesial temporal neural networks that bear the brunt of neurodegeneration. It has been already shown that motor learning and the transfer of motor skills requires constant practice for AD patients, for which is thus essential consistent repetition without interference to optimize learning. Without specific practice, 30% of patients deteriorated in ADLs such as walking, eating, dressing and continence [45].

Cognitive training in healthy older people and in patients in early stages of AD might also be helpful by improvising specific aspects of cognitive ability, with a recent meta-analysis and systematic review suggesting moderate benefit across a variety of training approaches [7].

7. BIOMARKERS IN AD DIAGNOSIS

As aforesaid, diagnostic criteria currently used for AD are based on clinical features supporting a probabilistic diagnosis with low specificity, particularly when these criteria are applied at very early stages of disease or used to monitor effects in drug development research. Moreover, symptomatology required for diagnosis is evident only a long time after initiation of pathological process, and since therapies are initiated only after diagnosis their modest benefit may be explained, in part, by the fact that some irreversible brain damage has already occurred at this time [46]. Hence, it has been emphasized the importance for new AD diagnosis criteria on defining preclinical AD and MCI phases, allowing to initiate a more earlier therapeutic intervention [26]. Indeed, the discovery of an effective treatment in the preclinical phase would in fact be a preventive therapy, though secondary prevention [2].

Discovery of new AD biomarkers is then essential for developing disease-modifying therapies and potentially reducing costs of clinical trials. In that way, new biomarkers are needed for early

diagnosis, ideally even before cognitive symptoms arise (sensitive biomarkers); accurate diagnosis, differential diagnosis between several kinds of dementia (specific biomarkers); and measurement of disease progression within the time of a clinical trial that could measure pathology directly or indirectly (surrogate biomarker) [2]. Further regarding clinical trials, biomarkers should facilitate selection of drug candidates, verify the mechanism of action, define dose effects, and thus diminish length and sample size of clinical trials [27].

Following this thoughts sequence, new AD biomarkers will need to be reliable (robust against main confounding factors such as age, gender and genotype), reproducible, easily obtainable, non-invasive, well-validated, more constant as possible throughout time in healthy people, and presents little variation due to unrelated comorbidities [2].

Furthermore, an accurate diagnosis of dementia enables detection of potentially treatable disorders that contribute to cognitive impairment, such as depression, vitamin deficiencies and hypothyroidism [7].

7.1. Current used AD biomarkers

The five most widely studied AD biomarkers corresponds to $A\beta_{42}$ and tau (total and phosphorylated form) levels in CSF, fluorodeoxyglucose uptake pattern on PET (FDG-PET), amyloid PET imaging (^{11}C-PiB), and structural MRI measures (Table 8). Each of them is well validated enough to be incorporated into AD renewed diagnosis criteria and used in therapeutic trials and large observational studies. Both CSF $A\beta_{42}$ and amyloid PET imaging are biomarkers of Aβ plaque deposition, while the others are related to neurodegeneration [20,29,45].

Table 8| Currently used AD biomarkers, according to NINCDS-ADRADA revised criteria and based in recent evidences.

Biomarker	Biomarker alteration in AD
Aβ plaque deposition/accumulation biomarkers	
amyloid PET imaging	abnormal tracer retention (^{11}C-PiB specifically binds to fibrillar Aβ, and not to soluble Aβ or to diffuse plaques)
[CSF $A\beta_{42}$]	low levels
Biomarkers of neuronal degeneration or injury	
[CSF tau_{total} and p-tau]	high levels
FDG-PET	decreased fluorodeoxyglucose uptake in a specific pattern involving temporoparietal cortex
Structural MRI	Atrophy specific pattern involving medial, basal and lateral temporal lobes, besides medial and lateral parietal cortices

The onset and progression of AD biomarkers appear to follow an ordered temporal pattern (Figure 6). Aβ biomarkers are indicative of initiating or upstream events which seem to be most dynamic before clinical symptoms appear, it has been suggested that they may become abnormal even 10-20 years before noticeable clinical symptoms. In other hand, biomarkers of neuronal injury and dysfunction are indicative of downstream pathophysiological processes which become dynamic later, with some studies suggesting that it might occur shortly before first symptoms arise. Besides, symptomatology progression closely parallels progressive worsening of neurodegenerative biomarkers [47].

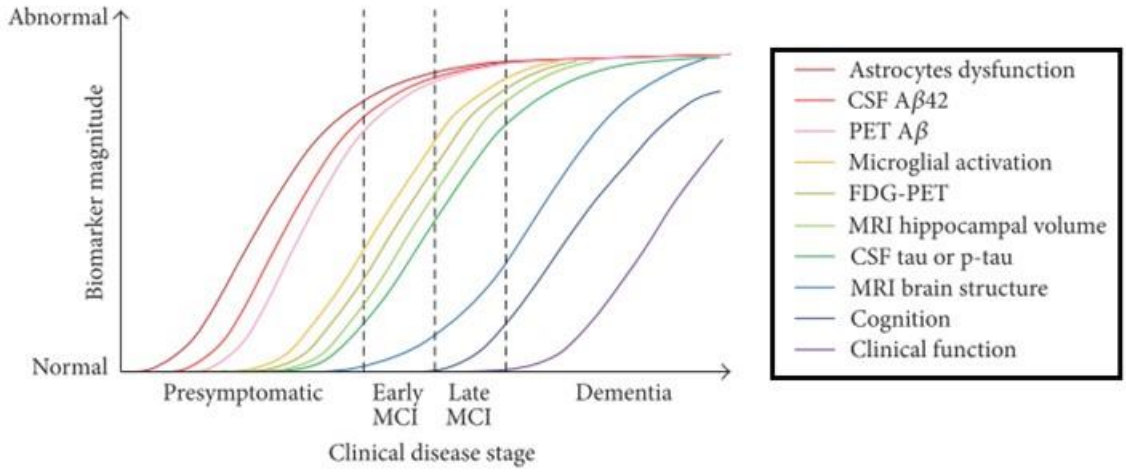

Figure 6|Chronobiological representation of AD biomarkers dynamic according to clinical disease stage progression. Each biomarker is represent by a different colour, correspondence in right board. Adapted from [19].

The temporal lag between AD pathological process appearance and emergence of AD associated clinical syndromes may be influenced by factors such as brain or cognitive reserve, besides aforesaid main risk factors [48].

FDG-PET, tau-CSF and volumetric MRI may be more pertinent biomarkers than Aβ-CSF PET at distinguishing early till late MCI. As cognitive behaviour alterations increase between early and late MCI and further progress during advance AD stage, volumetric MRI remains at present the sole biomarkers measuring differentially those alterations [19].

As aforesaid, in the preclinical phase, biomarkers are used to establish the presence of AD pathophysiology process in research subjects with no or very subtle overt symptoms. According to abovementioned biomarkers pattern (positive for presence and negative for absence of biomarker

alteration/abnormality), preclinical phase can be divided into three different stages (Table 9), currently for research proposes [45,46].

Table 9| Staging categories for preclinical AD research, with an important role of biomarkers. Adapted from [48].

Stage	Description	Aβ (PET/CSF)	Tau, sMRI, FDG-PET	Subtle cognitive change
Stage 1	Asymptomatic cerebral amyloidosis	+	-	-
Stage 2	Stage 1 + "downstream" neurodegeneration	+	+	-
Stage 3	Stage 2 + subtle cognitive/behavioural decline	+	+	+

sMRI: structural magnetic resonance

In MCI phase, biomarkers are used to establish the underlying etiology responsible for the clinical deficit. Besides biomarker severity, particularly neuronal injury biomarkers, indicates likelihood of imminent progression to AD dementia. In turn, at dementia phase, biomarkers are used as an attempt to increase certainty level that AD pathological process underlies the presented dementia [47].

7.2. Fluid AD biomarkers and further challenges

7.2.1.CSF biomarkers

CSF may be considered an ideal source for viable AD biomarkers, since it is in intimate contact with cerebral tissue and pathological brain alterations are often reflected in CSF. The obtained pattern of CSF concentrations of $A\beta_{42}$, total tau and phosphorylated tau in AD is commonly known as the "AD signature" in CSF (Table 10), which has good diagnostic accuracy to distinguish between normal aging and AD (>85%) and a predictive value (>90%) to determine dementia outcome in MCI patients. However, this predictive value becomes lower as patients get older, and its sensitivity/specificity is significantly lower at differentiate AD from other dementias (especially total tau whose increase is frequently observed in other diseases). The rates of change in total tau/$A\beta_{42}$ and p-tau/$A\beta_{42}$ ratios are considered more powerful predictors, rather than one of these measurements alone [47,48].

Table 10|Levels of core AD biomarkers in CSF. Adapted from [49].

[CSF] (pg/mL)	Reference range	AD
$A\beta_{42}$	> 550	365-535
total tau	<375	419-860
p-tau	<52	63-112

ELISA is one of the most common assays for measuring CSF concentration of these three core AD biomarkers. Besides $A\beta_{42}$ form, it is also possible ELISA measurement of truncated $A\beta_{42}$ fragments; all tau isoforms are detected, independently of phosphorylation state; most common measured p-tau are that is phosphorylated at residue 181 or 231. It has been developed multiparameter platforms based on xMAP® technology for simultaneous measurement of these biomarkers, however there are some drawbacks associated with these assays [48,49].

Besides from diagnosis, CSF biomarkers may be used for prognosis, assessing disease progression, developing treatments, monitoring treatment effects and studying disease mechanisms. Several analytes related to Aβ have been investigated as potential AD biomarkers, such as BACE1, sAPPα/sAPPβ and Aβ oligomers. It is though that these oligomers might be more toxic than fibrillar Aβ aggregates, they are able of inhibit hippocampal long-term potentiation and cause abnormal tau phosphorylation and neuritic dystrophy [50]. Recently it was developed a new technique, protein misfolding cyclic amplification assay (Aβ-PMCA), which allows detection of as little as 3 fmol of Aβ oligomers in CSF. This provides the proof-of principle basis for developing a highly sensitive and specific biochemical test for AD diagnosis, not only for Aβ oligomers detection in CSF, since detecting Aβ oligomers that may potentially be circulating in blood of AD patients might offer a great opportunity for more-routine testing [51].

There are several other interesting candidate CSF biomarkers associated to inflammatory response in AD, influence of cholesterol metabolism in pathological process, and endosomal vesicle recycling in affecting neurons [50].

7.2.2. Blood biomarkers

Although CSF represents the most suitable biological fluid to study neurodegenerative diseases since it can reflect the biochemical changes occurring in brain, its analysis is not always easily feasible for a large scale screening, because of the huge economic costs and procedures that are invasive, uncomfortable and not without risk. Thus, for a full screening and early diagnosis, biomarkers easily detectable in biological samples, such as plasma, are needed. Blood-based

biomarkers are minimally invasive and could increase diagnostic accuracy, be useful for prognosis and in monitoring therapeutic interventions [46].

Several biomarkers based on plasma proteins have been investigate through multiplex or proteomics approaches. None have yet been tested in phase 3 trials, but promising findings have been reported for complement factor H, alpha-2-macroglobulin and clusterin [7].

The valosin-containing protein (p97) is an ubiquitin-dependent ATPase with central role in ubiquitin proteasome system (UPS)-mediated protein degradation pathways. The p97 cleavage by caspase-6 (Casp6), which is a putative effector of AD neurodegeneration, has been related to UPS impairment. Indeed, Casp6 activation positively correlates with cognitive decline in aged individuals and occurs at all AD stages. It is thought that Casp6 may exacerbate ubiquitinated proteins accumulation through proteolytic processing of p97 [52]. Moreover, p97 soluble form has been suggested to be increased in blood of AD patients, although further studies are needed to confirm p97 as a reliable marker of AD [53].

It is important to note that only small hydrophobic, lipophilic molecules are more easily transported from CSF into blood, through BBB. This implies that the most relevant markers will be in low abundance in plasma, at least in normal healthy people. Nevertheless, there is increasing evidence for a compromised BBB in neurodegeneration, which will impact on the type of molecules leaking out of brain into blood circulation [2].

7.2.3. Main challenges for AD biomarkers research and development

Peripheral sources of biomarkers (plasma, serum, urine and saliva) present considerable advantages, such as easier collection, cheaper proceeding and repeated samplings can be performed for regular monitoring. However, these sources are further away from the brain. This implies peripheral markers will need to be correlated with accepted markers of AD pathology (observed in brain and CSF), to demonstrate that they reflect AD pathology [2]. Besides, these markers need to be determined as to whether they can be influenced by other organ systems, since AD patients also typically present comorbidities due to aging [54].

Besides all the potentiality of fluid biomarkers, there are some associated limitations, mainly the lack of anatomical precision in measurements and the lack of assay standardization. Thus, extensive standardization of every aspect of biomarkers analysis is now being addressed through initiation of an international quality-control program, which includes CSF reference materials and in the European Joint Programming project “Biomarkers for Alzheimer’s disease and Parkinson’s disease” (BIOMARKAPD) [48,49]. Besides, work to validation of both fluid-based and imaging biomarker thresholds is ingoing [48].

Other challenge for biomarkers research is the substantial overlap of major brain pathologies. Thus, a better understanding of how combinations of pathologies affect changes in biomarkers is needed [7]. Indeed, powerful and innovative bioinformatics tolls are be needed to unravel multivariate plasma AD signatures [2].

8. STRATEGIES FOR BIOMARKERS RESEARCH IN NEUROLOGICAL PATHOLOGY

Up to now, most of efforts in discovering new AD biomarkers have focused on measuring changes either directly in the brain or in cerebrospinal fluid (CSF). Although both PET and CSF analyses are very promising AD markers with potential for clinic application, they are respectively costly and sparsely available or evolve invasive procedures, besides neither is amenable to repeated sampling that is an important aspect of a biomarker's role and utility. Besides, these markers have not yet been shown to adequately predict early diagnosis or disease progression [2].

In the past decade, genomics has been used on identifying susceptibility AD factors. However, while risk genetic traits are important for identification they cannot be markers of disease state. Thus, for a true state marker other "omics" are needed, namely proteomics (related to protein translation, inclusive post-translational modifications), transcriptomics (measurement of mRNA levels for quantifying gene expression) or metabolomics (identification and/or quantitation of metabolites in a given biological sample) [2,55].

Biomarker discovery tends to take one of two options: target approach, which is hypothesis based and designed to investigate a specific molecule or group of molecules; nontargeted approach, using an unknown hypothesis and designed to analyse a large number of molecules in an unbiased manner. Within targeted approaches, commonly used techniques are nuclear magnetic resonance (NMR) and MRS, multiple mass spectrometry (MS)-based methods, and immunoassays (e.g. ELISA). Since there is an increasing trend for biological samples to be analysed without a specific target molecule, within nontargeted approaches metabonomics and metabolomics fields have been expanding, as it seen ahead. Besides, nontargeted approaches improved analytical equipment and data models make these a valuable alternative [56].

Proteomic technologies introduced the concept of a blood signature, arguing that a combination of plasma biomarkers (i.e. a signature) rather than a single marker will be needed to reflect the complexity of AD pathology [2]. Besides, proteomics has garnered recent attention mainly because proteins are readily available in body fluids and are more stable than mRNA and metabolites. This “omic” studies both structure and function of proteins by several methods, whether qualitative or

quantitative, allowing to reveal static or perturbation-induced changes in a protein profile [54]. Proteomics provides an unbiased approach to detecting protein biomarkers in complex sample mixtures such as plasma. It uses MS data coupled with protein database pattern recognition search algorithms to identify large numbers of proteins simultaneously. One of the most powerful protein identification strategies is liquid chromatography (LC) separation followed by MS analysis, usually ESI (electrospray ionization). Few studies have used proteomic methods to new AD plasma biomarkers discovery, making neuroproteomics an emerging technology. The plasma proteins that have been identified by these techniques are related with lipid or other molecules transportation, immune regulation and inflammation [57].

Moreover, it has been developed a new field called peptidomics, a proteomics analysis of peptides and small proteins, since proteins can be cleaved aberrantly (e.g. APP cleavage by α and β-secretases) direct de novo analysis of endogenous peptides could be invaluable for disease diagnosis [54].

8.1. Metabolomics approaches in biomarker identification

Although still a relatively nascent field, metabolomics is being developed and applied as a more global approach to neurodegenerative disorders biomarkers discovery. Metabolomics is now commonly defined as the detection and quantitation of all low-molecular-weight molecules and metabolites present in cells, tissues or organisms under a set of given conditions. Thus, it is able of quantify metabolite changes indicative of alterations in anabolic and catabolic processes in a given individual. In turn, metabonomics is described as the quantitative analysis of metabolic response of living systems to pathophysiological stimuli or genetic modification over time [2,55].

The metabolome is the collection of small molecules that are found within a biological system and whose identities, concentrations and fluxes are the final product of interactions between gene and protein expression, and the cellular environment. Thus, metabolomics information complements the obtained data from genomics, transcriptomics and proteomics [58].

Metabolomic techniques have been used to identify biochemical pathways perturbations related to several diseases, either in biological fluids (plasma, urine and CSF), animal models, and tissue or cell cultures [58]. Recently, several metabolic diseases such as diabetes, dyslipidaemia and hypertension have been associated with AD and progression of MCI to dementia phase. Additionally, several metabolic enzymes of the glycolytic, tricarboxylic and acid cycle and oxidative phosphorylation pathways are known to be impaired in AD, and pharmacological inhibition of metabolism further exacerbates AD pathology. Therefore, metabolic dysfunctions identification

using an unbiased metabolomics approach could provide a more comprehensive picture of the pathways involved in AD [26].

A typical metabolomics study includes four main steps: uniform sample collection, sample analysis (e.g. NMR, MS), statistical analysis (e.g. PCA, PLS-DA), and identification of significantly altered metabolites that could be translated into new disease biomarkers/pathways [26]. The main metabolic fingerprinting approaches used for disease diagnostics includes infrared and Raman spectroscopy, NMR and MS-based methods. Hence the multiple advantages and more widespread use of infrared spectroscopy, its role in metabolomics will be emphasized ahead [55].

One of the main metabolomics challenges is the development of standard protocols regarding sample collection and storage, chemical analyses, data processing, and information exchange. Indeed, it was already created the Metabolomics Standard Initiative (MSI), with support of the Metabolomic Society, to recommend standard protocols for use in all aspects of metabolomic research [58].

8.2. Potential of FTIR spectroscopy as metabolomics research tool

Fourier transform infrared (FTIR) spectroscopy has a significant and ongoing history of research into its potential as a diagnostic tool and allows for the extremely rapid, high-throughput and non-destructive analysis of a wide range of sample types. It uses vibration frequencies of molecules present in the analysed sample to produce a metabolic fingerprint, which is then specific for each sample. In terms of disease diagnosis, much of the work undertaken has concentrated on the mid-infrared (IR) region of electromagnetic spectrum (from 4000-600 cm^{-1} of wavelength). Although FTIR has been recognized as not as specific and sensitive as some of the MS-based techniques, the rapidity and reproducibility of FTIR is demonstrable through the extensive number of published research using this technology. Besides, it has been recognized as a valuable tool for metabolic fingerprinting as it is able to analyse carbohydrates, amino acids, fatty acids, lipids, proteins, nucleic acids and polysaccharides simultaneously with a minimum amount of sample preparation. Indeed, besides its rapidity (<10 seconds per sample is readily achievable), FTIR is an ideal candidate technology for high-throughput screening as it is possible to measure thousands of samples per day and obtain information-rich spectra using as little as 0,5 µl of sample. Also, FTIR is less expensive and more accurate rather other methods [55,59].

FTIR has been used in several pathology research fields besides neurodegenerative diseases, including oncology. Indeed, FTIR has been identified as an emergent technology in cervical cancer screening, and at differentiation between benign and malignant prostatic epithelium (i.e.

differentiate BPH from prostatic cancer). Besides, further studies have been undertaken on a range of cancers including breast, brain, bladder, thyroid tumours, colorectal adenocarcinoma sections, larynx, oesophagus and gastric cancer [55].

9. SIGNIFICANCE OF THE STUDY

AD is the most common and debilitating neurodegenerative disease among older population, with number of worldwide affected people prone to rise significantly giving the higher population aging. With no sufficiently accurate diagnosis in an earlier disease stage, nor either a disease-modifying therapy available, AD severely affects daily living of patients and their relatives. Besides the dramatic human suffering and loss, AD translates in a huge economic burden for countries health systems. Thus, it is sorely needed a simple, accurate and cost-effective early AD diagnosis in order to treat and even prevent first signs of disease, with introduction of reliable therapeutic approaches.

Hence, the main aims of this study pass through FTIR analysis of plasma samples, from both healthy (control) and putative AD (disease) subjects; identification of the main metabolic characteristics present in obtained FTIR spectra, inquiring if they could be related to AD pathology; differentiation of samples in groups (e.g. control vs AD) through data multivariate analysis, allowing not only to compare between groups but also to compare between samples of the same group; and identification of the more significant altered metabolites and their eventual role at the disease context.

CHAPTER 2

1. FTIR METHOD OVERVIEW

1.1. Fundamental principles

Fourier transform infrared spectroscopy (FTIR) is a type of infrared (IR) spectroscopy, and it constitutes the absorption measurement of different IR frequencies by a sample positioned in the path of an IR beam, some of this radiation is absorbed by the sample and some of it is passed through (transmitted). The resulting spectrum represents molecular absorption and transmission, creating a molecular fingerprinting of the analysed sample. In spectrum, absorption peaks correspond to the frequencies of vibrations of sample chemical bonds, allowing to identify sample functional groups and/or elucidate molecular structure (qualitative analysis); besides, the size of these peaks is correlated with the amount of each functional group (quantitative analysis). Through utilization of several sampling accessories, IR spectrometers are able to analyse a wide range of sample types such as gases, liquids and solids [60,61].

IR spectral region (Figure 7) ranges from the red end of visible spectrum at 780 nm (12820 cm^{-1} of wavenumber) to the onset of microwave region at a wavelength of 1 mm (10 cm^{-1}). In turn, IR range is further subdivided into the near-infrared (NIR), mid-infrared (MIR) and far-infrared (FIR) regions. MIR covers the range 4000-400 cm^{-1} and is the region that usually provides the fingerprint characteristics of molecular species. Besides, MIR includes the rich absorptions spectrum corresponding to fundamental vibrations of the species being probed. MIR absorption positions are reported in units of wavenumbers (cm^{-1}, the inverse of wavelengths in centimetres) [62].

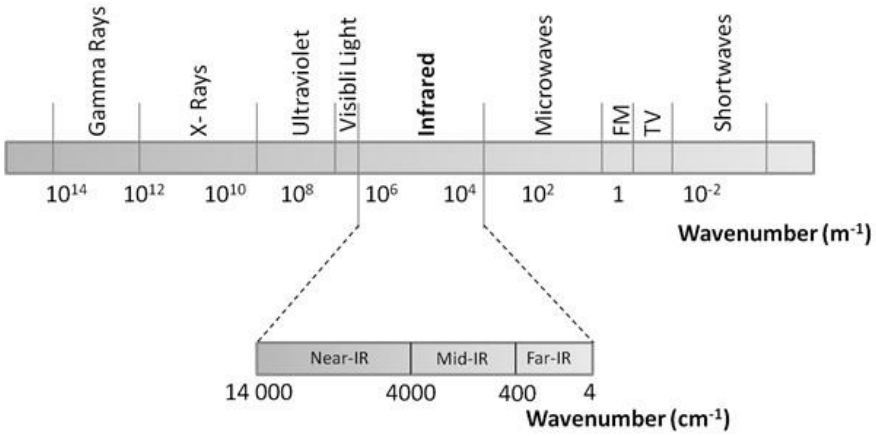

Figure 7| The electromagnetic spectrum, with IR region magnified. Adapted from [63,64].

1.2. Vibration of molecules

The energy possessed by a molecule at any given moment is defined as the sum of contributing energy terms: translational energy, related to the molecules displacement in space as a function of normal thermal motions of matter; rotational energy, the tumbling motion of a molecule which results from the energy absorption within the microwave region; vibrational energy, which is a higher energy term and corresponds to the energy absorption by a molecule as the component atoms vibrate about the mean centre of their chemical bonds; electronic energy, which is linked to energy transitions of electrons as they are distributed throughout the molecule [65]. IR radiation does not have enough energy to induce electronic transitions as seen with ultraviolet (UV) radiation. Absorption of IR is restricted to compounds with small energy differences in the possible vibrational and rotational states. The fundamental requirement for IR activity and consequent IR absorption by molecules is that vibrations or rotations within a molecule must cause a net change in the molecule dipole moment. It is known that the alternating electrical field of radiation interacts with fluctuations in the molecular dipole moment. If radiation frequency matches vibrational frequency of the molecule then radiation will be absorbed, leading to a change in molecular vibration amplitude [66]. In general, the larger the dipole change, the stronger the band intensity in the IR spectrum [67].

Rotational transitions are of little use to posterior FTIR spectrum interpretation. Rotational levels are quantized and IR absorption by gases yields line spectra; however, in liquids or solids, these lines broaden into a continuum due to molecular collisions and other interactions [66].

Each atom has three degrees of freedom, corresponding to motions along any of the Cartesian coordinate axes (x, y, z), thus a polyatomic molecule of n atoms has 3n total degrees of freedom. Nevertheless, 3 degrees of freedom are required to describe translation, and other 3 correspond to rotation of the entire molecule. Thus, the remaining 3n-6 degrees of freedom are fundamental vibrations for nonlinear molecules, while linear molecules possess 3n-5 fundamental vibrational modes since only 2 degrees of freedom are sufficient to describe rotation. Among the 3n-6 or 3n-5 fundamental vibrations, also known as normal vibration modes, those that produce a net change in the dipole moment may result in an IR activity and those that give polarizability changes may give rise to Raman activity. Indeed, some vibrations can be both IR and Raman active [61].

Therefore, atomic positions in molecules are not fixed, since they are subject to several vibrations. The major types of molecular vibrations (Figure 8) are stretching, change in inter-atomic distance along bond axis; and bending, change in angle between two bonds, that present four different types

(i.e. rocking, scissoring, wagging and twisting) [66]. Bending vibrations occur at lower frequencies than corresponding stretching vibrations [67].

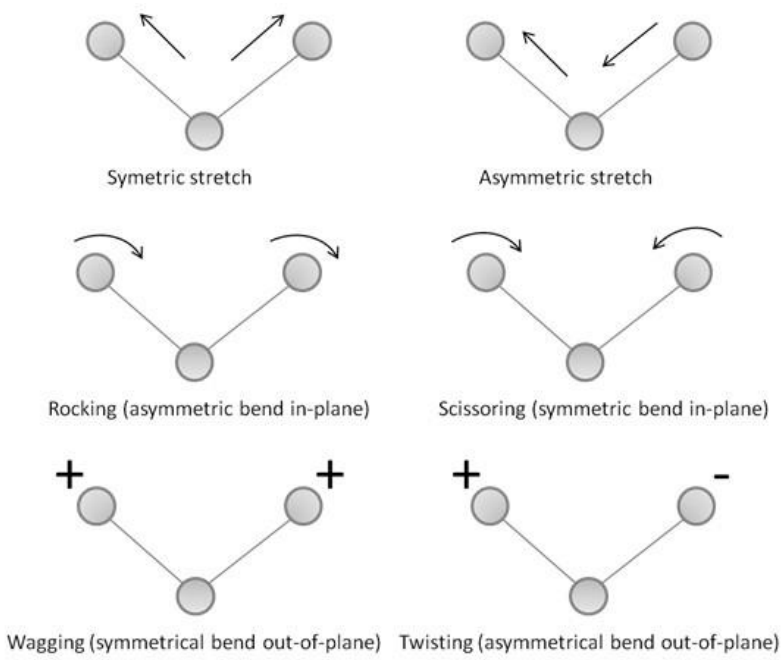

Figure 8| The different vibrational modes of molecules, divided on stretching type (upper line) and on bending type (central and lower lines). Adapted from [68].

Besides the aforesaid vibrations types, interaction between vibrations (coupling) can occur if vibrating bonds are joined to a single and central atom. In this turn, vibrational coupling is influenced by several factors:

- ✓ Strong coupling of stretching vibrations occurs when there is a common atom between two vibrating bonds;
- ✓ Bending vibrations coupling occurs if there is a common bond between vibrating groups;
- ✓ Coupling between a stretching vibration and a bending vibration occurs if the stretching bond is one side of an angle varied by bending vibration;
- ✓ Greatest coupling takes place when coupled groups have roughly equal energies;
- ✓ There is no coupling between groups separated by two or more bonds [66].

1.3. FTIR equipment and functioning

There are three basic FTIR spectrometer components: radiation source, interferometer and detector. Besides, an FTIR analysis can be divided in 5 steps (Figure 9) [60,61].

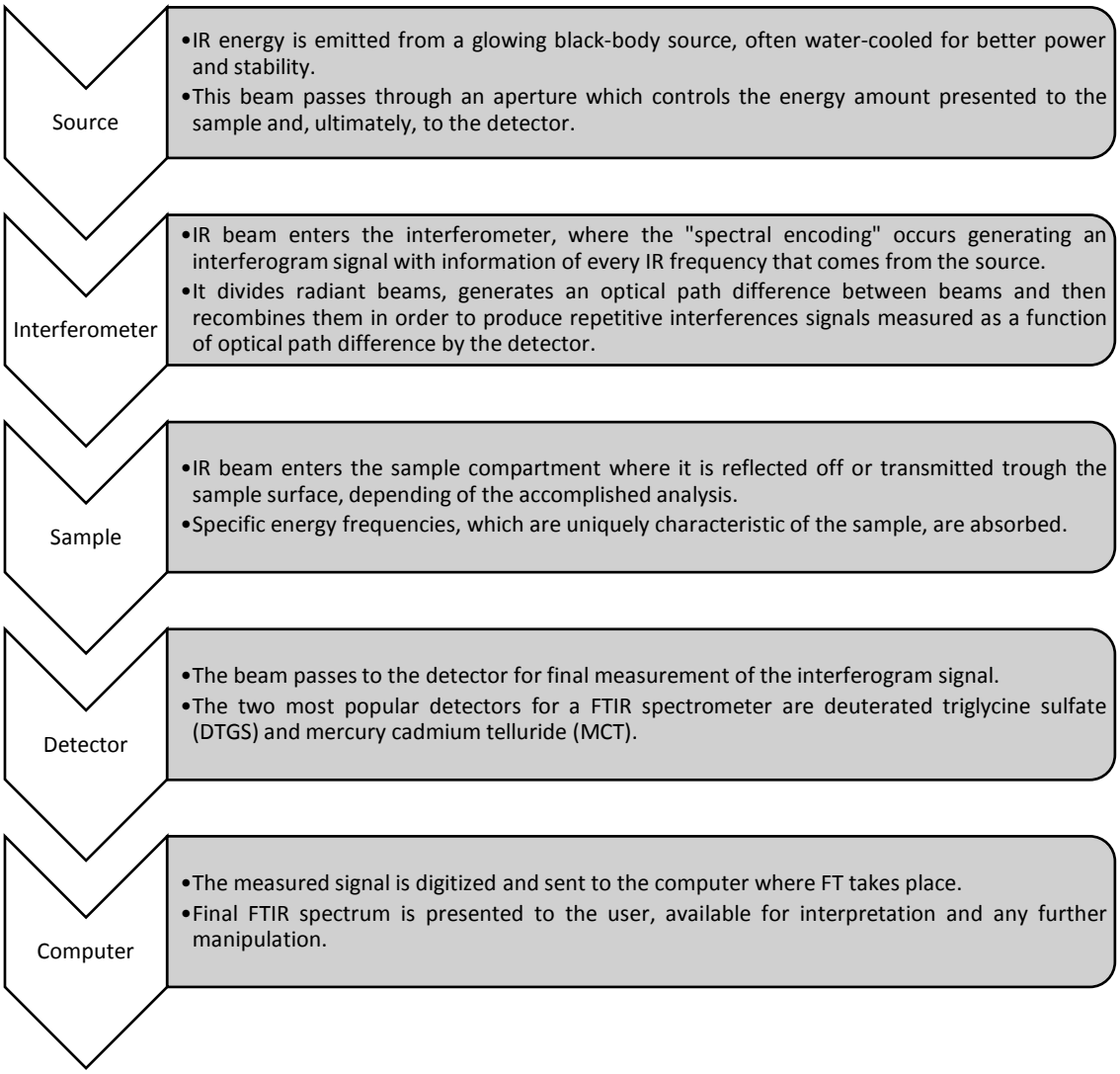

Figure 9| Main steps of FTIR process, presenting prime roles of the three basic spectrometer components.

Michelson interferometer (Figure 10) is the most commonly used and it consists of three active components: moving mirror, fixed mirror and beamsplitter. These two mirrors are perpendicular to each other, while the beamsplitter is a semireflecting device often made by depositing a thin germanium film onto a flat KBr substrate. Radiation from the broadband IR source is collimated and directed into the interferometer and impinges on the beamsplitter, where half the IR beam is transmitted to the fixed mirror and the remaining half is reflected to the moving mirror. After reflection of divided beams from the two mirrors, they are recombined at the beamsplitter.

Changes in the relative position of the moving mirror to the fixed mirror generate an interference pattern. The resulting beam then passes through the sample and is eventually focused on detector [61].

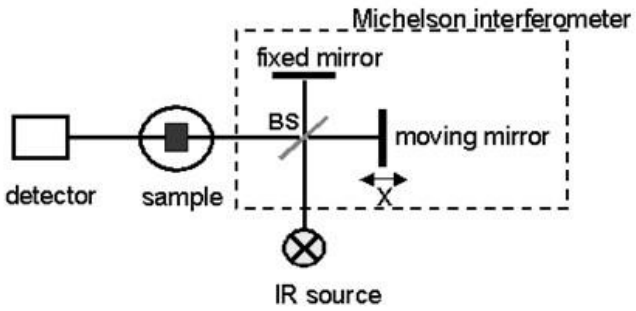

Figure 10|Schematic representation of a FTIR spectrometer, showing their main compartments. BS: beamsplitter; X: relative position variation of moving mirror [69].

Since interferogram present every data point, as a time domain spectrum that records detector response changes versus time within the mirror scan, all frequencies are measured simultaneously, thus resulting in extremely fast IR measurements. This interferogram signal cannot be interpreted directly, because it is required a frequency spectrum (plot of intensity at each individual frequency) in order to make an identification. Therefore, a mathematical technique called Fourier transformation (FT) is performed by the computer so as to "decoding" individual frequencies, converting interferogram to the final IR spectrum, which is the familiar frequency domain spectrum showing intensity versus frequency [60,61].

A background spectrum must also be measured, since it is needed to have a relative scale for absorption intensity. This is a measurement with no sample in the beam, generating a spectrum without any instrumental characteristic. Thus, all present spectral features are strictly due to the sample [60].

1.3.1. Golden Gate™ Diamond ATR

The technique of attenuated total reflectance (ATR) has been revolutionized solid and liquid sample FTIR analyses, since it combats the most challenging aspects of IR analyses, namely sample preparation and spectral reproducibility. Besides their complexity, sample preparation methods can be very messy, time consuming and further complicated by fragility and hydroscopic nature of the involved materials. In turn, ATR requires little or no sample preparation for most samples (high

sample throughput). It is especially useful for IR analyses of difficult sample that cannot be readily examined by the normal transmission method, being this technique suitable for studying thick or highly absorbing solid and liquid materials, including films, coatings, powders, threads, adhesives, polymers and aqueous samples. Therefore, ATR technique provides faster sampling, improves sample-to-sample reproducibility and minimize user to user spectral variation [61,70,71].

An ATR accessory (Figure 11) measures the occurred changes in a totally internally reflected IR beam when the beam comes into contact with a sample. The IR beam is directed onto an optically dense crystal with high refractive index at a certain angle, and internally reflected through the crystal with a single or multiple reflections, with both reflections number and penetration depth decrease with increasing incidence angle. This internal reflectance creates an evanescent wave that extends a few microns (0,5µ– 5µ) beyond the crystal surface into the sample held in contact with crystal (Figure 11). In regions of IR spectrum where the sample absorbs energy, the evanescent wave will be attenuated or altered, with attenuated energy of each wave being passed back to the IR beam, which then exits the opposite end of crystal and is passed to the spectrometer detector. Thus, for this technique to be successful, it is required a direct contact between sample and ATR crystal, and that crystal refractive index is significantly greater than that of the sample or else internal reflectance will not occur – the light will be transmitted rather than internally reflected in the crystal [61,70].

There are several crystal materials available for ATR, with zinc selenide (ZnSe) and germanium being the most common used for HATR (horizontal ATR, in which the crystal is a parallel-sided plate, typically about 5 cm by 1 cm, with the upper surface exposed). Nevertheless, diamond is by far the best ATR crystal material because of its robustness and durability [70].

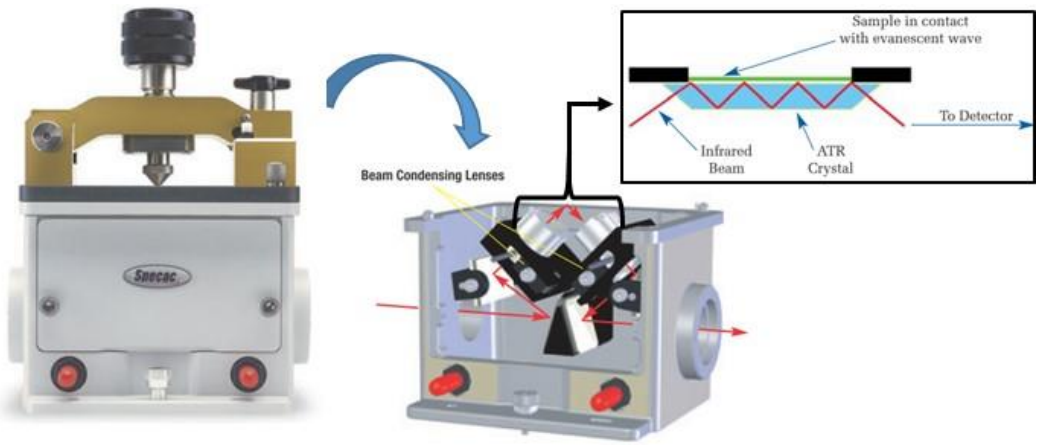

Figure 11|Golden Gate™ Diamond ATR instrument, showing its single internal reflection system (central and right picture). Note the evanescent wave formation under the diamond crystal (right picture). Adapted from [70,71].

In liquids analyses, after cleaning the crystal and collecting an IR background, sample is simply poured onto the crystal, which must be whole covered if performing a quantitative or qualitative analysis. Crystal is recessed into the metal plate to retain sample [70].

ATR improved spectral acquisition and reproducibility leads to better quality database building, for more precise material verification and identification. This makes of ATR an extremely robust and reliable technique for quantitative studies involving liquids. Besides it is one of the most versatile sampling techniques [61,70].

1.4. FTIR advantages

Major advantages of FTIR over the traditional dispersive technique include:

- Speed: since all frequencies are measured simultaneously, it mostly takes seconds (known as Felgett Advantage);
- Sensitivity: dramatically improved with FTIR, since detectors employed are much more sensitive and optical throughput is much higher (Jacquinot Advantage), which results in lower noise levels; besides fast scans enable coaddition of several scans in order to reduce random measurement noise to any desired level (signal averaging);
- Mechanical Simplicity: the interferometer moving mirror is the only continuously moving part in FTIR instrument, so there is little possibility of mechanical breakdown;
- Internally Calibrated: FTIR instruments employ a HeNe laser as an internal wavelength calibration standard (Connes Advantages), which make them self-calibrating [60].

1.5. MIR spectroscopy applied to biological samples

Clinical and diagnostic applications of MIR spectroscopy have been one of the most active areas of research and development since the 1990s [72]. IR spectra of cells, tissues and biofluids are the sum expression of cellular chemistry/biochemistry and give a snapshot on cell division, differentiation, growth and metabolism. Besides physiological characterization, IR spectra may report the response of biological entities to environmental stress, which makes of biological IR spectroscopy a "phenotypic" and explorative analysis modality that can be used into diagnoses of disease or dysfunction in cells, tissues and biofluids via "spectral fingerprints". It also may change in response to drug intervention, environmental stress or genetic modifications [73].

Biological fluids such as plasma, serum, synovial fluid and amniotic fluid, are routinely analysed in clinical chemistry since these fluids can easily be isolated from the body [73].

1.5.1. FTIR at blood-based samples analysis

FTIR plays critical role at diagnosing and monitoring a wide variety of disorders. The classification of disease-related spectral pattern has also been called "diagnostic pattern recognition" (DPR), whose concept has been successfully applied in the last decade to establish diagnostic MIR based blood analysis, or serum assays for diagnosis of DM, metabolic syndrome, rheumatoid arthritis and transmissible spongiform encephalopathies [62,73]. It was already well demonstrated how the information-rich MIR spectra may be used to estimate clinically important blood analytes such as glucose, proteins, cholesterol, urea, triglycerides, and uric acid when measured in plasma [74].

Since each biomolecule exhibit a unique FTIR spectrum, representing the vibrations of its structural bonds, a plasma FTIR spectrum exhibit absorption peaks related to its major components [62,74]. Proteins are the major component of plasma, with albumin representing 65% of plasma proteins and 45% of total plasma mass. The spectral contribution of albumin (4000 – 500 cm^{-1}) represents 39,9% of total plasma FTIR spectral area. Thus, it is not surprising that after spectra subtraction of 20 biomolecules, the mean total spectral area of the remaining spectrum corresponds to 24,2% of the initial plasma FTIR spectral area. Indeed, in the FTIR spectra of complex biological samples such as plasma, the absorption spectra of the more abundant biomolecules may first be subtracted to uncover other absorption patterns [75]. Nevertheless, since that in the present study it is used a metabolomics approach, this subtraction method could eventually lead to a significant signal loss, especially of some lower weight metabolites, and thus it will not be applied in the current study.

In order to obtain plasma, an anticoagulant like EDTA or heparin is added to full blood previous collected, following by removal of blood cells. There is a good reproducibility of metabolite concentrations in plasma, which may result from the simple collecting procedure for plasma, as it does not require time to coagulate [76]. Removal of cellular component from blood, in order to obtain plasma, allows to exclude perturbations of the chemical analysis or to ensure that blood cells metabolism does not falsify metabolite concentration values. This latter point is particularly important for glucose identification, since its concentration begins to decrease immediately after sampling because of the glycolytic action of erythrocytes and leucocytes [77].

It is important to note that water is the most abundant compound of all biological fluids, which is reflected in IR spectra [62]. Following in this chapter some methodologies are presented in order to circumvent this water signal overlap within IR spectra.

2. FTIR EXPERIMENTAL OPTIMIZATION

FTIR acquisition methodology has been already optimized in a pilot exploratory study occurred last year [78]. Thus, at the present study it was implemented the same optimized methodology.

2.1. Sample collection

In order to optimize acquisition methodology and to overcome water signals overlap, it was used a blood sample from an apparently healthy elderly that belongs to a project approved by ethics committee of the Regional Health Centre - Coimbra, protocol number 012 804 of April 4, 2012. All blood samples of this project were received in proper time after its collection, and pre-processing was performed immediately [78].

From each sample were prepared plasma aliquots: it was used tubes K2 EDTA 5 mL with gel separator and then it was applied a centrifugal force of 1800g during 15 minutes at 8ºC, wherein blood cells were separated from plasma. The obtained plasma was transferred and resuspended in a 5 mL tube. For the present study, were performed plasma aliquots of 30 µL, which were stored at -80ºC [78].

2.2. FTIR spectral acquisition

Plasma samples were thawed at room temperature and homogenized with vortex for around 8 seconds, immediately before spectroscopic analysis. Spectra were acquired with Perkin-Elmer Spectrum BX FT-IR™ spectrometer in the range of 4000-600 cm^{-1}, at resolution of 8 cm^{-1}, with 64 co-added scans. During acquisition, room temperature and humidity were kept at ± 23ºC and ± 39%, respectively.

For spectral acquisition using drying process the attainment of background single beam was performed against air (empty crystal). Then, 8 µL of plasma were placed on the ATR diamond crystal. Drying time was achieved and established after approximately 40 minutes, which corresponds to 16 consecutive spectra acquisition.

2.2.1. Drying process

It was demonstrated, for each sample, that 40 minutes of drying time allows to obtain a spectrum with more spectroscopic information and enhanced signal-to-noise ratio (SNR) whose peaks can be assigned, enabling a qualitative analysis of the sample. It was additionally made a comparison of different methods for minimize water signals of samples, included drying process, arithmetic subtraction of water spectrum to the plasma spectra, and a third method that uses pure water in

the background single beam acquisition which is later used to make the ratio with sample single beam. Apart from the apparent less subjectivity, drying process, even time consuming, requires less computational manipulations and was shown to be capable of eliminate water spectral contribution, maintaining a reasonable SNR [78].

Thus, by simply allowing water to evaporate from the sample, while spectra are being acquired, it is possible observe alterations in spectroscopic signals over time, ensuring that the last spectrum obtained reached a constant drying stage. This information is not available by a single spectrum acquisition of the film at the end of drying process [78].

Therefore, drying process was the chosen method for samples acquisition spectra, which are analysed in the follow chapter.

CHAPTER 3

1. METHODS OF STUDY

1.1. Study group

Inclusion criteria for the present study group were: age between 50-90 years, resident in Aveiro region, with complaints including objective memory impairment or other cognitive complains. In other hand, exclusion criteria comprise individuals undergoing chemotherapy or radiotherapy, suffering from psychiatric illness (e.g. bipolar disease, schizophrenia), or using illicit drugs.

Cognitive evaluation of individuals was carried out at several centres for primary health care from Aveiro region, with application of the following cognitive tests: CDR, MMSE and Geriatric Depression Scale (GDS). This latter test allowed exclusion from the study of depressed individuals.

The project was approved by the ethics committee of the Regional Health Centre - Coimbra, protocol number 012 804 of April 4, 2012.

According to cognitive evaluation, 45 individuals were subdivided in 3 groups: the age and sex matched control group, presenting negative result for all the 3 cognitive tests; the putative AD group, with a positive result for CDR and MMSE scales but negative for GDS and other neuropathologies; the other neuropathologies group, which includes subjects suffering from other pathologies or mixed disorder and thus also positive on CDR and MMSE scales. It was also reunited other clinical data related to presence of some AD risk factors, namely the manifestation of comorbidities such as DM, dyslipidaemia or hypertension (HTN).

Table 11| Characterization of study samples group according to sex, age and cognitive evaluation.

Sex	Age	Condition	MMSE	CDR	Sex	Age	Condition	MMSE	CDR
F	65	Control	-	-	F	79	Control	-	-
F	81	Control	-	-	F	72	Control	-	-
F	78	Control	-	-	M	80	AD	+	-
F	65	Control	-	-	F	65	AD	+	-
F	72	Control	-	-	F	84	AD	+	+
F	72	Control	-	-	F	74	AD	+	+
F	78	Control	-	-	F	49	AD	+	+
F	73	Control	-	-	M	83	AD	+	+
M	82	Control	-	-	F	74	AD	+	+
F	81	Control	-	-	F	72	AD	+	+
M	74	Control	-	-	M	74	AD	+	+
F	49	Control	-	-	F	78	AD	+	+
F	75	Control	-	-	F	85	AD	+	+
F	84	Control	-	-	F	78	AD	+	+
F	75	Control	-	-	F	76	AD	+	+
M	78	Control	-	-	F	82	AD	+	+
F	75	Control	-	-	F	86	AD	+	+
F	72	Control	-	-	M	80	AD	+	-
F	77	Control	-	-	F	88	AD	+	+
F	75	Control	-	-	F	80	AD	+	+
M	81	Control	-	-	F	76	Other/mixed dementia	+	+
M	82	Control	-	-	F	76	Other/mixed dementia	+	+
F	80	Control	-	-					

1.2. Experimental procedure from blood collection to final results

The blood collection and plasma sample preparation followed the procedure stated in the previous chapter, with application of optimized method for FTIR applied to plasma samples. The spectra were obtained by mid infrared spectroscopy (MIR), being recorded a total of three independent aliquots (replicates) for each sample, and with the spectrometer diamond crystal being carefully cleaned with distilled water between all replicates analyses. This is important for increase confidence of obtained results. Room temperature and humidity values were always controlled and spectra were only acquired when these room conditions were fulfilled.

After spectra acquisition, data underwent multivariate analysis to allow differentiate between disease and control samples, with identification of relevant spectra regions/bands and their corresponding assignments to chemical functional groups and/or compounds families.

1.3. Multivariate data analysis

Apart from several analytical procedures that result in quantitative data, for diagnostic purposes it is important to define some categorical differentiable classes for the obtained data, most

commonly by dividing samples in healthy or disease affected classes. This important area of chemometric data processing is called classification, whose main aims are pattern recognition and discrimination analysis. Univariate analysis methods can consider only a single characteristic of the sample as the dependent variable is in a selected given independent variable. Thus, it is usually necessary to use multivariate pattern recognition methodologies, which allows the evaluation of several sample properties simultaneously [79]. Multivariate analysis uses mathematical, statistical and computer sciences to efficiently extract useful information from data generated via chemical measurements [80].

Multivariate classification techniques can be further divided into two categories: unsupervised and supervised learning procedures. In this first category, it is not required an *a priori* knowledge about training set samples (i.e. the class membership of the training samples), therefore, samples will be grouped into a number of classes with certain communalities without initial qualification of samples and their class assignment. Thereby, even without initial knowledge about the expected differences, structure with certain data sets may be recognized. Examples of unsupervised methods are principal component analysis (PCA) and cluster analysis (CA). In the other hand, supervised pattern recognition requires *a priori* knowledge about the classes contained within the training samples, i.e. which sample belongs to which class (e.g. clearly identifying samples from disease cases vs. samples from healthy subjects). Examples of supervised methods are discriminant analysis (DA) and artificial neural network (ANN) [80, 81].

Hence, unsupervised patter-recognition techniques are exploratory methods for data analysis, which seek inherent similarities of data. Using this method, unexpected grouping within a training sample set that might not be initially evident may be discovered then, e.g. that a group of disease samples might be additionally separated into two or more distinctly different classes [80].

1.4. Main MIR regions of interest for study aims

For biological applications, the MIR region can be divided into spectral windows of interest where strong absorption bands can be directly related to specific components (Figure 12). These spectral regions include: fatty acids region; amide region, ascribed primarily to proteins and peptides; mixed region, ascribed to carboxylic groups of proteins, free amino acids and polysaccharides; and the polysaccharide region. Besides, there are others spectral regions such as the one that is relevant to RNA, DNA and phospholipid content [82].

The 900-600 cm^{-1} region exhibits a variety of weak but extremely characteristic features superimposed on an underlying broad spectral contour. This region may contain weakly expressed

bands arising from aromatic ring vibrations of phenylalanine, tyrosine, tryptophan, and the various nucleotides. Hence valid assignments can hardly to achieve, with the exception of only a few peaks (e.g. a band near 720 cm^{-1}, resulting from CH_2 rocking modes of fatty-acid chains), this spectral domain can be named as to the “true fingerprint region” [83].

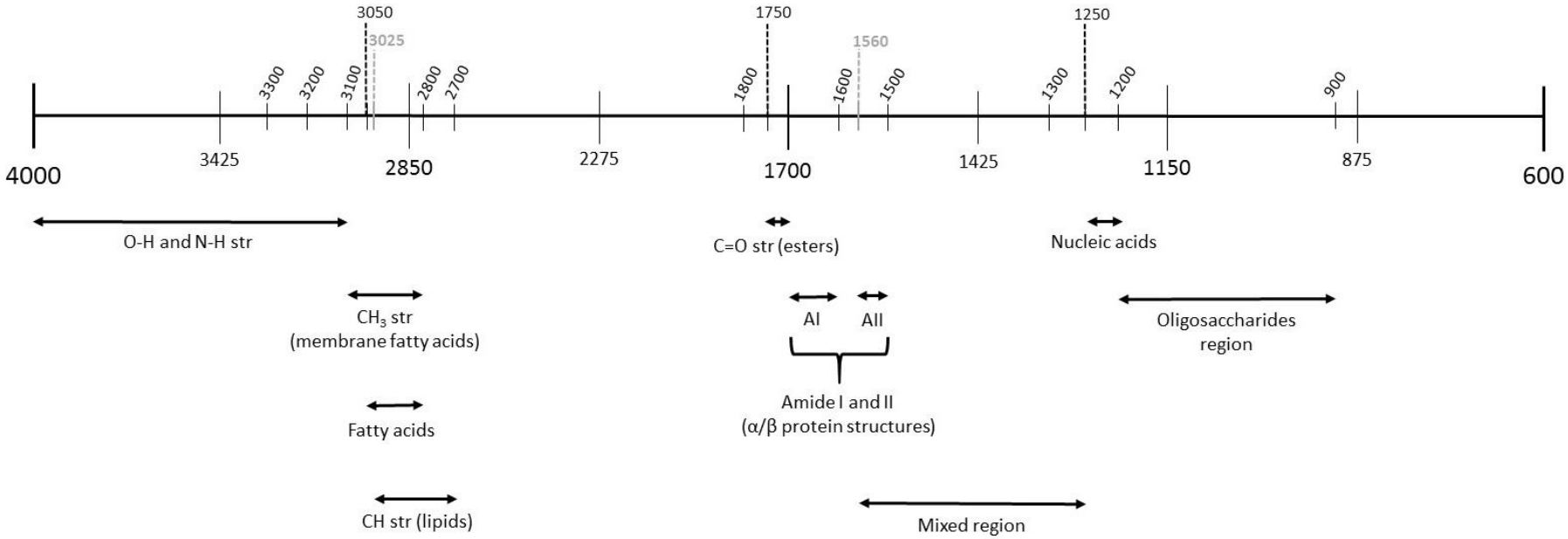

Figure 12| Main regions of FTIR spectra in a range of 4000 – 600 cm^{-1}. The mixed region refers to oligosaccharides, free amino acids and nucleic acids. Str: stretching

2. RESULTS AND DISCUSSION

2.1. Spectral analysis

At this section the obtained spectra is subject of direct analysis with observation of general vibrational/chemical pattern of whole plasma samples (Figure 13), and identification of main maximum wavenumber peaks of the average control and disease samples (Figure 14).

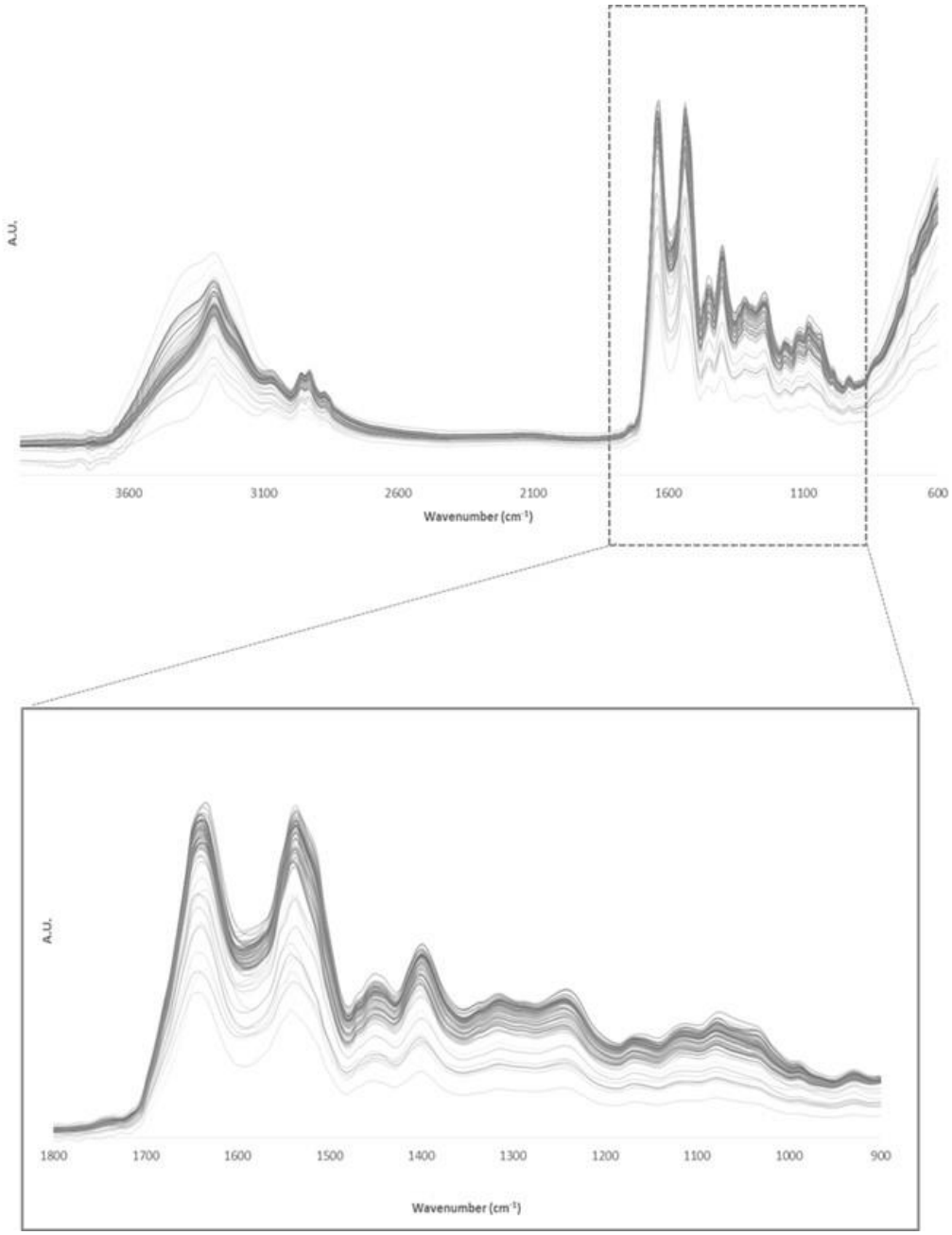

Figure 13| FTIR spectra of all plasma samples that have been used in the present study, in a wavenumber range of 4000 – 600 cm^{-1}. The FTIR spectra region of 1800-900 cm^{-1} has been magnified (down side) for better visualization. X-axis: wavenumber (cm^{-1}); Y-axis: arbitrary units (A.U.)

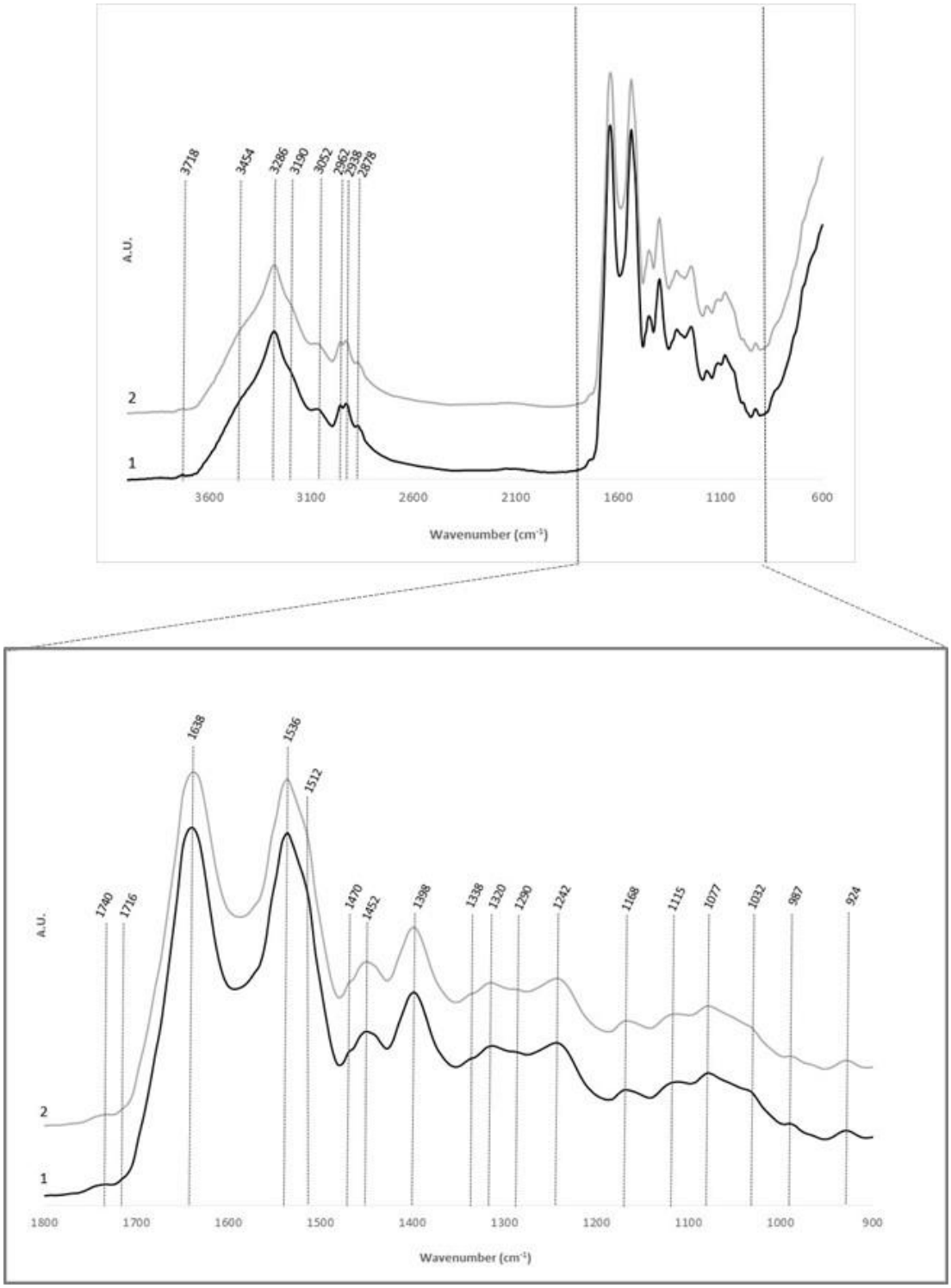

Figure 14|The 4000-600 cm^{-1} FTIR spectral region of two average plasma samples, one of a control subject (black line) and other of an AD subject (grey line), showing maximum wavenumber peaks. The downer picture is a magnification of the 1800-900 cm^{-1} FTIR spectra region acquired from the first spectra, showing maximum wavenumber peaks. X-axis: wavenumber (cm^{-1}); Y-axis: arbitrary units (A.U.)

During direct analysis of FTIR spectra (Figure 14), it was possible to identify the maximum wavenumber peaks at both control and disease samples. Each of these spectral signals have one or more assignment (specific type of molecular vibration), that corresponds to a certain chemical group and/or chemical family of compounds. This correspondence allows to establish a specific chemical pattern of plasma samples, with identification of the main chemical components (Table 12).

Table 12| Maximum wavenumber peaks founded in FTIR spectra and its main assignments and correspondents plasma contents.

Peaks (cm^{-1})	**Assignments**	**Plasma contents**	**Ref.**
≈ 3718	O-H stretching and an intermolecular vibration of CO_2 and phenol**	Presence of gaseous CO_2	[84]
≈ 3454	N-H stretching	Proteins (amide A)	[85]
≈ 3286	N-H stretching, H-O-H symmetric and asymmetric stretching*	Proteins (amide A)	[86,87]
≈ 3190	N-H symmetric stretching	mainly cis-ordered sub-structures	[88]
≈ 3052	N-H stretching	Proteins (amide B)	[88]
≈ 2962	C-H asymmetric stretching of CH_3 group*	Lipid acyl chains in lipid bilayers (phospholipids)	[82,83,86,89]
≈ 2938	C-H stretching of CH_2 and CH_3 group*	Fatty acids	[83,85,86]
≈ 2878	C-H symmetric stretching of CH_3 group*	Lipid acyl chains in lipid bilayers (phospholipids)	[82,83,86,89]
≈ 1740	C=O stretching	Fatty acid esters (triglycerides), lipid bilayers (phospholipids)	[79,82,86]
≈ 1716	C=O stretching	Carbonic acid, phospholipid sub-structures, purine bases from nucleic acids	[79,83,86,90]
≈ 1638	C=O stretching*; NH_3^+ asymmetric in plane bending (rocking)*	Proteins (amide I for β-sheet); Membrane lipids (phospholipids)	[83,86,89,91]
≈ 1536	N-H bending in plane, C-N stretching*	Proteins (amide II)	[83,86,87]
≈ 1512	CC (phenyl ring) stretching, CH in plane bending*	tyrosine band (proteins side chain)	[83,86,92]
≈ 1470	CH_2 bending; C-H asymmetric bending; CH_2 symmetric in plane bending (scissoring)*	Proteins; Carbohydrates; Lipid acyl chains in lipid bilayers (phospholipids)	[79,83,88,89]
≈ 1452	CH_2 bending and CH_3 asymmetric in plane bending (rocking)*; C-O symmetric stretching	Proteins, membrane lipids (phospholipids); Carbohydrates	[79,82,88,89]
≈ 1398	C=O symmetric stretching of COO^- group, C-O symmetric stretching*; C-O bending (carboxylate ions)*; CH_3 and $N^+(CH_3)_3$ symmetric bending*	Proteins and carbohydrates; Mixed region (carboxylic groups); Membrane lipids (phospholipids)	[79,82,87,89]
≈ 1338	CH_2 wagging*	Membrane lipids (phospholipids)	[87,89]
≈ 1320	C-O stretching	Carbohydrates	[79]
≈ 1290	N-H bending in plane, C-N stretching*;	Proteins (amide III);	[79,86–88]

	C-O stretching; N-H thymine/cytosine deformation	Carbohydrates; Nucleic acids	
≈ 1242	N-H bending in plane, C-N stretching*; P=O asymmetric stretching of PO_2^- group	Proteins (amide III, mainly α-helix conformation); Phosphodiester groups of nucleic acids	[86–88]
≈ 1168	Ester and CO-O-C antisymmetric stretching*; C-O, C-C stretching and C-O-H, C-O-C deformation*	Membrane lipids (phospholipids); Carbohydrates	[86,87,89]
≈ 1115	C-O, C-C stretching, C-O-H, C-O-C deformation and C-O-C asymmetric stretching*; P-O-C symmetric stretching, C-O stretching of C-OH group	Carbohydrates; Phosphodiesters, RNA	[79,86,88]
≈ 1077	C-O, C-C stretching, C-O-H, C-O-C deformation and C-O-C asymmetric stretching*; PO_2^-, CO-O-C symmetric stretching*;	Carbohydrates; Membrane lipids (phospholipids) and nucleic acids sugar backbone	[79,86,88,89]
≈ 1032	C-O, C-C stretching, C-O-H, C-O-C deformation*; C-O symmetric stretching	Carbohydrates; Nucleic acids sugar backbone	[79,86,88]
≈ 987	C-O, C-C stretching, C-O-H, C-O-C deformation, C-H bending*; CH_3-N asymmetric stretching	Carbohydrates; Membrane lipids (phospholipids)	[79,86]
≈ 924	C-O, C-C stretching, C-O-H, C-O-C deformation*; $N^+(CH_3)_3$ symmetric stretching*	Carbohydrates; Membrane lipids (phospholipids)	[86,89]

*Characteristic band assignments of biological samples (not specific for plasma)
**Not characteristic of biological samples

The spectral band at 3718 cm^{-1} might be related to a higher level of plasma acidity, which is usually found at perturbations of acid/base blood balance mechanisms that in turn might be associated to presence of general oxidative stress responses. Indeed, in acidic conditions such as generated by brain ischemia and hypoxia, especially related to hyperglycaemia as in DM, I2 PP2A (inhibitor-2 of protein phosphatase-2A) is cleaved into a C-terminal and an N-terminal fragments that are known to bind to PP2A (protein phosphatase-2A) catalytic subunit inhibiting its activity. Since it has been suggested that a decrease in PP2A is a cause of the protein tau abnormal hyperphosphorylation in AD, it might be possible the involvement of brain acidosis in AD pathogenesis [93].

The peptide bond could exhibit nine characteristic IR-active amide bands (A, B and I-VII). Nonetheless, at the present study only amide A, B and I-III were identified in FTIR spectrum. The N-H stretching vibration gives rise to the amide A band between 3310 and 3270 cm^{-1}, it is exclusively localized on the NH group and is therefore insensitive to the conformation of polypeptide backbone, nevertheless its frequency depends on the strength of the hydrogen bond. The amide A

band is usually part of a Fermi resonance doublet with the second component absorbing weakly between 3100 and 3030 cm^{-1} (amide B) [85,87,94]. This resonance doublet originates between the first overtone of amide II and the N-H stretching vibration. Amides I and II, as mentioned below (2.2.2), are the major bands in the protein FTIR spectrum, with amide I providing the most insight into secondary structure. Amides III and IV are very complex bands resulting from mixtures of several coordinate displacements. Out-of-plane motions could be found in amides V, VI and VII. Given the technical and theoretical limitations, only amide bands I, II and III are used for analysis of protein secondary structure [85,87].

It is believed that under oxidative stress and low anti-oxidant defence condition, as appear to occur in neurodegenerative disorders, there is a significant lipid damage in the brain tissues, where lipids have an important role in modifying the structure, fluidity and function of cellular and subcellular membranes. In FTIR spectrum, lipids have characteristic C-H stretching vibrations between 3025 and 2700 cm^{-1}. Specifically, the long hydrocarbon chains in lipids yield intense asymmetric and symmetric C-H stretching vibrations from the aliphatic $–CH_2$ functional group, which fall at ≈2920 and 2850 cm^{-1}, respectively. For $-CH_3$ functional groups, the asymmetric and symmetric C-H stretching modes are found at ≈ 2957 and 2872 cm^{-1}, respectively. In addition, unsaturated olefinic C=C-H stretching vibration has a unique vibrational frequency of 3012 cm^{-1}, which is well distinguishable from the saturated aliphatic peaks. Thus, the unsaturated lipid content (e.g. PUFAs), which is highly vulnerable to oxidative attack given its fullness in double bonds, could be monitored by using this olefinic C=C-H stretching mode [90,95].

The presence of a carbonyl group in a compound can be identified by the strong IR band at the region 1650-1850 cm^{-1}, which corresponds to the C=O stretching vibration. At the present study, FTIR spectra analysis reveals some peaks in this region (1740, 1716 and 1638 cm^{-1}), which might be related to lipid hyperoxidation, especially 1740 cm^{-1} band. As result of lipid peroxidation, which begins with a free radical attack to polyunsaturated lipids, reactive carbonyls are generated. Reactive carbonyls are known to influence protein function by alkylation and crosslinking, contributing to mitochondrial dysfunction and disrupting of cell cytoskeleton. Furthermore, they have been implicated in neurodegenerative disease as intermediates in toxicity [96–98]. Indeed, the 1638 cm^{-1} band corresponds to β-sheet of amide I, which can be related to conformational changes of protein α-helices. Since protein secondary structure is stabilized by hydrogen bonding of peptide backbone, the exposure of proteins to free radicals provokes damage of hydrogen bonds, thus the chains opens and are more prone to free radicals injury, leading to the aforesaid structural changes [96].

Of the aromatic side chains, tyrosine (Tyr) has been most intensely studied due to its interesting properties: it may take part in proton and electron transfer reactions. Tyrosine is a relative strong infrared absorber due to its polar character and the ring mode near 1517 cm^{-1} is one of its most intensive bands [92].

FTIR also provides information about nucleic acid biochemistry, being the more characteristic spectra findings of nucleic acids the C=O stretching vibrations from the purine (1717 cm^{-1}) and pyrimidine (1666 cm^{-1}) bases, besides antisymmetric (1224 cm^{-1}) and symmetric (1087 cm^{-1}) PO_2^- stretching vibrations at the 1500-1000 cm^{-1} region [90].

Besides secondary structure information, some details of protein tertiary structure may also appeared to change in AD at the 780-739 cm^{-1} spectral range [99]. However, it was not possible to identify significant maximum peaks in this spectral range.

At a first glance in Figure 14, it is not possible to achieve and identify significant differences between control and disease samples. Therefore, as it will be presented next, PCA methodology was applied to data allowing a better comparison between samples and its characterization.

2.2. PCA analysis and identification of main sample groups

With PCA methodology and analysis of both scores and loadings of profile, it was possible to identify and characterize different sub-groups of sample, within control and AD major groups. The spectral regions with assignments suggestive of biochemical alterations (Table 12) were submitted to PCA analysis.

2.2.1. Spectral range of 3500-2700 cm^{-1}

This spectral range is related to the presence of lipids (e.g. saturated or unsaturated), especially fatty acids and phospholipids, and its implications for cognitive health and dementia states. Besides, some information of amide A and B regions of proteins could be found in this range.

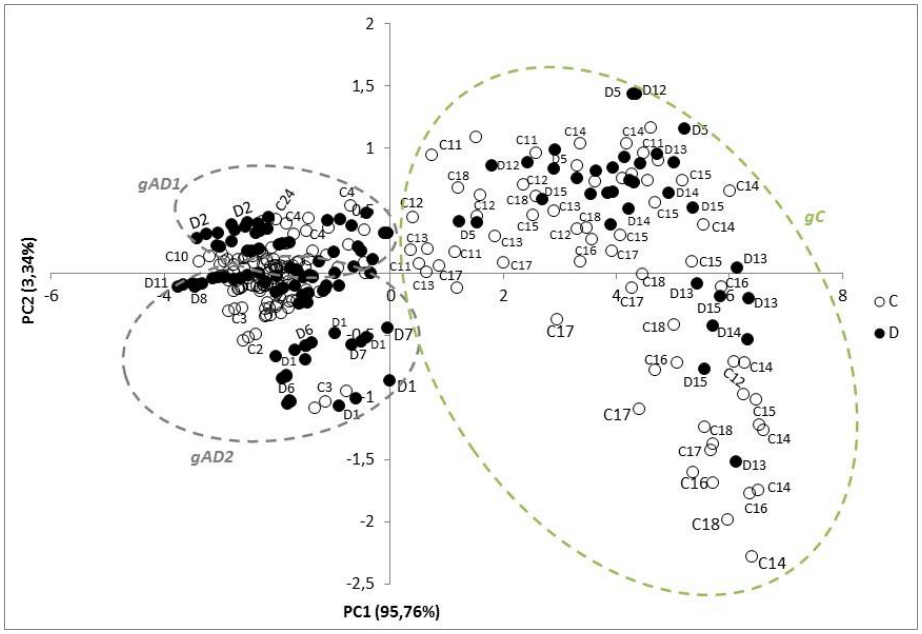

Figure 15| PCA scores of 3500-2700 cm^{-1} spectral region showing spread of samples at a PC1 x PC2 scores diagram. It is possible to identify three distinct groups of samples: cognitive impairment groups (gAD1 and gAD2) and control group (gC). C: control samples; D: dementia/cognitive impairment samples

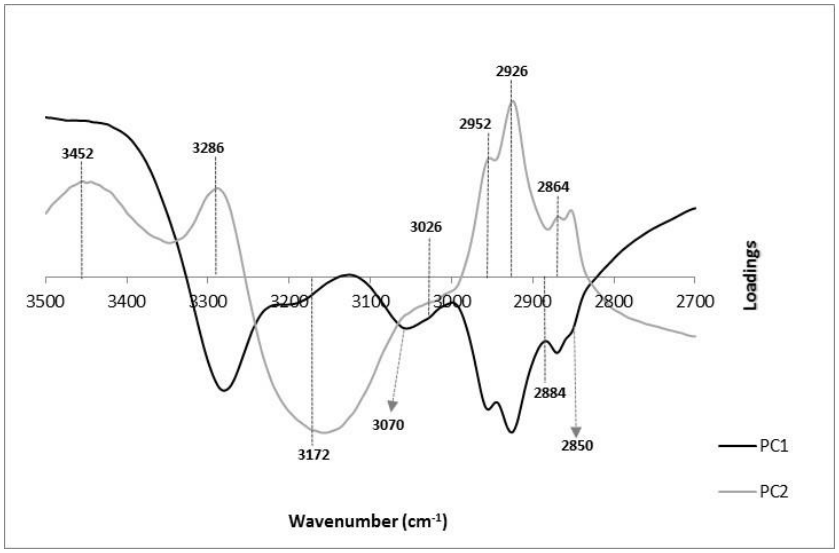

Figure 16| PCA loadings of 3500-2700 cm^{-1} spectral region showing the main maximum wavenumber peaks.

By analysis of Figure 15 it is possible to achieve that although there are control samples present in all quadrant scores the great part of them are distributed among positive PC1 (Q1/Q4). In the other hand, despite the fact of disease samples are present in all quadrants, they are mainly concentrated in negative PC1 (Q2/Q3), where they also appear to have a more distinct pattern between them.

Indeed, PCA loadings analysis turns possible to divide disease samples into two distinct groups, according to the presence of different kinds of molecular alterations (Table 13). Besides, disease samples present at positive PC1 (Q1/Q4) express a more disperse distribution among control samples group.

It is important to note that the obtained biochemical data cannot be only related to absence/presence of dementia, since it might be influenced by other relevant factors, such as the presence of comorbidities, disorder of mixed nature, medication, or even factors as age or sex of the subjects.

Table 13| Assignments of the main maximum peaks from PCA loadings (range of 3500-2700 cm^{-1}).

Peak (cm^{-1})	PCs	Assignment	Score (group)	Ref.
3400	PC1 (+)	N-H stretching of amide A	gC	[87]
3286	PC1 (-) PC2 (+)	N-H stretching of amide A	gAD1	[86]
3172	PC1 (-) PC2 (-)	O-H stretching band of carboxylic acids	gAD2	[68]
3070		N-H stretching of amide B	gAD2	[90]
3026		N-H stretching of amide B	gAD2	[83]
2952	PC1 (-) PC2 (+)	C-H asymmetric stretching of -CH_3 (fatty acids)	gAD1	[68,82,100]
2926		C-H asymmetric stretching of -CH_2 (fatty acids)	gAD1	[68,82,87]
2884		C-H asymmetric stretching of -CH_2 (membrane lipids)	gAD1	[89]
2864		C-H symmetric stretching of -CH_3 (membrane fatty acids)	gAD1	[68,82,89]
2850		C-H symmetric stretching of -CH_2 (membrane fatty acids)	gAD1	[82,89,100]

The spectral region 4000-3100 cm^{-1} is dominated by rather broad spectral features resulting from O-H stretching modes (≈3400 cm^{-1}) and from N-H stretching vibrations (amide A and amide B). The region between 3100 and 2800 cm^{-1} presents C-H stretching vibrations of –CH_3 and –CH_2 functional groups and, hence, it is generally dominated by fatty acids of the several membrane amphiphiles (e.g. phospholipids) and by some amino acid side-chain vibrations. Complementary information can be deduced from the spectral region 1470-1400 cm^{-1}, where the various deformation modes of these functional groups are present [83].

Group AD1: cognitive impairment with altered metabolism of lipids

As aforesaid, the unsaturated lipid content (e.g. PUFAs) could be monitored by using the olefinic C=C-H stretching mode at the frequency of 3012 cm^{-1}, whose intensity is proportional to the amount of unsaturated lipid in the analysed tissue. At healthy conditions, PUFAs as part of phospholipid

membranes have a key structural role being critical for brain normal function (e.g. membrane fluidity, single transduction). It is even believed that these lipids are capable of confer protection against amyloidogenesis, since it was already shown in AD transgenic mouse models and cell culture experiments that they could diminished amyloid burden, possibly by disruption of amyloidogenic pathway and/or increase of Aβ clearance mechanisms [90,95].

At the current study, it was not possible to identify any peak close to 3012 cm^{-1}, which could indicate very low content of unsaturated lipids that makes the signal to much weak for being detected. Significant low levels of PUFAs in brain tissue are usually related to AD condition, being a possible evidence of lipid peroxidation with presence of protein carbonyl formation and high content of lipid peroxidation products. This may translate in a higher risk and severity of AD, with progression of amyloidogenesis. It is thought that these events take place in an early stage of amyloid plaques formation [95].

Moreover, frequency changes in the spectral range 3025-2800 cm^{-1}, especially CH_2 stretching vibrations, can be used as a marker of alterations in the lipid order of the biological system. Indeed, it was possible to identify several peaks in this region (i.e. 2952 cm^{-1}, 2926 cm^{-1}, 2884 cm^{-1}, 2864 cm^{-1} and 2850 cm^{-1}), all of them are related to the presence of saturated lipids. In addition to the absence of unsaturated content spectra signal, this means that there is an unbalance between the content of saturated and unsaturated lipids, favouring the first one. Besides the aforesaid potential brain damage, a high content of saturated lipids is related to vascular disturbances and atherogenic processes, which translates in higher risk for cerebrovascular occurrences leading to ischemia and oxidative stress events. This kind of vascular perturbations are strong correlated with higher risk of dementia development [68,89,90,96].

Group AD2: cognitive impairment with changes in protein conformation

These group are mainly characterized by the presence of carboxylic acids, related to strong O-H stretching vibrations at 3172 cm^{-1}. As mentioned above, this kind of compounds are usually related to lipid hyperoxidation, production of reactive carbonyls and protein structural and functional disturbances, being implicated in the neurodegeneration process. Therefore, the presence of these carboxylic compounds might be related to the changes in protein conformation that can be verify trough 3070 cm^{-1} peak, which translates in a modified localization of amide B region [68,90,96,97]

Group C: control samples

This group is mainly constituted by control samples that appear to have a biochemical pattern without any issues that might be related to neurodegeneration process, being characterised by the presence of assignment for amide A related to the peak 3400 cm^{-1}, a common band found at proteins spectra [87]. Besides, there are also present inside its frontiers some dispersed disease samples, which have less contribute from negative PC1 related peaks.

Giving the presence of some controls at negative PC1, this might be associated to the fact that these samples could present similar biochemical pattern to the respective disease samples that belongs to gAD1 and gAD2, which could translate in a higher risk of developing dementia or even the presence of cognitive impairment in a pre-clinical stage, and thus not detectable by cognitive tests.

2.2.2.Spectral range of 1700-1400 cm^{-1}

As already presented above, this spectral range corresponds mainly to protein conformation mode trough analysis of protein secondary structure (amide I and II), although it might be related also to chemical properties of nucleic acids bases, fatty acids and carbohydrates.

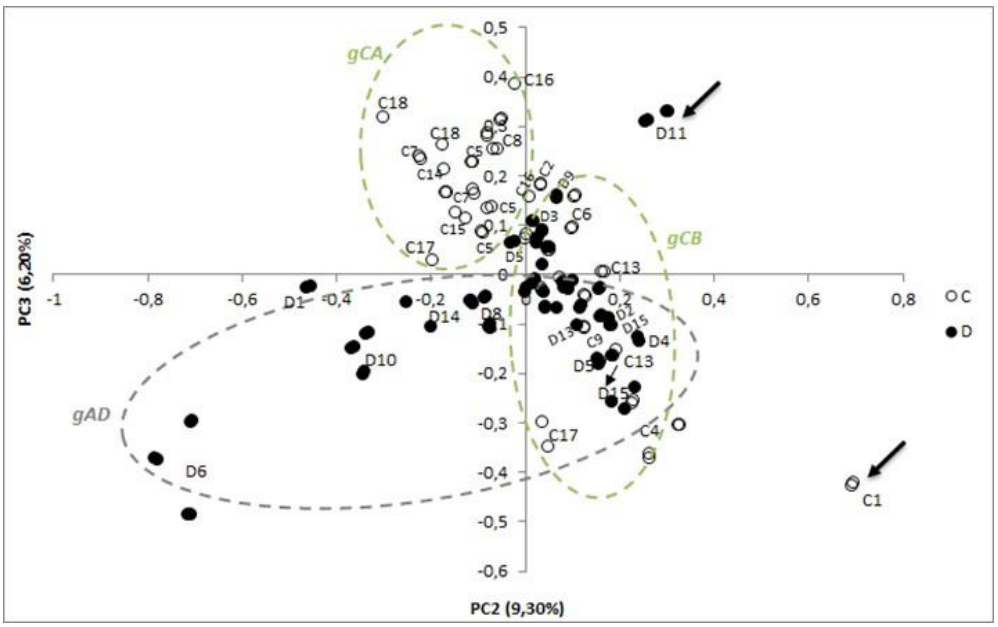

Figure 17| PCA scores of 1700-1400 cm^{-1} spectral region showing spread of samples at a PC2 x PC3 scores diagram. It is possible to identify three distinct groups of samples: cognitive impairment one (gAD) and control groups (gCA and gCB). Samples D11 and C1 as potential outliers. C: control samples; D: dementia/cognitive impairment samples

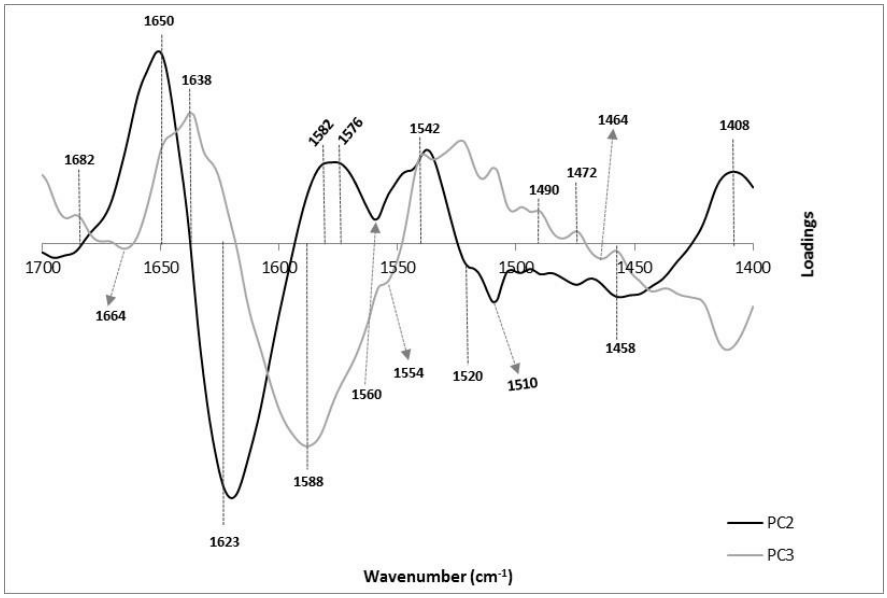

Figure 18| PCA loadings of 1700-1400 cm^{-1} spectral region showing the main maximum wavenumber peaks.

Trough analysis of Figure 17 is possible to verify that there is a predominance of dementia subjects with negative PC3 value (Q3 and Q4), while majority of control samples presents positive PC3 (mainly founded at Q2) despite existence of some control subjects at Q4 (negative PC3). This distributional pattern of samples, accounting with additional information from PCA loadings (Figure 18) and additional clinical data, allow to identify three distinct groups of samples: dementia group (gAD) and control groups (gCA and gCB). Dementia sample group is localized in negative region of PC3, while control sample groups are located in positive PC3 region (gCA and part of gCB) and positive PC2 (gCB). It is believed that C1 and D11 samples (signalled by an arrow) appear to be outliers given the significant lower age of their subjects, comparably to the others.

A better characterization of these groups is only possible with analysis of correspondent assignments of loadings signals peaks (Table 14).

Table 14| Assignments of the main maximum peaks from PCA loadings (range of 1700-1400 cm^{-1}).

Peak (cm^{-1})	PCs	Assignments	Scores (group)	Ref.
1682	PC3 (+)	C=O guanine deformation N-H in plane; unordered random coils, turns and loops (amide I)	gCB	[85,88,101]
1664	PC2 (+)	C=O band of α-helical structure (amide I)*, turns and loops	gCB	[85,96]
1650	PC2 (+)	C=O symmetric stretching band of α-helical structure (amide I)	gCB	[86,100]
1638	PC3 (+)	C=O stretching band of parallel β-sheet (amide I)	gCB	[86]
1623	PC3 (+)	C=O stretching band of parallel β-sheet (amide I)	gCB	[85,90,101]
1588	PC3 (-)	N-H bending in plane and C-N stretching (amide II); benzene ring vibrations from arginine	gAD	[68,87,88]
1582	PC3 (-)	C=N imidazole ring stretching (nucleic acids); benzene ring vibrations from arginine	gAD	[68]
1576	PC3 (-)	N-H bending in plane and C-N stretching (amide II); NH_3^+ symmetric bending (membrane lipids); C=N imidazole ring stretching (nucleic acids)	gAD	[68,82,89]
1560	PC2 (+)	N-H bending in plane and C-N stretching of amino acids (amide II); CO_2^- asymmetric stretching from glutamic acid	gCB	[68,87]
1554	PC2 (+)	N-H deformation mode of α-helical band (amide II)*; CO_2^- asymmetric stretching from glutamic acid	gCB	[68,85]
1542	PC2 (+)	N-H bending in plane and C-N stretching of amino acids (amide II)	gCB	[87,88,100]
1520	PC2 (-) PC3 (+)	N-H bending in plane and C-N stretching of amino acids (amide II);	gCA	[85,91]
1510	PC2 (-) PC3 (+)	N-H bending in plane and C-N stretching of amino acids (amide II); C-H in plane bending of phenyl rings (tyrosine)	gCA	[85,91,92]
1490	PC2 (-) PC3 (+)	$N^+(CH_3)_3$ asymmetric bending (membrane lipids)	gCA	[68,89]
1472	PC2 (-) PC3 (+)	CH_2 scissoring of proteins and CH_3 scissoring of phospholipids (membrane lipids)	gCA	[68,86,89]
1464	PC3 (-)	CH_2 scissoring and CH_3 scissoring and asymmetric bending of phospholipids (membrane lipids)	gAD	[68,86,89]
1458	PC3 (-)	C=O symmetric stretching of COO^- of amino acid side chains; CH_2 bending of mainly fatty acids (membrane lipids)	gAD	[89,102]
1408	PC3 (-)	C=O symmetric stretching of COO^- of amino acid side chains and fatty acids; $N^+(CH_3)_3$ symmetric bending (membrane lipids)	gAD	[68,100,102]

*related to structural analysis of synthetic polypeptides

The typical protein spectrum has two prominent features, amide I (1600-1700 cm^{-1}) and amide II (1500-1560 cm^{-1}) bands, where the former arise from the C=O stretching vibration and the latter is attributed to the N-H bending and C-N stretching vibrations of peptide backbone. The frequency of amide I band is particularly sensitive to secondary structure based on different hydrogen-bonding environments for α-helix, β-sheet, turn and unordered conformations. For example, α-helices and β-sheets have amide I vibrational frequencies at approximately 1655 and 1630 cm^{-1}, respectively. This makes of FTIR a valuable technique for assessing protein aggregation at neurodegenerative

disorders. The amide I vibrational frequency of an aggregated protein falls around 1685-1695 and 1620-1630 cm^{-1}, due to the distinct hydrophobic environment [85,90].

Group AD: cognitive impairment with alterations in lipids and nucleic acids biochemistry

Oxidative stress and free radical damage have been recognized as important factors in degenerative disorders such as AD. Indeed, Aβ can induce free radical formation, which contributes even more for the inflammatory mechanisms related AD pathological development. Besides, inflammatory proteins are thought to exacerbate AD pathogenic process by stimulating Aβ production, and thus facilitating its aggregation in plaques and increasing its neuronal cytotoxicity [90,102].

Therefore, it is not surprising that there is a decreased intensity of 1455 cm^{-1} centred peak (Table 12), which is close to the 1458 cm^{-1} peak identified at the present study (Figure 18). This results from deformation and stretching vibrations of CH_2 groups particularly in fatty acids (present in membrane lipids) [89,102]. The brain is known to have a high content of easily peroxidizable unsaturated fatty acids (especially arachidonic and docosahexaenoic acids) and a high content of iron, which are key factors for neuronal membrane lipoperoxidation. Indeed, isoprostanes (specifically generated from arachidonic acid) were considered as stable markers of oxidative lipid damage in AD patients [102].

Besides, the 1582 cm^{-1} band might be associated to alteration of conformational state and structural stability of nucleic acid molecules. The same may also be stated for 1576 cm^{-1}, to which is added structural changes in lipids. Once again, it could be found in 1588 cm^{-1} peak a different localization for amide II, related to altered protein conformation and presence of protein aggregates typical of AD. In other hand, similarly to the aforesaid for 1458 cm^{-1} peak, 1464 cm^{-1} and 1408 cm^{-1} peaks are due mainly to structural changes of associated membrane lipids, namely fatty acids and phospholipids, which are the principal targets of free radicals, oligomers and other damage-inducing agents [68,86,87,89].

Although β-sheet content in oligomers is lower than in fibrils (where this content is about to 75%), it is significant and have already shown to reach 48-57% of total oligomer constitution. This lower content in secondary protein structure and faster dynamics exchange probably reflects a higher flexibility of Aβ in soluble oligomers than in fibrils, which could be related to lower stability and higher toxicity of oligomer forms comparatively to fibrils. In fact, it is thought that soluble oligomers, also known as protofibrils or ADDLs (Aβ-derived diffusible ligands), may interact with cellular lipid bilayers and causing its perturbation and/or permeabilization [103].

Indeed, several recent studies in the field of protein-folding diseases suggest that the neuron toxicity arises from the initial oligomeric species, rather than the largest protein plaques. The mechanism of oligomer toxicity is still under debate, but includes formation of transmembrane pores that disrupt ion transport through cells. Pore-forming oligomeric structures have been described with Aβ in AD and α-synuclein in Parkinson's disease [90].

A previous study was already shown that the spectral region 1480-1428 cm^{-1} provided the largest differentiation between control and disease samples, suggesting that oxidative stress-dependent processes in AD lead to modified lipid and nucleic acid structures [90,102].

Almost all of patients that belongs to AD group present comorbidities, which may be translated in higher severity and faster progression of the disease condition.

Patient D5

The patient D5 are present at both Q1 and Q4 scores, being related to the presence of altered protein conformation and cell damage trough oxidative stress, namely membrane lipids and nucleic acid molecules. This might be translated into a more advanced and severe stage of disease comparably to the reminder patients, or instead it may be possible that this patient suffer from a mixed pathology and thus present a different plasma biochemical pattern. D5 shows a positive value for MMSE score but a negative one for CDR scale, besides the existence of both DM and HTN comorbidities, which enforces the aforesaid picture.

Group CA: pure control subjects

These control group is a pure one, with all samples inside group borders being controls. Besides, this appear to present an unaltered proteins conformation, without any signal that could indicate protein aggregation or presence of intermediate damaging forms like oligomers. This is consistent with biochemical pattern of a control sample and it is related to 1520 cm^{-1} and 1510 cm^{-1} peaks [85,91].

Nevertheless, the other peaks related to CA group (i.e. 1472 cm^{-1} and 1490 cm^{-1}), are associated to structural properties of membrane lipids, and the 1490 cm^{-1} peak is particularly connected to membrane injury probably due to the action of oxidative stress and free radicals inductors of cell damage. The brain is particularly vulnerable to oxidative damage (as could be possible of being detected trough IR plasma analysis) for reasons already mentioned above, which in addition of the diminished oxidative defences characteristically from the normal aging process and the presence of comorbidities (i.e. DM and HTN) provides the perfect picture for developing dementia and/or

some other related neurodegenerative disorder [68,86,89,104,105]. Indeed, all subjects from CA group suffer from comorbidities such as DM and HTN. Given the possibility of these subjects had already achieve the pre-MCI or initial phase of MCI state, it would be important theirs clinical monitoring.

Group CB: control subjects with potential picture of MCI

This group comprises control samples dispersed among Q1/Q4 and a small cluster of disease samples located in Q1, which are related to changes in protein conformation.

Giving their coordinates and their match to amide I region of aggregated proteins, peaks present at 1682 cm^{-1}, 1638 cm^{-1}, 1623 cm^{-1} could be related to disease samples present among CB group (Figure 17). Indeed, 1623 cm^{-1} peak had been considered as characteristic of a protein in an aggregated state, during FTIR analysis of cerebral tissue from AD patients [85,90,101].

Contrarily to fibrils, oligomers present both 1630 and 1695 cm^{-1} peaks, which corresponds to an anti-parallel β-sheet conformation. This 1695 cm^{-1} peak is not present in PCA loadings (Figure 18), and there is two peaks near to 1630 cm^{-1} (i.e. 1623 cm^{-1} and 1638 cm^{-1}), which is related to highly stable parallel β-sheet that in turn is usually associated to the presence of fibrils. Since it is believed that Aβ soluble oligomers are an intermediate form that precedes Aβ fibrils, it is not difficult to believe that a higher proportion of Aβ fibril forms is related to a later stage of the disease. Still, it is needed to considerer that the 1695 cm^{-1} peak signal is five times weaker than the signal related to 1630 cm^{-1} peak, and thus, the absence in PCA loadings (Figure 18) of the former peak signal does not mean the complete lack of oligomer forms in the analysed samples. Actually, the 1695/1630 cm^{-1} intensity ratio is proportional to the percentage of anti-parallel β-sheet content in Aβ aggregates. Once again, given the absence of 1695 cm^{-1} peak, it is suggested that Aβ fibrils are present in higher content than Aβ oligomers [103].

Moreover, it must not be forgotten that most of the proteins present a mixture of secondary structures, and thus, the amide I band represents a combination of these components [85,90]. Indeed, the 1670-1685 cm^{-1} region is related to the presence of non-β structure in protein fibrils, especially turns and loops. Thus, in addition to the parallel β-sheet core related to 1638 cm^{-1} and 1623 cm^{-1} peaks, Aβ fibrils present in lower content non-β structures related mainly to 1682 cm^{-1} band. Besides, amorphous aggregates also may present a spectral band at 1623 cm^{-1}, and they are not associated to a higher content of β-sheet structure, contrarily to protein fibrils. Since a 1623 cm^{-1} band has been identified (Figure 18), this might indicate that besides protein fibrils there are

also some amorphous aggregates, arising from a relatively unfolded-like partially folded and a native like conformation, respectively [101].

Likewise, it was found during analysis of synthetic polypeptides that components of C=O band with α and β forms are related to spectral peaks at 1658 cm^{-1} and 1629 cm^{-1}, respectively. Besides, the N-H deformation mode had presented a signal peak at 1550 cm^{-1}, which showed to correspond to α form [85]. At the present study, it is possible to find 1664 and 1623 cm^{-1} peaks related to α and β forms, in addition to the identified peaks at 1554 and 1542 cm^{-1} that are linked to N-H deformation mode (Table 14).

In the other hand, control samples could be associated to signal peaks identified at 1664 cm^{-1} and 1650 cm^{-1} that are related to the typical localization of amide I of proteins mainly constituted by α-helix structures. This is complemented by protein structural information given by 1560 cm^{-1}, 1554 cm^{-1}, 1542 cm^{-1} and 1538 cm^{-1} peaks [85–87,100]. Nevertheless, giving the proximity of these samples to the disease ones, from both Q1 (protein aggregates) and Q4 (lipid and nucleic acids altered biochemistry), it is possible that control samples share some biochemical characteristics with disease samples. Besides, almost all control subjects from CB group (exception for C4) suffer from comorbidities such as DM and HTN, which can be translated *per se* in a higher risk of developing some demented disorder comparatively to the average healthy cognitive population that not present this kind of comorbidities. Therefore, it is quite plausible that control subjects have already been suffering with a pre-clinical form of cognitive impairment (i.e. beginning of MCI).

2.2.3. Spectral range of 1200-900 cm^{-1}

The spectral region 1200 - 900 cm^{-1} is usually dominated by the symmetric stretching of PO_2 groups in nucleic acids and a complex sequence of peaks due mainly to strongly coupled C-C, C-O stretching and C-O-H, C-O-C deformation modes of several oligosaccharides [83]. Besides oligosaccharides and nucleic acids structural and functional information, it is possible to identify signal peaks related to membrane lipids.

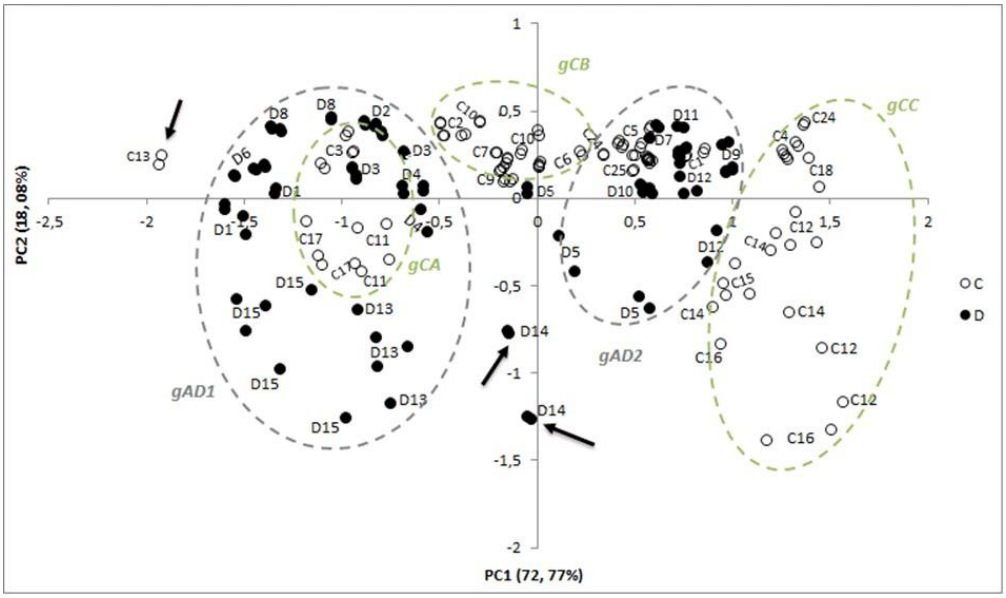

Figure 19| PCA scores of 1200-900 cm^{-1} spectral region showing spread of samples at a PC1 x PC2 scores diagram. It is possible to identify five distinct groups of samples: cognitive impairment ones (gAD1 and gAD2), and control groups (gCA, gCB and gCC). Samples C13 and D14 as potential outliers. C: control samples; D: dementia/cognitive impairment samples

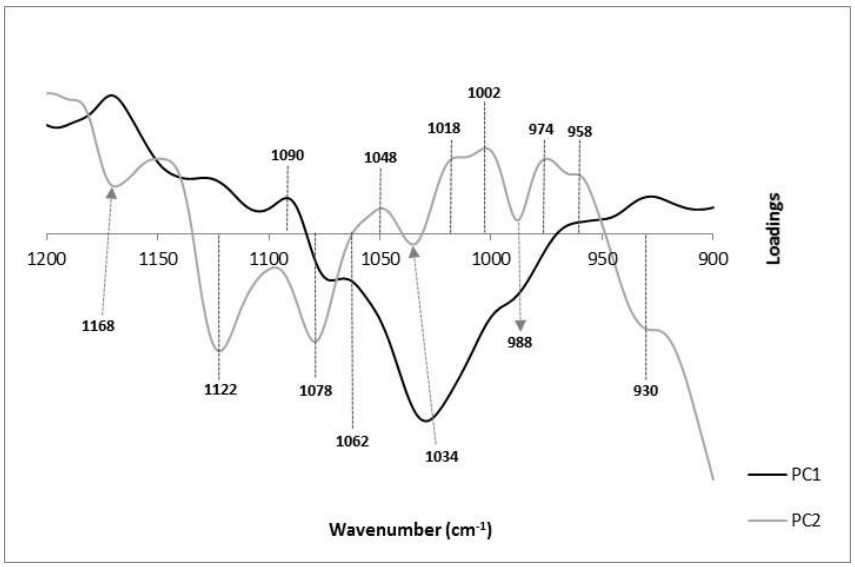

Figure 20| PCA loadings of 1200-900 cm^{-1} spectral region showing the main maximum wavenumber peaks.

Through analysis of Figure 19 it is possible to distinguish disease samples into two well delimited groups, with gAD1 at Q2/Q3 and gAD2 at Q1/Q4. In the other hand, control samples are divided into three groups, with gCA at Q2/Q3 and inside gAD1 frontiers, gCB at Q1/Q2 and gCC at Q1/Q4.

Table 15| Assignments of the main maximum peaks from PCA loadings (range of 1200-900 cm^{-1}).

Peaks (cm^{-1})	PCs	Assignments	Score (group)	Ref.
1168	PC1 (+)	C-O stretching of ribose from nucleic acids; CO-O-C asymmetric stretching (membrane lipids)	gAD2	[68,86,89,102]
1122		PO stretching of phosphodiester backbone and C-O stretching of deoxyribose and ribose (nucleic acids)	gAD2	[68,102]
1090		PO_2^- symmetric stretching of sugar rings (nucleic acids) and membrane lipids	gAD2	[68,82,89,90]
1078	PC1 (-)	CO-O-C symmetric stretching (membrane lipids)	gAD1	[68,89]
1062		Ester C-O-C symmetric stretching (phospholipids); ribose C-O stretching (nucleic acids)	gAD1	[68,86]
1048		C-O stretching of sugar rings (nucleic acids)	gAD1	[68,102]
1034		C-N symmetric stretching of amino acid (aliphatic amines); ribose C-O stretching (RNA)	gAD1	[68,100]
1018		C-O stretching in osidic and protein structures; symmetric stretching of dianionic phosphate monoester (nucleic acids, especially DNA)	gAD1	[68,102]
1002		C-O stretching in osidic and protein structures; uracil ring bending (RNA); symmetric stretching of dianionic phosphate monoester (nucleic acids, especially DNA)	gAD1	[68,102]
988		C-O stretching in osidic and protein structures; symmetric stretching of dianionic phosphate monoester (nucleic acids, especially DNA)	gAD1	[102]
974		C-O stretching in osidic and protein structures; $N^+(CH_3)_3$ asymmetric stretching (membrane lipids); symmetric stretching of dianionic phosphate monoester (nucleic acids, especially DNA)	gAD1	[68,86,89,102]
958	PC1 (+)	C-O stretching in osidic and protein structures; symmetric stretching of dianionic phosphate monoester (nucleic acids, especially DNA)	gAD2	[102]
930		C-O-H out of plane bending of carboxylic acids; C-O stretching in osidic and protein structures; symmetric stretching of dianionic phosphate monoester (nucleic acids, especially DNA)	gAD2	[68,102]

The wavenumber components characteristics of each sample group are difficult to define since all these groups are distributed among PC1 region, thus having less contribute from PC2. Therefore, the analysis of main maximum peaks presented in PCA loadings (Table 15) does not allow to distinguish clearly the biochemical pattern between gAD1 and gAD2, with both presenting structural and functional alterations mostly in nucleic acids, but also in membrane lipids and proteins. Besides, it is not equally possible to differentiate the three control groups from each other through PCA loadings, since it has not been identified spectral bands that could be related to control characteristics.

Nevertheless, according to group's distribution among PC1 region, gAD1 show to have more contribute from negative PC1 signal peaks, while gCC presents more contribution from positive PC1

signal peaks. This might indicate that gCC, presented in Figure 19 as a pure control group, have opposing biochemical characteristics in relation to gAD1, which could translate in opposing clinical profiles. In the other hand, gCB comprises control samples from subjects with some similar characteristics, namely sex and age, besides almost all these subjects suffer from vascular comorbidities that translates in a higher risk for developing cognitive impairment.

Groups AD1 and AD2: cognitive impairment with lipid and nucleic acids disturbances

The C-O stretching bands, especially from the 1150-1000 cm^{-1} spectral region, are related to the presence of hydroxyl compounds, which are products of lipid peroxidation and have already been reported as markers of oxidative damage in AD [99]. Besides, the 1200-1100 cm^{-1} region is related to the presence of saturated lipids (aliphatic esters), which may be translated into a higher content of saturation associated to a higher risk of membrane damage and vascular events. It is already known that hyperoxidation of lipids, phospholipids and membranes takes place during the atherogenesis process, and since the majority of patients from both gAD1 and gAD2 have comorbidities such as DM, HTN or dyslipidaemia, this might confer the risk of a more severe picture of neurodegeneration [68,96]. The presence of atheromatous formations in the extracranial and intracranial blood vessels predisposes to ischemic events, both subclinical brain infarction and stroke, as well as small vessel disease and amyloid angiopathy, provoke white matter damage and even cerebral haemorrhagic events. Both cerebral ischemia and haemorrhage are known to interact with AD pathology in a bidirectional way. In the same manner, high blood pressure may damage small blood vessels, affecting cognition by disruption of subcortical neuronal circuits [106]. Nucleic acids molecules, especially DNA, represent a major target for free radicals when capacity of intracellular free radical scavengers and antioxidants is overcome, as it is possible to verify trough the identified spectral peaks at 1122 cm^{-1}, 1090 cm^{-1}, 1048 cm^{-1}, and the ones that belong to the 1020-930 cm^{-1} region. Some studies *in vitro* have shown that hydroxyl radicals are able to attack the deoxyribose moiety, generating a variety of products that result from hydrogen abstractions of the pentose ring and provoke loss of phosphoric acid and breaking of strands. Although many repair enzymes systems have evolved to remove and replace the damaged nucleosides and repair the broken strands, there is a high rate of DNA damage as it was already shown by the high plasmatic levels of 8-OHdG (8-hydroxydeoxyguanosine) found in AD patient samples. It is believed that cumulative DNA damage contributes to progressive neuronal cell loss because nonrepaired DNA damage can trigger programmed cell death [102].

3. CONCLUDING REMARKS

Direct analysis of spectra allowed to identify the main chemical FTIR assignments in plasma, which is essential for establish a pattern of chemical vibrations and identify the principal spectral regions that could present significant information. However, giving the complexity of biological samples and the resultant overlaps of the main biomolecules absorptions, direct analysis of spectra proved to be insufficient to distinguish between the spectra of control and dementia samples. Thus, it was needed to apply multivariate data analysis methodology, namely PCA technique, to draw out the significant and no redundant spectra information.

Trough multivariate analysis, it was possible to achieve spectrum data with important information from the main IR relevant regions, namely from lipids (3500-2700 cm^{-1}), protein conformation (1700-1400 cm^{-1}), and also from carbohydrates and nucleic acids structure (1200-900 cm^{-1}). At the analysis of the first spectral region, it was noted that in disease samples there is an unbalance between the content of saturated and unsaturated lipids, favouring the first one. This translates in a high potential brain damage, since a high content of saturated lipids is related to vascular disturbances and atherogenic processes, leading to cerebrovascular occurrences and to ischemia and oxidative stress events. Hence, it could be shown the presence of carboxylic acids that are usually related to lipid hyperoxidation, production of reactive carbonyls and protein structural and functional disturbances, being implicated in the neurodegeneration process. Relatively to 1700-1400 cm^{-1} spectral range, it was identified the existence of protein aggregates and the change in protein conformation for highly stable parallel β-sheet, which is usually associated to the presence of Aβ fibrils. Samples D3, D5 and D9 appear to be the ones that most influence these findings. Since it is believed that Aβ soluble oligomers are an intermediate form that precedes Aβ fibrils, it is not difficult to believe that a higher proportion of Aβ fibril forms is related to a later stage of the disease. In 1200-900 cm^{-1} region, it was possible to find products of lipid peroxidation related to impairment of membranes, and nucleic acids oxidative damage. In a previous work involving FTIR analysis of plasma samples, it was denoted a higher risk of vascular damage in cognitive impaired subjects, besides evidences of potential oxidative stress that are also present in the current project [78].

Giving the presence of several comorbidities in the majority of subjects, it is possible to suggest that vised controls are at higher risk of developing dementia rather than average healthy population, and in turn, vised cognitive impaired patients are prone to develop a more insidious and severe disorder picture with a faster neurodegeneration process. Moreover, biochemical data that had result from this project cannot be only related to absence/presence of dementia, or even to occurrence of aforesaid comorbidities, there are also other relevant clinical factors that could

influence results, such as the presence of a neurodegenerative disorder of mixed nature, unknown and/or undiagnosed genetic predisposed factors, or use of medication capable of affect biochemical plasma levels.

As a final remark, FTIR analysis could have the potential to be applied in future not only for cognitive impairment diagnosis but also for identification of disease stage and prognostic evaluation, besides assessment of disease developing risk for control subjects. To make it possible it will be required further clinical trials with data sets more approximate from general population, besides it will be needed a sustainable and efficient validation model to transfer potential biomarkers from these clinical trials to clinical practice.

BIBLIOGRAPHY

[1] M. Kosicek and S. Hecimovic, “Phospholipids and Alzheimer’s disease: alterations, mechanisms and potential biomarkers.,” *Int. J. Mol. Sci.*, vol. 14, no. 1, pp. 1310–22, Jan. 2013.
[2] C. Bazenet and S. Lovestone, “Plasma biomarkers for Alzheimer’s disease: much needed but tough to find.,” *Biomark. Med.*, vol. 6, no. 4, pp. 441–54, Aug. 2012.
[3] R. Arking, *The Biology of Aging: Observations & Principles*, Third edit. Oxford University Press, 2006.
[4] L. Alves, A. S. a Correia, R. Miguel, P. Alegria, and P. Bugalho, “Alzheimer’s disease: a clinical practice-oriented review.,” *Front. Neurol.*, vol. 3, no. April, p. 63, Jan. 2012.
[5] P. Kumar and M. Clarck, *Kumar & Clark’s Clinical Medicine*, Seventh ed. Saunders Elsevier, 2009, p. 1343.
[6] C. M. Porth, *Pathophysiology: Concepts of Altered Health States*, 7th editio. Lippincott Williams & Wilkins, 2005.
[7] C. Ballard, S. Gauthier, A. Corbett, C. Brayne, D. Aarsland, and E. Jones, “Alzheimer’s disease.,” *Lancet*, vol. 377, no. 9770, pp. 1019–31, Mar. 2011.
[8] Alzheimer Portugal, “Plano Nacional de Intervenção Alzheimer,” 2009.
[9] R. J. Castellani, R. K. Rolston, and M. A. Smith, “Alzheimer disease.,” *Dis. Mon.*, vol. 56, no. 9, pp. 484–546, Sep. 2010.
[10] The Regents of the University of California, “Alzheimer’s Disease,” 2014. [Online]. Available: http://memory.ucsf.edu/education/diseases/alzheimer.
[11] R. Taipa, J. Pinho, and M. Melo-Pires, “Clinico-pathological correlations of the most common neurodegenerative dementias.,” *Front. Neurol.*, vol. 3, no. May, p. 68, Jan. 2012.
[12] F. J. Wippold, N. Cairns, K. Vo, D. M. Holtzman, and J. C. Morris, “Neuropathology for the neuroradiologist: plaques and tangles.,” *AJNR. Am. J. Neuroradiol.*, vol. 29, no. 1, pp. 18–22, Jan. 2008.
[13] WebPat, “The Internet Pathology Laboratory for Medical Education,” 2014. [Online]. Available: http://library.med.utah.edu/WebPath/TUTORIAL/CNS/CNSDG004.html.
[14] M. Goedert and M. G. Spillantini, “A century of Alzheimer’s disease.,” *Science*, vol. 314, no. 5800, pp. 777–81, Nov. 2006.
[15] A. M. Palmer, “Neuroprotective therapeutics for Alzheimer’s disease: progress and prospects.,” *Trends Pharmacol. Sci.*, vol. 32, no. 3, pp. 141–7, Mar. 2011.
[16] R. H. Swerdlow, “Is aging part of Alzheimer’s disease, or is Alzheimer's disease part of aging?,” *Neurobiol. Aging*, vol. 28, no. 10, pp. 1465–80, Oct. 2007.
[17] H. W. Querfurth and F. M. LaFerla, “Alzheimer’s disease.,” *N. Engl. J. Med.*, vol. 362, no. 4, pp. 329–44, Jan. 2010.
[18] S. Dong, Y. Duan, Y. Hu, and Z. Zhao, “Advances in the pathogenesis of Alzheimer’s disease: a re-evaluation of amyloid cascade hypothesis.,” *Transl. Neurodegener.*, vol. 1, no. 1, p. 18, Jan. 2012.
[19] B. Leclerc and A. Abulrob, “Perspectives in molecular imaging using staging biomarkers and immunotherapies in Alzheimer’s disease.,” *ScientificWorldJournal.*, vol. 2013, p. 589308, Jan. 2013.
[20] C. R. Jack, D. S. Knopman, W. J. Jagust, L. M. Shaw, P. S. Aisen, M. W. Weiner, R. C. Petersen, and J. Q. Trojanowski, “Hypothetical model of dynamic biomarkers of the Alzheimer’s pathological cascade.,” *Lancet Neurol.*, vol. 9, no. 1, pp. 119–28, Jan. 2010.
[21] L. Tillement, L. Lecanu, and V. Papadopoulos, “Alzheimer’s disease: effects of β-amyloid on mitochondria.,” *Mitochondrion*, vol. 11, no. 1, pp. 13–21, Jan. 2011.
[22] L. Martin, X. Latypova, and F. Terro, “Post-translational modifications of tau protein: implications for Alzheimer’s disease.,” *Neurochem. Int.*, vol. 58, no. 4, pp. 458–71, Mar. 2011.
[23] K. H. Ashe and A. Aguzzi, “Prions, prionoids and pathogenic proteins in Alzheimer disease.,” *Prion*, vol. 7, no. 1, pp. 55–9, 2013.
[24] S. Mondragón-Rodríguez, “Phosphorylation of tau protein as the link between oxidative stress, mitochondrial dysfunction and connectivity failure; implications for Alzheimer’s disease,” *downloads.hindawi.com*, vol. 2013, no. Figure 1, 2013.
[25] J.-H. Chen, K.-P. Lin, and Y.-C. Chen, “Risk factors for dementia.,” *J. Formos. Med. Assoc.*, vol. 108, no. 10, pp. 754–64, Oct. 2009.
[26] X.-H. Xu, Y. Huang, G. Wang, and S.-D. Chen, “Metabolomics: a novel approach to identify potential diagnostic biomarkers and pathogenesis in Alzheimer’s disease.,” *Neurosci. Bull.*, vol. 28, no. 5, pp. 641–8, Oct. 2012.

[27] H. Hampel, R. Frank, K. Broich, S. J. Teipel, R. G. Katz, J. Hardy, K. Herholz, A. L. W. Bokde, F. Jessen, Y. C. Hoessler, W. R. Sanhai, H. Zetterberg, J. Woodcock, and K. Blennow, "Biomarkers for Alzheimer's disease: academic, industry and regulatory perspectives.," *Nat. Rev. Drug Discov.*, vol. 9, no. 7, pp. 560–74, Jul. 2010.

[28] G. M. McKhann, D. S. Knopman, H. Chertkow, B. T. Hyman, C. R. Jack, C. H. Kawas, W. E. Klunk, W. J. Koroshetz, J. J. Manly, R. Mayeux, R. C. Mohs, J. C. Morris, M. N. Rossor, P. Scheltens, M. C. Carrillo, B. Thies, S. Weintraub, and C. H. Phelps, "The diagnosis of dementia due to Alzheimer's disease: recommendations from the National Institute on Aging-Alzheimer's Association workgroups on diagnostic guidelines for Alzheimer's disease.," *Alzheimers. Dement.*, vol. 7, no. 3, pp. 263–9, May 2011.

[29] M. S. Albert, S. T. DeKosky, D. Dickson, B. Dubois, H. H. Feldman, N. C. Fox, A. Gamst, D. M. Holtzman, W. J. Jagust, R. C. Petersen, P. J. Snyder, M. C. Carrillo, B. Thies, and C. H. Phelps, "The diagnosis of mild cognitive impairment due to Alzheimer's disease: recommendations from the National Institute on Aging-Alzheimer's Association workgroups on diagnostic guidelines for Alzheimer's disease.," *Alzheimers. Dement.*, vol. 7, no. 3, pp. 270–9, May 2011.

[30] B. Dubois, H. H. Feldman, C. Jacova, S. T. Dekosky, P. Barberger-Gateau, J. Cummings, A. Delacourte, D. Galasko, S. Gauthier, G. Jicha, K. Meguro, J. O'brien, F. Pasquier, P. Robert, M. Rossor, S. Salloway, Y. Stern, P. J. Visser, and P. Scheltens, "Research criteria for the diagnosis of Alzheimer's disease: revising the NINCDS-ADRDA criteria.," *Lancet Neurol.*, vol. 6, no. 8, pp. 734–46, Aug. 2007.

[31] B. Dubois, H. H. Feldman, C. Jacova, J. L. Cummings, S. T. Dekosky, P. Barberger-Gateau, A. Delacourte, G. Frisoni, N. C. Fox, D. Galasko, S. Gauthier, H. Hampel, G. a Jicha, K. Meguro, J. O'Brien, F. Pasquier, P. Robert, M. Rossor, S. Salloway, M. Sarazin, L. C. de Souza, Y. Stern, P. J. Visser, and P. Scheltens, "Revising the definition of Alzheimer's disease: a new lexicon.," *Lancet Neurol.*, vol. 9, no. 11, pp. 1118–27, Nov. 2010.

[32] O. V Forlenza, B. S. Diniz, and W. F. Gattaz, "Diagnosis and biomarkers of predementia in Alzheimer's disease.," *BMC Med.*, vol. 8, no. 1, p. 89, Jan. 2010.

[33] S. Weintraub, A. H. Wicklund, and D. P. Salmon, "The neuropsychological profile of Alzheimer disease.," *Cold Spring Harb. Perspect. Med.*, vol. 2, no. 4, p. a006171, Apr. 2012.

[34] D. a. Lowe, S. Balsis, T. M. Miller, J. F. Benge, and R. S. Doody, "Greater Precision when Measuring Dementia Severity: Establishing Item Parameters for the Clinical Dementia Rating Scale," *Dement. Geriatr. Cogn. Disord.*, vol. 34, no. 2, pp. 128–134, 2012.

[35] C. Hill, "Neuropsychological Testing Used In The Evaluation Of Alzheimer's Disease," 2014. [Online]. Available: http://alzheimers.about.com/od/diagnosisofalzheimers/tp/neuropsychtests.htm.

[36] A. Rosenzweig, "Alzheimer's Tests Screening Tests for Alzheimer's Disease and Other Dementias," 2010. [Online]. Available: http://alzheimers.about.com/od/testsandprocedures/tp/Alzheimers-Tests.htm.

[37] A. Rosenzweig, "The Mini-Mental State Exam and Its Use as an Alzheimer's Screening Test," 2010. [Online]. Available: http://alzheimers.about.com/od/testsandprocedures/a/The-Mini-Mental-State-Exam-And-Its-Use-As-An-Alzheimers-Screening-Test.htm.

[38] S. Crutch, "The Mini Mental State Examination (MMSE)," 2012. [Online]. Available: http://www.alzheimers.org.uk/site/scripts/documents_info.php?documentID=121.

[39] B. T. Hyman, C. H. Phelps, T. G. Beach, E. H. Bigio, N. J. Cairns, M. C. Carrillo, D. W. Dickson, C. Duyckaerts, M. P. Frosch, E. Masliah, S. S. Mirra, P. T. Nelson, J. a Schneider, D. R. Thal, B. Thies, J. Q. Trojanowski, H. V Vinters, and T. J. Montine, "National Institute on Aging-Alzheimer's Association guidelines for the neuropathologic assessment of Alzheimer's disease.," *Alzheimers. Dement.*, vol. 8, no. 1, pp. 1–13, Jan. 2012.

[40] S. Karantzoulis and J. Galvin, "Distinguishing Alzheimer's disease from other major forms of dementia," pp. 1579–1592, 2011.

[41] B. Mollenhauer, H. Förstl, G. Deuschl, A. Storch, W. Oertel, and C. Trenkwalder, "Lewy body and parkinsonian dementia: common, but often misdiagnosed conditions.," *Dtsch. Arztebl. Int.*, vol. 107, no. 39, pp. 684–91, Oct. 2010.

[42] Medscape, "Imaging Neurodegeneration in Parkinson's Disease Dementia and Parkinson's Disease," 2014. [Online]. Available: http://www.medscape.org/viewarticle/572271_8.

[43] F. Mangialasche, A. Solomon, B. Winblad, P. Mecocci, and M. Kivipelto, "Alzheimer's disease: clinical trials and drug development.," *Lancet Neurol.*, vol. 9, no. 7, pp. 702–16, Jul. 2010.

[44] M. Sweetlove, “Phase III CONCERT Trial of Latrepirdine,” *Pharmaceut. Med.*, vol. 26, no. 2, pp. 113–115, Aug. 2012.
[45] B. H. Dobkin, *The Clinical Science of Neurologic Rehabilitation*, Second edt. Oxford University Press, 2003.
[46] F. Di Domenico, R. Coccia, D. A. Butterfield, and M. Perluigi, “Circulating biomarkers of protein oxidation for Alzheimer disease: expectations within limits.,” *Biochim. Biophys. Acta*, vol. 1814, no. 12, pp. 1785–95, Dec. 2011.
[47] C. R. Jack, M. S. Albert, D. S. Knopman, G. M. McKhann, R. a Sperling, M. C. Carrillo, B. Thies, and C. H. Phelps, “Introduction to the recommendations from the National Institute on Aging-Alzheimer’s Association workgroups on diagnostic guidelines for Alzheimer's disease.,” *Alzheimers. Dement.*, vol. 7, no. 3, pp. 257–62, May 2011.
[48] R. a Sperling, P. S. Aisen, L. a Beckett, D. a Bennett, S. Craft, A. M. Fagan, T. Iwatsubo, C. R. Jack, J. Kaye, T. J. Montine, D. C. Park, E. M. Reiman, C. C. Rowe, E. Siemers, Y. Stern, K. Yaffe, M. C. Carrillo, B. Thies, M. Morrison-Bogorad, M. V Wagster, and C. H. Phelps, “Toward defining the preclinical stages of Alzheimer’s disease: recommendations from the National Institute on Aging-Alzheimer's Association workgroups on diagnostic guidelines for Alzheimer's disease.,” *Alzheimers. Dement.*, vol. 7, no. 3, pp. 280–92, May 2011.
[49] C. Teunissen, “C EREBROSPINAL FLUID BIOMARKERS FOR A LZHEIMER ’ S DISEASE : EMERGENCE OF THE,” vol. 65, no. Figure 1, pp. 3–4, 2013.
[50] C. Rosén, O. Hansson, K. Blennow, and H. Zetterberg, “Fluid biomarkers in Alzheimer’s disease - current concepts.,” *Mol. Neurodegener.*, vol. 8, p. 20, Jan. 2013.
[51] N. Salvadores, M. Shahnawaz, E. Scarpini, F. Tagliavini, and C. Soto, “Detection of Misfolded Aβ Oligomers for Sensitive Biochemical Diagnosis of Alzheimer’s Disease,” *Cell Rep.*, pp. 1–8, Mar. 2014.
[52] D. Halawani, S. Tessier, D. Anzellotti, D. a Bennett, M. Latterich, and A. C. LeBlanc, “Identification of Caspase-6-mediated processing of the valosin containing protein (p97) in Alzheimer’s disease: a novel link to dysfunction in ubiquitin proteasome system-mediated protein degradation.,” *J. Neurosci.*, vol. 30, no. 17, pp. 6132–42, Apr. 2010.
[53] J. Wiltfang, P. Lewczuk, P. Riederer, E. Grünblatt, C. Hock, P. Scheltens, H. Hampel, H. Vanderstichele, K. Iqbal, D. Galasko, L. Lannfelt, M. Otto, H. Esselmann, a. W. Henkel, J. Kornhuber, and K. Blennow, “Consensus Paper of the WFSBP Task Force on Biological Markers of Dementia: The role of CSF and blood analysis in the early and differential diagnosis of dementia,” *World J. Biol. Psychiatry*, vol. 6, no. 2, pp. 69–84, Jan. 2005.
[54] M. Shi, W. M. Caudle, and J. Zhang, “Biomarker discovery in neurodegenerative diseases: a proteomic approach.,” *Neurobiol. Dis.*, vol. 35, no. 2, pp. 157–64, Aug. 2009.
[55] D. I. Ellis, W. B. Dunn, J. L. Griffin, J. W. Allwood, and R. Goodacre, “Metabolic fingerprinting as a diagnostic tool.,” *Pharmacogenomics*, vol. 8, no. 9, pp. 1243–66, Sep. 2007.
[56] L. Whiley and C. Legido-Quigley, “Current strategies in the discovery of small-molecule biomarkers for Alzheimer’s disease.,” *Bioanalysis*, vol. 3, no. 10, pp. 1121–42, May 2011.
[57] F. Song, A. Poljak, G. a Smythe, and P. Sachdev, “Plasma biomarkers for mild cognitive impairment and Alzheimer’s disease.,” *Brain Res. Rev.*, vol. 61, no. 2, pp. 69–80, Oct. 2009.
[58] A. El-Ansary, “Biomarker discovery in neurological diseases: a metabolomic approach,” *Open Access J. Clin. Trials*, pp. 27–41, 2009.
[59] Y. Ma, P. Zhang, Y. Yang, F. Wang, and H. Qin, “Metabolomics in the fields of oncology: a review of recent research.,” *Mol. Biol. Rep.*, vol. 39, no. 7, pp. 7505–11, Jul. 2012.
[60] Thermo Nicolet Corporation, “Introduction to Fourier Transform Infrared Spectrometry,” 2001.
[61] S. Hsu, “Infrared spectroscopy,” in *Handbook of Instrumental Techniques for Analytical Chemistry*, Prentice-Hall, Inc., 1997, pp. 247–284.
[62] R. Shaw and H. Mantsch, “Infrared spectroscopy in clinical and diagnostic analyses,” *Encyclopedia of Analytical Chemistry*. John Wiley & Sons, Ltd, 2000.
[63] D. Finkenthal, *Introduction to the electromagnetic spectrum*. General Atomics, 1996.
[64] B. C. Smith, *Fundamentals of Fourier Transform Infrared Spectroscopy*, Second edi. CRC Press, 2011, p. 207.
[65] J. Coates, “Interpretation of Infrared Spectra , A Practical Approach,” *Encyclopedia of Analytical Chemistry*. John Wiley & Sons Ltd, pp. 10815–10837, 2000.

[66] Sheffield Hallam University, “Infra-Red Absorption Spectroscopy Theoretical Principles.” [Online]. Available: http://teaching.shu.ac.uk/hwb/chemistry/tutorials/molspec/irspec1.htm.
[67] University of Colorado, Boulder, Dept of Chem and Biochem., “Infrared spectroscopy: theory,” in *Handbook for Organic Chemistry Lab*, 2002, pp. 155–164.
[68] B. H. Stuart, *Infrared Spectroscopy: Fundamentals and Applications*. Chichester, UK: John Wiley & Sons, Ltd, 2004.
[69] Institute of Biophysics Ulm University, “The Fourier Transform Infra-Red (FTIR) Technique,” 2012. [Online]. Available: https://www.uni-ulm.de/en/nawi/institute-of-biophysics/research/research-ag-prof-dr-u-nienhaus/methoden/ftir.html.
[70] PerkinElmerInc., “FT-IR Spectroscopy Attenuated Total Reflectance (ATR),” 2005.
[71] Specac, “Specac Product Catalogue 2013.” 2013.
[72] J. Krinsley, K. Bochicchio, C. Calentine, and G. Bochicchio, “Glucose Measurement of Intensive Care Unit Patient Plasma Samples Using a Fixed-Wavelength Mid-Infrared Spectroscopy System,” *J. Diabetes Sci. Technol.*, vol. 6, no. 2, pp. 294–301, Mar. 2012.
[73] A. Barth and P. I. Haris, *Biological and Biomedical Infrared Spectroscopy*. IOS Press, 2009, p. 448.
[74] J. Krinsley, K. Bochicchio, C. Calentine, and G. Bochicchio, “Glucose Measurement of Intensive Care Unit Patient Plasma Samples Using a Fixed-Wavelength Mid-Infrared Spectroscopy System,” *J. Diabetes Sci. Technol.*, vol. 6, no. 2, pp. 294–301, Mar. 2012.
[75] C. Petibois, G. Cazorla, a Cassaigne, and G. Déléris, “Plasma protein contents determined by Fourier-transform infrared spectrometry.,” *Clin. Chem.*, vol. 47, no. 4, pp. 730–8, Apr. 2001.
[76] Z. Yu, G. Kastenmüller, Y. He, P. Belcredi, G. Möller, C. Prehn, J. Mendes, S. Wahl, W. Roemisch-Margl, U. Ceglarek, A. Polonikov, N. Dahmen, H. Prokisch, L. Xie, Y. Li, H.-E. Wichmann, A. Peters, F. Kronenberg, K. Suhre, J. Adamski, T. Illig, and R. Wang-Sattler, “Differences between human plasma and serum metabolite profiles.,” *PLoS One*, vol. 6, no. 7, p. e21230, Jan. 2011.
[77] G. Janatsch, J. D. Kruse-Jarres, R. Marbach, and H. M. Heise, “Multivariate calibration for assays in clinical chemistry using attenuated total reflection infrared spectra of human blood plasma,” *Anal. Chem.*, vol. 61, no. 18, pp. 2016–2023, Sep. 1989.
[78] R. Cerdeira Silva, “Identification of Alzheimer biomarkers by FTIR - a pilot study,” University of Aveiro, 2013.
[79] M. de la Guardia and S. Garrigues, Eds., *Handbook of Green Analytical Chemistry*, 1ª Ed. John Wiley & Sons, Ltd, 2012, p. 519.
[80] L. Wang and B. Mizaikoff, “Application of multivariate data-analysis techniques to biomedical diagnostics based on mid-infrared spectroscopy.,” *Anal. Bioanal. Chem.*, vol. 391, no. 5, pp. 1641–54, Jul. 2008.
[81] R. Davis and L. J. Mauer, “Fourier tansform infrared (FTIR) spectroscopy: A rapid tool for detection and analysis of foodborne pathogenic bacteria,” in *Current Research, Technology and Education Topics in Applied Microbiology and Microbial Biotechnology*, A. Mendez-Vilas, Ed. Formatex Research Center, 2010, pp. 1582–1594.
[82] D. I. Ellis, G. G. Harrigan, and R. Goodacre, *Metabolic Profiling: Its Role in Biomarker Discovery and Gene Function Analysis*. Boston, MA: Springer US, 2003, pp. 111–124.
[83] D. Naumann, “FT-INFRARED AND FT-RAMAN SPECTROSCOPY IN BIOMEDICAL RESEARCH,” *Appl. Spectrosc. Rev.*, vol. 36, no. 2–3, pp. 239–298, Jun. 2001.
[84] S. D. Smolarek, “UV and IR laser spectroscopy of isolated molecular structural dynamics,” FNWI: Van ’t Hoff Institute for Molecular Sciences (HIMS), 2011.
[85] S. Kumar, S. Chaudhary, and D. C. Jain, “Vibrational Studies of Different Human Body Disorders Using FTIR Spectroscopy,” *Open J. Appl. Sci.*, vol. 04, no. 03, pp. 103–129, 2014.
[86] A. Barth and P. I. Harris, Eds., *Biological and Biomedical Infrared Spectroscopy*. IOS Press, 2009, p. 448.
[87] P. Garidel and H. Schott, “Fourier-Transform Midinfrared Spectroscopy for Analysis and Screening of Liquid Protein Formulations Part 2: Details Analysis and Applications,” *Bioprocess Int.*, vol. 1, pp. 48–55, 2006.
[88] Z. Movasaghi, S. Rehman, and D. I. ur Rehman, “Fourier Transform Infrared (FTIR) Spectroscopy of Biological Tissues,” *Appl. Spectrosc. Rev.*, vol. 43, no. 2, pp. 134–179, Feb. 2008.
[89] L. K. Tamm and S. A. Tatulian, “Infrared spectroscopy of proteins and peptides in lipid bilayers.,” *Q. Rev. Biophys.*, vol. 30, no. 4, pp. 365–429, Nov. 1997.

[90] F. Severcan and P. I. Harris, *Vibrational Spectroscopy in Diagnosis and Screening*. IOS Press, 2012, p. 432.
[91] A. Jabs, "Determination of Secondary Structure in Proteins by Fourier Transform Infrared Spectroscopy (FTIR)," 10-Jul-2005. [Online]. Available: http://jenalib.fli-leibniz.de/ImgLibDoc/ftir/IMAGE_FTIR.html.
[92] A. Barth, "The infrared absorption of amino acid side chains.," *Prog. Biophys. Mol. Biol.*, vol. 74, no. 3–5, pp. 141–73, Jan. 2000.
[93] G. Basurto-Islas and K. Iqbal, "A molecular mechanism by which acidosis of the brain can lead to Alzheimer's disease," *Alzheimer's Dement.*, vol. 9, no. 4, p. P307, Jul. 2013.
[94] A. Barth, "Infrared spectroscopy of proteins," *Biochim. Biophys. Acta*, vol. 1767, no. 9, pp. 1073–101, Sep. 2007.
[95] A. C. Leskovjan, A. Kretlow, and L. M. Miller, "Fourier transform infrared imaging showing reduced unsaturated lipid content in the hippocampus of a mouse model of Alzheimer's disease.," *Anal. Chem.*, vol. 82, no. 7, pp. 2711–6, Apr. 2010.
[96] V. Dritsa, "FT-IR Spectroscopy in Medicine," in *Infrared Spectroscopy - Life and Biomedical Sciences*, T. Theophile, Ed. InTech, 2012, pp. 271–288.
[97] M. J. Calkins, D. A. Johnson, J. A. Townsend, M. R. Vargas, J. A. Dowell, T. P. Williamson, A. D. Kraft, J.-M. Lee, J. Li, and J. A. Johnson, "The Nrf2/ARE pathway as a potential therapeutic target in neurodegenerative disease.," *Antioxid. Redox Signal.*, vol. 11, no. 3, pp. 497–508, Mar. 2009.
[98] J. D. Roberts and M. C. Caserio, "CARBONYL COMPOUNDS ALDEHYDES AND KETONES. ON REACT OF THE CARBONYL GROUP," in *Basic Principles of Organic Chemistry*, 2nd ed., W. A. Benjamin, Inc., 1977, pp. 671–734.
[99] P. Carmona, M. Molina, M. Calero, F. Bermejo-Pareja, P. Martínez-Martín, and A. Toledano, "Discrimination analysis of blood plasma associated with Alzheimer's disease using vibrational spectroscopy.," *J. Alzheimers. Dis.*, vol. 34, no. 4, pp. 911–20, Jan. 2013.
[100] N. Kanagathara, M. Thirunavukkarasu, E. Jeyanthi C, and P. Shenbagarajan, "FTIR AND UV-VISIBLE SPECTRAL STUDY ON NORMAL BLOOD SAMPLES," *Int. J. Pharm. Biol. Sci.*, vol. 1, no. 2, pp. 74–81, 2011.
[101] B. Shivu, S. Seshadri, J. Li, K. A. Oberg, V. N. Uversky, and A. L. Fink, "Distinct β-sheet structure in protein aggregates determined by ATR-FTIR spectroscopy.," *Biochemistry*, vol. 52, no. 31, pp. 5176–83, Aug. 2013.
[102] E. Peuchant, S. Richard-Harston, I. Bourdel-Marchasson, J.-F. Dartigues, L. Letenneur, P. Barberger-Gateau, S. Arnaud-Dabernat, and J.-Y. Daniel, "Infrared spectroscopy: a reagent-free method to distinguish Alzheimer's disease patients from normal-aging subjects.," *Transl. Res.*, vol. 152, no. 3, pp. 103–12, Sep. 2008.
[103] E. Cerf, R. Sarroukh, S. Tamamizu-Kato, L. Breydo, S. Derclaye, Y. F. Dufrêne, V. Narayanaswami, E. Goormaghtigh, J.-M. Ruysschaert, and V. Raussens, "Antiparallel beta-sheet: a signature structure of the oligomeric amyloid beta-peptide.," *Biochem. J.*, vol. 421, no. 3, pp. 415–23, Aug. 2009.
[104] A. L. Mitchell, K. B. Gajjar, G. Theophilou, F. L. Martin, and P. L. Martin-Hirsch, "Vibrational spectroscopy of biofluids for disease screening or diagnosis: translation from the laboratory to a clinical setting.," *J. Biophotonics*, vol. 7, no. 3–4, pp. 153–65, Apr. 2014.
[105] D. H. Burns, S. Rosendahl, D. Bandilla, O. C. Maes, H. M. Chertkow, and H. M. Schipper, "Near-infrared spectroscopy of blood plasma for diagnosis of sporadic Alzheimer's disease.," *J. Alzheimers. Dis.*, vol. 17, no. 2, pp. 391–7, Jan. 2009.
[106] F. Rincon and C. B. Wright, "Vascular cognitive impairment.," *Curr. Opin. Neurol.*, vol. 26, no. 1, pp. 29–36, Mar. 2013.